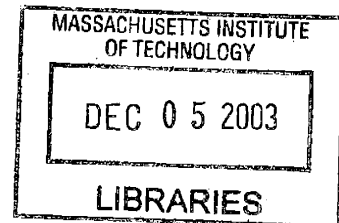


Synthesis and Evaluation of Actinide Imprinted Resins

by

Karen Lynn Noyes

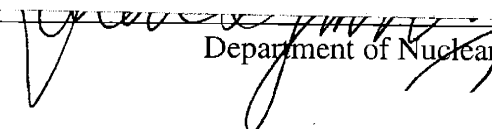
S.B., Nuclear Engineering (1999)
Massachusetts Institute of Technology




Submitted to the Department of Nuclear Engineering
in partial fulfillment of the requirements for the degree of
Doctor of Science in Nuclear Chemical Engineering and Waste Management
at the Massachusetts Institute of Technology
September 2003

© 2003 Massachusetts Institute of Technology. All rights reserved.


Signature of Author


Department of Nuclear Engineering
June 6 2003


Certified by


Kenneth R. Czerwinski
Associate Professor of Nuclear Engineering
Thesis Supervisor

Certified by


Michéline Draye
Associate Professor of Analytical Chemistry
Ecole Nationale Supérieure de Chimie de Paris
Thesis Reader

Accepted by


Jeffrey Coderre
Chairman, Committee on Graduate Students
Department of Nuclear Engineering

ARCHIVES

Synthesis and Evaluation of Actinide Imprinted Resins

by

Karen Lynn Noyes

Submitted to the Department of Nuclear Engineering
on June 6, 2003 in Partial Fulfillment of the
Requirements for the Degree of Doctor of Science in
Nuclear Chemical Engineering and Waste Management

ABSTRACT

Organic resins have previously shown good results with application to actinide separations. Large portions of recent research have been dedicated to the synthesis and evaluation of resins with phenolic-type functional groups. Other recent chemical research with lighter metals has developed a technique known as ion imprinting which can provide greater selectivity for the target metal ion. Initial work with ion imprinting and phenolic-type resins has shown these two areas to be largely incompatible. Identifying the ion imprinting technique as potentially the more valuable of the two, further work was undertaken with resins that incorporate a carboxylic acid-type functionality. These new resins are synthesized via a radical polymerization method, which proved to be very compatible with both actinides and the ion imprinting procedure.

Polymer-based resins were synthesized without a metal template as well as ion imprinted, or templated, with U(VI), Th(IV), Np(V), and a resin for use with Am(III). Each of these resins were individually characterized and evaluated for use with their respective target metals. Characterization provides a means of comparing theoretical binding capacities of various resins, which the evaluations define the binding characteristics of interest (capacity, selectivity, kinetics, etc.). Based on the initial results for the selectivity of the U(VI) and Th(IV) ions, a new type of resin was developed in an effort to further increase the selectivity of the resin for the target metal ion. This new resin, known as a "capped" resin, seeks to remove the binding capability of any potential binding sites not involved in the ion imprinting process.

Results show that the ion imprinting technique can be successfully applied in the synthesis of resins for actinide separations with good success. The resins created through this process also show an affinity for their target metals over both competing ions as well as ions of similar ionic charge and radii. The removal of so-called random binding sites is also possible, with the addition of a few synthetic steps.

Thesis Supervisor: Kenneth R. Czerwinski
Associate Professor of Nuclear Engineering

Thesis Reader: Micheline Draye
Associate Professor of Analytical Chemistry
ENSCP-University of Paris

Acknowledgements

First, I would like to thank the people who honestly and truly helped me make it through this whole process. Of course I have to thank my advisor, Professor Ken Czerwinski, for having me in his lab for six years and two theses. Actinides really are groovy! I would also like to thank Professor Micheline Draye of ENSCP-University of Paris for her help, support, and for the inspiration to go into actinide separations in the first place. I am also grateful to Nathalie Charton for her help and assistance with my project (I really hope that she enjoys Australia). For the day-to-day support, I have to thank my group. I'm really going to miss you guys and the French relations stick when we're all torn asunder.

Second, I would like to thank my friends and family for not yelling at me too much when I went into the nuclear business. To my dad for finally deciding that maybe being a nuke isn't so bad after all. To my sister, for doing my laundry countless times, making me dinner, and always reminding me of important things that I would have otherwise forgotten—you've been an invaluable presence for the past four years. To Amanda for not only supporting me, but also following in my footsteps. To Rachel, for being one of the dearest friends that anyone can have and a spectacular human being who is a hell of a lot tougher than anyone ever would have expected. To Idahlia and Gene for treating me like one of their own, helping to pick me up when I was down, and for all of the spectacular art and conversation.

Third, I would like to thank the people that make MIT the place that hasn't quite given me an ulcer yet. Among them, and very dear to me, is James E. Tetazoo, III. To the Muddy Charles Pub, always full of wonderful old-school MIT folk, cheap beer, and support. To Dwight, for teaching me how to sail, for sliming me in to LSC (which sucks, and always will), and for never actually sh@#ing in my sink. To Chuck Vest, for making my time more interesting with countless media-prompted knee-jerk reactions.

I dedicate this work of chemistry to my mother. You always encouraged me, truly helped me believe that I actually could do anything that I wanted to do, and you sacrificed so much to make all of my accomplishments possible. Someday I hope that I can give you even a small fraction of what you gave me. I'll never be able to thank you enough!

-Karen Lynn Noyes

Author Biography

I was born and raised in small-town New England (a.k.a. Westminster, MA), where the cracker factory doesn't make crackers anymore, but the crackers still have a picture of the cracker factory on them anyway. When I was 15, I moved to a town that was roughly four times the size of my birthplace, which is where I graduated from Dracut Senior High School on my 18th birthday (June 9, 1995, in case you're not familiar with my birth) and still list as my hometown, even though my heart's not in it. After that I moved to yet another town in Massachusetts to attend the infamous Massachusetts Institute of Technology. Upon surviving four glorious years that generally lacked sleep, I received an S.B. degree in nuclear engineering slightly before my 22nd birthday in 1999. Fearing that I hadn't yet spent enough time at MIT, I decided to stay on for a long haul as a graduate student. Now that I've made it through another four years, it looks like I'll be getting another degree (right on schedule, or so it seems). Although the stars aligned for MIT's commencement to be on my 26th birthday (June 9, 2003), I won't be participating in this year's ceremony. In any event, here is a list of my accomplishments (publications, etc) at MIT, not including these:

Manuscript in preparation: **Synthesis and evaluation of resins for americium separations.** K.L. Noyes, N. Charton, M. Draye, and K.R. Czerwinski. For Separation Science and Technology.

Synthesis and evaluation of resins for americium separations. K.L. Noyes, N. Charton, M. Draye, and K.R. Czerwinski. American Institute of Chemical Engineers Proceedings (2003), Recent Advances in Chemical Separation Process for Tank Waste Treatment. [Submitted for publication]

Synthesis and evaluation of resins for actinide separations. K.L. Noyes, M. Draye, A. Favre-Reguillon, J. Foos, A. Guy, and K.R. Czerwinski. Materials Research Society Symposium Proceedings (2003), Scientific Basis for Nuclear Waste Management XXVI. [Submitted for publication]

Synthesis and evaluation of uranium and thorium imprinted resins. K.L. Noyes, M. Draye, A. Favre-Reguillon, J. Foos, A. Guy, and K.R. Czerwinski. Materials Research Society Symposium Proceedings (2002), Scientific Basis for Nuclear Waste Management XXV, 901-906.

Hafnium hydroxide complexation and solubility: the impact of hydrolysis reactions on the disposition of weapons-grade plutonium. G. Cerefice, M. Draye, K. Noyes, and K. Czerwinski. Mater. Res. Soc. Symp. Proc. (1999), Scientific Basis for Nuclear Waste Management XXII, 1025-1032.

Environmental behavior of hafnium for the disposal of weapons-grade plutonium. G. Cerefice, M. Draye, K.L. Noyes, and K. Czerwinski. WM'98 Proc. (1998), 1862-1872. Publisher: American Nuclear Society, La Grange Park, IL.

Presentation in preparation: **Synthesis and evaluation of resins for americium separations.** K.L. Noyes, N. Charton, M. Draye, and K.R. Czerwinski. To be presented by K.L. Noyes at American Institute of Chemical Engineers (AIChE) spring meeting in March, 2003, in New Orleans, LA.

Synthesis and evaluation of resins for actinide separations. K.L. Noyes, N. Charton, M. Draye, and K.R. Czerwinski. Presented by K.L. Noyes at Materials Research Society (MRS) fall meeting in Boston, MA, in November, 2002.

- Selectivity batch studies of thorium- and uranyl-imprinted resins.** K.L. Noyes, M. Draye, and K.R. Czerwinski. Presented by K.L. Noyes at American Nuclear Society annual meeting in Hollywood, FL, in June, 2002.
- Synthesis and evaluation of uranium and thorium imprinted resins.** K.L. Noyes, M. Draye, A. Favre-Reguillon, J. Foos, A. Guy, and K.R. Czerwinski. Presented by K.L. Noyes at MRS fall meeting in Boston, MA, in November, 2001.
- Differentiation of ion-selective resins using a nuclear magnetic resonance (NMR) tracer method.** D.F. Caputo, K.L. Noyes, D.G. Cory, M. Draye, Marc Vial, and K.R. Czerwinski. This poster was presented at Atalante 2000: Scientific Research on the Back-End of the Fuel Cycle for the 21st Century, located in Avignon, France, in October, 2000.
- Complexation of Eu and Cm with fulvic acid: comparison with expected trends.** K.L. Noyes and K.R. Czerwinski. This poster was presented in September 1999 at Migration 99 in Incline Village, NV.

TABLE OF CONTENTS

	TITLE PAGE.....	1
I.	ABSTRACT.....	3
	ACKNOWLEDGEMENTS.....	4
	TABLE OF CONTENTS.....	7
	LIST OF FIGURES.....	9
	LIST OF TABLES.....	11
II.	THESIS SUMMARY.....	13
III.	INTRODUCTION.....	25
	3.1 Project Overview	
	3.2 Thesis Overview	
	3.3 The Development of a Need for Actinide/Lanthanide Separations Processes	
	3.4 Actinide Separations: A Brief History	
IV.	BACKGROUND.....	45
	4.1 Physico-Chemical Properties of the Actinides and Lanthanides	
	4.2 The Origin of Actinide/Lanthanide Separations	
	4.3 The Inherent Difficulties in Actinide/Lanthanide Separations	
	4.4 Principles of Molecular and Ion Imprinting	
	4.5 Applications and Advantages of Molecular and Ion Imprinting	
V.	ANALYTICAL TECHNIQUES.....	59
	5.1 ICP-AES	
	5.2 ICP-MS	
	5.3 Synchrotron Techniques	
	5.4 Spectroscopy	
VI.	PHENOLIC RESIN SYNTHESSES.....	77
	6.1 Introduction	
	6.2 Background	
	6.3 Experimental	
	6.4 Results and Discussion	
	6.5 Conclusions	
VII.	URANIUM AND THORIUM EXPERIMENTS.....	87
	7.1 Introduction	
	7.2 Background	
	7.3 Experimental	
	7.4 Results and Discussion	
	7.5 Conclusions	
VIII.	NEPTUNIUM EXPERIMENTS.....	105
	8.1 Introduction	
	8.2 Background	
	8.3 Experimental	
	8.4 Results and Discussion	
	8.5 Conclusions	

IX.	AMERICIUM EXPERIMENTS.....	111
	9.1 Introduction	
	9.2 Background	
	9.3 Experimental	
	9.4 Results and Discussion	
	9.5 Conclusions	
X.	CAPPING OF URANIUM TEMPLATED RESIN.....	129
	10.1 Introduction	
	10.2 Background	
	10.3 Experimental	
	10.4 Results and discussion	
	10.5 Conclusions	
XI.	CONCLUSIONS.....	135
XII.	REFERENCES CITED.....	143

LIST OF FIGURES

1. ABSTRACT
2. THESIS SUMMARY
3. INTRODUCTION
 - 3.1 Once-through fuel cycle
 - 3.2 Fuel cycle with U reuse
 - 3.3 Fuel cycle with U and Pu reuse
 - 3.4 Radioactivity of Np, Am, and Cm as a function of time
 - 3.5 Flow chart of PUREX process
4. BACKGROUND
 - 4.1 Elemental and +3 ionic radii for lanthanide series
 - 4.2 Actinide radii for elemental, +3, +4, and +5
 - 4.3 Schematic representation of the molecular imprinting technique
 - 4.4 Schematic of non-covalent vs. covalent approaches of molecular/ion imprinting techniques
5. ANALYTICAL TECHNIQUES
 - 5.1 ICP-AES basic arrangement
 - 5.2 Detail of basic ICP-AES configuration
 - 5.3 ICP-AES plasma torch operation
 - 5.4 Major components of an ICP-MS
 - 5.5 Typical synchrotron setup
 - 5.6 Typical EXAFS sample analysis setup
 - 5.7 Sample XANES (“edge”) spectra
 - 5.8 Sample k^3 weighted EXAFS oscillation spectrum
 - 5.9 An example of a Fourier transformed EXAFS spectrum
 - 5.10 Basic diagram of FTIR spectroscopy setup
 - 5.11 Liquid scintillation counting
6. PHENOLIC RESIN SYNTHESIS
 - 6.1 Basic setup for phenolic type resin synthesis
 - 6.2 Closeup of catechol synthesis after packing with ice and addition of all reagents
7. URANIUM AND THORIUM EXPERIMENTS
 - 7.1 Uranyl resin synthesis before polymerization
 - 7.2 Thorium resin at reaction completion
 - 7.3 Synthesis of Uranium and Thorium Imprinted Resins
 - 7.4 Experimental and theoretical sorption values for uranium and thorium sorption to uranium- and thorium-imprinted resins. The plot shows the results of PEC experiments as well as the binding results seen in tables 7.1 and 7.2
 - 7.5 Selectivity results for uranium-imprinted resin vs. pH
 - 7.6 Selectivity results for thorium-imprinted resin vs. pH
 - 7.7 FTIR spectra of uranium-imprinted resins and uranium nitrate
 - 7.8 Uranium L3 edge spectra for uranium and thorium loaded resins
 - 7.9 Diagram of uranyl-imprinted resin complex consistent with EXAFS data
 - 7.10 EXAFS data for uranium-resin binding characteristics

8. NEPTUNIUM EXPERIMENTS

- 8.1 Neptunium, as received
- 8.2 Picture of Np before dried

9. AMERICIUM EXPERIMENTS

- 9.1 Fourier transforms and fits of EXAFS data
- 9.2 EXAFS data and fits for the Sm-imprinted resin
- 9.3 Influence of pH on Eu-resin binding for Sm-, Nd-, Pr-, and non-templated resins at 200 % of loading capacity
- 9.4 Influence of pH on Gd-resin binding for Sm-, Nd-, Pr-, and non-templated resins at 200 % of loading capacity
- 9.5 D_{cx} values for Eu vs. pH at 200 % of loading capacity
- 9.6 D_{ex} values for Gd vs. pH at 200 % of loading capacity
- 9.7 D_{ex} values for Am vs. pH at 100 nM
- 9.8 D_{ex} results for Am, presented with respect to ionic radii at 100 nM
- 9.9 K values for Eu vs. pH at 50 % of loading capacity
- 9.10 K values for Gd vs. pH at 50 % of loading capacity
- 9.11 K values for Am vs. pH at 100 nM

10. CAPPING OF URANIUM TEMPLATED RESIN

11. CONCLUSIONS

LIST OF TABLES

1. ABSTRACT
2. THESIS SUMMARY
3. INTRODUCTION
 - 3.1 Summary of separations processes
4. BACKGROUND
 - 4.1 Oxidation states of An elements
 - 4.2 Molecularly imprinted polymers and their potential areas of applications
 - 4.3 Some characteristics of molecular or ion imprinted polymers
5. ANALYTICAL TECHNIQUES
6. PHENOLIC RESIN SYNTHESIS
 - 6.1 Summary of results for resorcinol and catechol resins
 - 6.2 Summary of results for remainder of resin syntheses
7. URANIUM AND THORIUM EXPERIMENTS
 - 7.1 Experimental data for the sorption of UO_2^{2+} on uranyl templated resin
 - 7.2 Experimental data for the sorption of the Th^{4+} on thorium templated resin
8. NEPTUNIUM EXPERIMENTS
9. AMERICIUM EXPERIMENTS
 - 9.1 Proton exchange capacities and theoretical sorption capacities of the resins
 - 9.2 Loading capacities of the resins
10. CAPPING OF URANIUM TEMPLATED RESIN
11. CONCLUSIONS

II. THESIS SUMMARY

This document is a summary of the thesis prepared by Karen Lynn Noyes in partial fulfillment of requirements for a Doctor of Science degree in Nuclear Chemical Engineering and Waste Management at the Massachusetts Institute of Technology. It consists of an overview of each section as it appears in the main thesis document.

2.1 Abstract

Organic resins have previously shown good results with application to actinide separations. Large portions of recent research have been dedicated to the synthesis and evaluation of resins with phenolic-type functional groups. Other recent chemical research with lighter metals has developed a technique known as ion imprinting which can provide greater selectivity for the target metal ion. Initial work with ion imprinting and phenolic-type resins has shown these two areas to be largely incompatible. Identifying the ion imprinting technique as potentially the more valuable of the two, further work was undertaken with resins that incorporate a carboxylic acid-type functionality. These new resins are synthesized via a radical polymerization method, which proved to be very compatible with both actinides and the ion imprinting procedure.

Polymer-based resins were synthesized without a metal template as well as ion imprinted, or templated, with U(VI), Th(IV), Np(V), and a resin for use with Am(III). Each of these resins were individually characterized and evaluated for use with their respective target metals. Characterization provides a means of comparing theoretical binding capacities of various resins, which the evaluations define the binding characteristics of interest (capacity, selectivity, kinetics, etc.). Based on the initial results for the selectivity of the U(VI) and Th(IV) ions, a new type of resin was developed in an effort to further increase the selectivity of the resin for the target metal ion. This new resin, known as a "capped" resin, seeks to remove the binding capability of any potential binding sites not involved in the ion imprinting process.

Results show that the ion imprinting technique can be successfully applied in the synthesis of resins for actinide separations with good success. The resins created through this process also show an affinity for their target metals over both competing ions as well as ions of similar ionic charge and radii. The removal of so-called random binding sites is also possible, with the addition of a few synthetic steps.

2.2 Introduction

Other recent work in the area of actinide separations undertaken by our collaborators has been mainly involved in the development of resins with phenolic-based functional groups. These resins had slow kinetics, which was the large reason that this work examines carboxylic acid type functionality resins. A technique known as molecular, or ion, imprinting was also implemented in the synthetic process. Although this technique has been widely applied for a number of applications, there has been little use with the lanthanides and actinides.

The purpose in undertaking this project was to produce new research in the area of actinide separations, which is becoming a lost art in the United States due to proliferation concerns. In the past few years, there has been renewed activity in the development of the nuclear industry. Hundreds of millions of dollars have been dedicated to research into the feasibility of nuclear transmutation.

This project went into the development of resins for solid-liquid extraction methods, rather than liquid-liquid, which was once the industry standard. The reason for this is that the solid provides a reusable binding source, is entirely incinerable, and does not produce by-products. By-products previously produced in liquid-liquid extraction processes are well known to degrade solvents, to be unstable, and to be explosive in nature. Based on work with other metals and molecules, solid-liquid extraction development was limited to molecular- or ion-imprinted resins.

The concept of molecular-imprinted polymers was developed more than 20 years ago [1] and shows a potential for applications in analytical chemistry [2-4]. The technique of molecular imprinting can be used for the production of selective ion exchange resins. Both simple organic compounds and polymers have been created using these methods in order to separate lanthanides [5] and actinides [6]. The more traditional simple organic compounds utilized functional groups such as phenols, resorcinol, and catechol. The problems with these previous resins include slow kinetics and difficulty with creating a molecularly imprinted product. This led to the investigation of templated resins with carboxylic functional groups.

The actinides are of prime importance in the nuclear industry, hence the concentration on the development of resins for the actinide elements uranium, thorium, neptunium, and plutonium. Uranium is important for its value as a fuel; plutonium and thorium may become valuable fuel resources; and neptunium is a large contributor to the radiation inventory of spent nuclear fuel [7].

There is a desire to develop simple, fast, and accurate separation techniques and methods for actinides, both for analytical and potentially industrial purposes. Previous methods using unimprinted resins were slow and although effective, there is room for improvement. By imprinting resins, potential binding sites are tailored for the target metal in terms of both ion size and charge, thereby increasing efficacy.

Separations can be improved by both changing input conditions and by altering elution methods, which provides many options for elements such as actinides which have very complex solution chemistry behavior. By tailoring both the resin and the separation conditions, improved techniques can be developed for actinide separations.

2.3 Background

Actinide/lanthanide inter- and intra-group separations are among the most difficult chemical separations, and may become necessary in future fuel cycles. Chemical separation techniques have been key to the nuclear since its dawn. Separations were required in order to manufacture both weapons and fuel, for both military and civilian enterprises. Since the lanthanides are fission products and Pu for weapons use is produced in nuclear reactors, the Pu is produced side-by-side with lanthanides.

Lanthanides have high neutron absorption cross-sections, thereby making them nuclear reaction “poisons,” and their removal necessary to retain the integrity of the reaction. Given that future fuel cycles propose making use of transmutation techniques, which utilize a neutron source in order to lower the overall radioactivity of waste and/or produce power, there is a definite need for fast, efficient actinide/lanthanide separations.

Past fuel cycles or military uses mainly focused on the partitioning of U and Pu. Their separation from the lanthanides is easily achieved by exploiting the extractability of the higher oxidation states of these particular actinides. Future fuel cycles will also require the partitioning of Am and Cm, which are trivalent actinides and therefore chemical homologs for the trivalent lanthanides. Am and Cm will need to be separated from the trivalent lanthanides in order to produce targets or blanket fuel pins which are free of neutron poisons such as Gd [8].

This section also includes relevant background information on the chemistry of the lanthanides, actinides, the inherent difficulties in the separation of lanthanides from actinides, the chemical principles behind the molecular imprinting technique, and the advantages of using the molecular imprinting technique.

2.4 Analytical Techniques

Metal ion concentrations for the lanthanides, thorium, and uranium were determined via inductively coupled plasma atomic emission spectroscopy (ICP-AES). The principles behind this analytical technique as well as the sample preparation, standard preparation, and data analysis are described in this section.

Metal ion concentrations from the uranium and thorium resin competition experiments, as detailed in section VII, were analyzed via inductively coupled plasma mass spectrometry (ICP-MS). The change in analysis methods was made due the detection limits of the ICP-AES for some metals involved in the experiments.

A synchrotron was used as a source of intense, high energy X-rays in order to probe the average local structure of some Sm-, Th-, and U-bearing samples. Extended X-ray absorption fine structure (EXAFS) is an ideal method for probing the local structure of actinide and lanthanide bearing materials because of their high atomic masses. Here, EXAFS was used to confirm oxidation states, suspected structures of the resins, and to examine the binding of the metals to the resins.

Two spectroscopic techniques were used for sample analysis: Fourier transform infrared (FTIR) and liquid scintillation spectroscopy. The FTIR spectroscopy was used for analysis of some U- and non-templated resins, as well as some U-templated resins that were bound to U. Liquid scintillation spectroscopy was used for metal concentration analysis of both Np and Am due to their radioactive alpha emissions. Due to the small quantities of Np and Am used in experiments, as well as the inability to analyze them by traditional methods of solution concentration quantification, this was an ideal method.

2.5 Phenolic Resin Synthesis

Many resins have been created which make use of a phenol-type functional group to bind the metals of interest. These have included resorcinol, catechol, phenol, 8-quinolinol, and chelating resins. Some of these resins have been modified to include soft donors in the backbone in order to create a higher binding affinity for the target An and Ln metals. None of these resins have been made with the application of an ion imprinting technique.

Given the harsh conditions of these types of resin syntheses, it may not be possible to keep the target ion in solution during resin production, which is required by the ion imprinting technique. Work undertaken in this section seeks to investigate the limits of synthetic conditions

for phenolic resins and possible compatibility with ion imprinting techniques. Experiments were limited to syntheses and visual observations of the final products.

In general, the only potential success in this task was the production of a phenol imprinted resin, which is very limiting and may not be applicable with further modifications, such as adding soft donors to the back bone or adding chelators. Given these severe limitations, ion imprinting is not deemed to be a compatible technique with phenolic-type resin syntheses. Other types of resin syntheses could show more promise for this technique and are investigated throughout the remainder of this thesis, as well as by other researchers for use with other, lighter metals.

2.6 Uranium and Thorium Experiments

A uranium selective polymer has yielded promising results and was used as the synthetic basis for the work described in this paper [6]. This paper examines the creation and qualification of a new polymer-based thorium selective resin and a similar uranium selective resin. The separation of uranium from other metals has been used by the nuclear industry, mainly for fuel production and the handling of waste streams. Thorium is an important element in advanced nuclear fuels and therefore a desire to separate it from other metals was seen. In addition the synthesis of a Th selective resin can prove the methodology for template synthesis using higher valent metal ions.

With the success of the uranium-imprinted resin synthesis given below, a modified synthetic route was developed in order to create a thorium-imprinted resin. The final, successful process is also outlined below. The proton exchange capacities of the synthesized templated resins were determined. The interaction of U and Th with their respective templated resin as a first step towards competitive reactions was investigated.

These studies show that polymer-based resins templated with uranyl and thorium(IV) ions sorb their target metal ions. The ability of the resin to sorb the target metal ion while competing with metal ion of differing oxidation states yielded some unexpected results in that strong competition was coming from unexpected players. This may indicate that a fair amount of binding is occurring at random sites, or binding sites which were not produced via the imprinting process. An addition to the synthesis should be investigated in order to remove these random binding sites, which should further increase the selectivity of the resin.

The breakthrough of solutions containing the target metal in a resin column also must be determined in order to consider column feasibility. The syntheses of this study will also be used as a basis for templating higher actinides, such as neptunium and plutonium. One of the initial goals of this work was to produce a resin with rapid kinetics, and these experiments have indicated success. The values for the metal binding indicate charge neutralization, which is confirmed with the EXAFS data. The reusability of the resin also remains to be proven, and will be investigated in another experiment.

2.7 Neptunium Experiments

The imprinting process generally requires the use of gram quantities of the target metal ion, which is difficult to accomplish when the target is Np(V), due to both radioactivity and the ability to procure necessary quantities. For these reasons, the synthetic process was modified for use in very small quantities (roughly 250 times smaller than previous syntheses, seen in chapter 7, 9, or 10).

If there is a move toward transmutation, it is critical to separate Np from An and Ln in a coherent manner in order to control the amounts of Np present, an important aspect of both fuel production and criticality control. The experiments presented in this section intend to show that it is possible to produce an imprinted ion exchange resin for Np separations that could be used to control the flow of Np in output streams.

The successful imprinting of a resin with the Np(V) ion proves that it is possible to template both more radioactive metals and run the synthesis on very small scales. Other successes of the synthesis include starting with a wet (i.e. aqueous) target, which is notable since water easily and completely halts the radical synthesis involved in the formation of the imprinted resin. The resin preparation method was also altered in order to account for both the small amount of product and the radioactivity involved. All in all, this is a success that can be further applied to other elements in the future, such as Pu.

2.8 Americium Experiments

Molecular imprinting techniques have shown great promise for applications in chemical separations, including those involving lanthanides and actinides. This work examines the production of a selective resin for Am separations. Due to practical difficulties, resins were not imprinted with Am, rather 3 resins were created with each of Sm, Nd, and Pr as the template ions. An analogous “blank” or unimprinted resin was also created. The nitrate salt of the target

metal ion was dissolved in CCl_2H_2 and the resin was created around the ions to provide a unique structure based upon each metal. These resins were synthesized by a radical polymerization method, producing a reusable organic solid. The resins were qualified by obtaining values for their proton exchange capacities and data to define their complexation thermodynamics. Proton exchange capacities were determined using an indirect titration and were found to be 10.08 meq/g for the Sm-imprinted resin, 7.25 meq/g for the Nd resin, and 7.14 meq/g for the Pr resin. Data for the resins' thermodynamics were obtained at pH 1-7 in steps of 0.5 units. Results show that the templated resins rapidly removed the target actinide from aqueous solution under experimental conditions. Better separation results for Am, rather than Eu or Gd, were obtained with the Nd imprinted resin.

When compared with other published results, the results of these syntheses and experiments show that the imprinted resins have lower PEC values than those of phenolic-based resins such as CF, RF, CQF, and RQF by factors of 2-3 [9]. Although the D_{ex} values are lower than those for CF, RF, CQF, and RQF, at pH 4, the values are comparable at pH 6 [9]. Other comparisons for Kd values show that the imprinted Nd resin at a pH value of 6 has very comparable values with CMPO, roughly 300 (as calculated in the reference paper) [10]. In comparison with other imprinted polymers, the resins tested for effectiveness with Am can only be compared with a resin meant to complex (i.e. imprinted with) Gd. For this comparison, the values for the Am complexation with the Nd-imprinted resin at pH 6 were compared with the results for the Gd-imprinted resin produced by others; the Am was about 99% complexed by the resin, whereas the Gd was 48% extracted [11]. This may be a bit misleading, as the Gd-imprinted resin is based on a vinylpyridine synthesis, as opposed to my carboxylic acid type, but the two resins do have the same backbone structure.

So far, the use of lanthanides as templates for ion-imprinted resins for use with Am seems to be working quite well and shows better separation factors than the non-templated resin. The Nd resin shows the most promise and all future work should be concentrated on further evaluating this resin for use in Am separations. Previous issues with slow kinetics have been solved and no Am is needed for the templating process.

The initial testing for reusability via EXAFS analysis shows a good possibility for reuse of the resin, as there is little change in the binding structure after a second loading. Also, the kinetics results show a very fast equilibrium, achieved in 20 minutes or less. The Nd resin shows a

higher than theoretical loading capacity for Am, the intended target metal of this process. Column studies also need to be run in the future to determine potential for column separations and elution methods.

Overall, the resins indeed sorb metals and the Nd resin in particular seems very promising for use in Am separations. Since the content of Nd in waste relative to other trivalent metals tends to be small, there is not much concern for the metal used in the templating process significantly interfering with the separation scheme. However, experiments still need to be run to confirm a resin preference for Am when other trivalent metals are in direct competition, as in a realistic waste stream. Based on previous successes along with the successes from the experiments presented in this paper, the same method is currently being applied for templating Np and Pu resins.

2.9 Capping of Uranium Resin

An ion exchange resin was created to complex UO_2^{2+} from aqueous solutions. The nitrate salt of the target metal ion was dissolved in CCl_2H_2 , while the resin was created around the ions to provide a unique structure based upon each metal, followed by a process to remove potential binding sites which were not involved in the initial imprinting process. This resin was synthesized by a radical polymerization method, producing a reusable organic solid and is based upon the original work as seen in chapter 7. The resin was qualified by obtaining a value for its proton exchange capacity. Proton exchange capacities were determined using an indirect titration and were found to be 14.39 meq/g for the new uranium-based resin. A new resin preparation process had to be developed to prepare this new type of resin (“capped”) for use in experiments. Once loaded with metal, the ions can easily be removed with 5 M HNO_3 and reused.

This work proves that the resin synthesis, as developed throughout chapters 7, 8, and 9, can be further modified for both other applications or for more specific separations. This section modifies the synthetic process much more than the previous changes, seen within chapter 7, 8, and 9, which further attests to the robust quality of the final product. The modifications made to the resin in this section (chapter 10) require significantly more processing and caution in the synthesis itself, so the process is no longer as simple as that seen in previous chapters. However, the benefits may end up outweighing the detractions, since it is likely that in future work this “capped” resin will prove to be more selective than its predecessors.

2.10 Conclusions

The most important conclusion of this work is that it is possible to apply the ion imprinting method to the synthesis of resins that are applicable for actinide separations processes. This is a notable achievement, since ion imprinted products are well-known to be highly selective for their target metals and that efficient separations processes will likely be needed in the near future for most currently proposed nuclear fuel cycles.

Initially, the ion imprinting technique was applied to phenolic resin syntheses, which have been widely used and synthesized for experiments in actinide/lanthanide separations. Due to the harsh, inhospitable conditions inherent to the phenolic-based resin syntheses, the ion imprinting technique was extremely difficult to accomplish in a reliable manner (for details on this section of the work, see chapter 6). For these reasons, a very common application of ion imprinting was tapped: ion imprinted polymers.

Since there had been a previous success with the imprinting of a polymer with the uranyl ion, this work began with a similar synthesis based on that initial work. A resin imprinted with uranyl was successfully produced and tested for effectiveness (see chapter 7 for details on results/tests). This success led to modifications to the synthesis so that a product imprinted with Th(IV) ions was successfully produced. This resin was also tested for effectiveness (results can be seen in detail in chapter 7).

The successes of the imprinting of resins with the uranyl and Th(IV) ions, the work was further adapted for application to Np(V) ions (see chapter 8 for details). Due to the small advantage in selectivity, the synthesis was further modified in order to remove any binding sites which were not involved in the original synthetic imprinting process. This methylation of unimprinted binding sites is referred to as “capping.” The capping technique was only applied to the uranyl ion, which provided the simplest reaction conditions and the least number of preliminary modifications (details on this work can be found in chapter 10).

Although the fruitful application to Np(V) showed that it was possible to template relatively radioactive metals, when the technique was extended to produce a resin for Am(III) separations, four resins were created for use with Am(III), none of which were actually imprinted with Am(III). Given the chemical similarity of Am(III) to the lanthanides, the following four resins were produced: Sm(III)-, Pr(III)-, Nd(III)-, and un-imprinted. A series of experiments were run in order to test the effectiveness and applicability of each of the resins to Am(III) separations.

The most notable conclusion to come out of the work is the following: the most effective resin for application to Am(III) separations was the resin templated with Nd(III). This is notable, since the size of the template ion can be proven to matter. The ion which had a smaller ionic radius than that of Am(III) was not very effective; the most effective turned out to be that which was just slightly larger than Am(III), proving that the cavity produced in the templating process must be at least as large as the desired target (for details on this section, please reference chapter 9).

Based on all of the applications of the ion imprinting technique detailed in this thesis, it can be seen that ion imprinting is a highly adaptable and widely applicable technique that is also useful for potential actinide/lanthanide separation schemes. The work in this thesis can easily be further extended to other actinides, lanthanides, or further still to other sections of the periodic table. The synthetic processes detailed throughout the thesis are easily scalable for either small- or large-scale processes. In cases of high activity or hard to get target materials, suitable resins can be created from chemically similar materials (note: the similarity must be in both size and charge). The creation of a more tailored resin is possible by adding additional synthetic steps onto the back-end of the resin production process, but requires significant and non-trivial modifications to the synthetic conditions. Finally, this work shows that the area of ion imprinting should be investigated further for the renewed development of actinide/lanthanide separation science.

2.11 References for Section II

1. G. Wulff, A. Sarhan, *Angew. Chem. Int. Ed. Eng.*, 1972, **11**, 341 ; R. Arshady, K. Mosbach, *Makromol. Chem.*, 1981, **182**, 687-692
2. a) A. Sarhan, G. Wulff, *Makromol. Chem.*, 1982, **183**, 85-92 ; b) G. Wulff, J. Haarer, *Makromol. Chem.*, 1991, **192**, 1329-1338
3. M. Kempe, K. Mosbach, *J. Chromatogr. A*, 1995, **694**, 3-13
4. a) B. Sellergren, M. Lepistö, K. Mosbach, *J. Am. Chem. Soc.*, 1988, **110**, 5853-5860 ; b) D. Spivak, M.A. Gilmore, K.J. Shea, *J. Am. Chem. Soc.*, 1997, **119**, 4388-4393
5. K. Uezu, M. Yoshida, M. Goto, S. Furusaki, *Chemtech*, 1999, 12-18
6. Saunders, G., Foxon, S., Walton, P., Joyce, M., and Port, S.: A Selective Uranium Extraction Agent Prepared by Polymer Imprinting. *Chem Commun.* 2000, **4**, 273-274.
7. Kazuba, J.P., Runde, W.H.: The Aqueous Geochemistry of Neptunium: Dynamic Control of Soluble Concentrations with Applications to Nuclear Waste Disposal. *Env. Sci. Tech.* 33, 4427-4433 (1999)
8. Nash, K.L. *Solvent Extr. and Ion Exch.*, 1993, 729-768.
9. Draye, M., Favre-Reguillon, A., Wruck, D., Foos, J., Guy, A., and Czerwinski, K. *Sep Sci Tech.*, 2001, 899-909.
10. Barr, M.E., Schulte, L.D., Jarvinen, G.D., Espinoza, J., Ricketts, T.E., Valdez, Y., Abney, K.D., and Bartsch, R.A. *Journal of Radioanalytical and Nuclear Chemistry*, 2001, 457-465.
11. Garcia, R., Vigneau, O., Pinel, C., and Lemaire, M. *Sep Sci Tech.*, 2002, 2839-2857.

III. Introduction

In this initial chapter, the project overview will be presented, along with the scope of the thesis and some introductory materials pertaining to previous work done in the area of the thesis work. In this general area of research, little recent work has been done in the United States, but here has been a desire to revisit the area of actinide separations for potential future applications in American nuclear fuel cycles. This desire stems largely from the Advanced Fuel Cycle Initiative (AFCI) program.

The goals of the AFCI program are to design effective technologies for spent fuel treatment, particularly for the following specific issues: the reduction of spent fuel volume, separate long-lived toxic elements, and utilize the potential energy of spent fuel [1]. To realize these goals, safe and effective chemical and nuclear technologies will need to be developed. The benefits of the AFCI philosophy are: increased capacity of the proposed geologic repository at Yucca mountain, the reduced need for a second repository, reduction in the long-term Pu content of fuel, reducing the toxicity of spent fuel, reducing the long term heat generation of spent fuel, providing a stable resource for nuclear energy, and the utilization of the Pu reservoir in spent fuel [1].

Thus far, the project has yielded a technology known as UREX, the uranium extraction process, which was developed by the DOE (Department of Energy). The process is proliferation resistant, as Pu is never separated from the other components. Phase one of the project looks to further demonstrate the capabilities of UREX, to potentially build a pilot scale plant, and to continue the development of aqueous waste processing techniques for eventual industrial scale separations. There is a second version of the process, known as UREX+, which would also separate out other actinides and fission products of interest for waste volume [1]. AFCI looks to further develop and test both of these methods.

3.1 Project Overview

This project overview summarizes the efforts completed in fulfillment of a doctoral thesis. Included in the overview is a description of the problem addressed in the thesis statement, research goals and objectives, and their significance, and a detailed description of each task.

3.1.1 Problem Description

Previous recent work in the area of resins for actinide separations by our colleagues has been mainly involved in the development of resins with phenolic-based functional groups. These resins had slow kinetics, which was the large reason that this work examines carboxylic acid type functionality resins. A technique known as molecular, or ion, imprinting was also implemented in the synthetic process. Although this technique has been widely applied for a number of applications, there has been little use with the lanthanides and actinides.

The purpose in undertaking this project was to produce new research in the area of actinide separations, which is becoming a lost art in the United States due to proliferation concerns. In the past few years, there has been renewed interest in the redevelopment of nuclear chemical engineering.

This project went into the development of resins for solid-liquid extraction methods, rather than liquid-liquid, which is still the industry standard. Liquid-liquid extraction is widely used in the hydrometallurgy of base and strategic metals², and for the spent nuclear fuels reprocessing. However, this technique exhibits important restrictions and drawbacks. In particular, the diluents and extractants, which constitute the organic solvents, the solutes are extracted in, are partly lost in the aqueous phases by solubility and mechanical dispersion as fine droplets and therefore may be the origin of an induced pollution. Furthermore, the use of large volumes of hydrocarbons as diluents may be hazardous. In addition, the solid provides a reusable binding source, is entirely incinerable (as long as it contains only H, C, O, or N), and does not produce by-products. By-products previously produced in liquid-liquid extraction processes are well known to degrade solvents, to be unstable, and can be explosive in nature. Based on work with other metals and molecules, solid-liquid extraction development was limited to molecular- or ion-imprinted resins.

The concept of molecular-imprinted polymers was developed more than 20 years ago [3] and shows a potential for applications in analytical chemistry [4-6]. The technique of molecular imprinting can be used for the production of selective ion exchange resins. Both simple organic compounds and polymers have been created using these methods in order to separate lanthanides

[7] and actinides [8]. The more traditional simple organic compounds utilized functional groups such as phenols, resorcinol, and catechol. The problems with these previous resins include slow kinetics and difficulty with creating a molecularly imprinted product. These reasons lead to the investigation of templated resins with carboxylic functional groups.

The actinides are of prime importance in the nuclear industry, hence the concentration on the development of resins for the actinide elements uranium, thorium, neptunium, and plutonium. Uranium is important for its value as a fuel; plutonium and thorium may become valuable fuel resources; and neptunium is a potentially large contributor to the dose inventory of spent nuclear fuel [9].

There is a desire to develop simple, fast, and accurate separation techniques and methods for actinides, both for analytical and potentially industrial purposes. Previous methods using unimprinted resins were slow and although effective, there is room for improvement. By imprinting resins, potential binding sites are tailored for the target metal in terms of both ion size and charge, thereby increasing efficacy. If selective extraction is seen by this templating method future research will be directed at improving selectivity through the introduction of specific binding sites on the resin functional group or backbone.

Separations can be improved by both changing input conditions and by altering elution methods, which provides many options for elements such as actinides that have very complex solution chemistry behavior. By tailoring both the resin and the separation conditions, improved techniques can be developed for actinide separations.

3.1.2 Research goals and objectives

The work presented in this thesis encompasses a number of resin syntheses and developments. The initial work describes attempts to stretch the limits of the synthesis of phenolic-based resins in order to try and incorporate an ion imprinting technique. These forays yielded limited ability and success, which prompted the switch to a polymer synthesis with a different functional group that would require smaller needs for changes in ambient synthetic conditions. All of the initial syntheses that involved imprinting were done with uranium, due to the low levels of activity and the ease in obtaining sufficient quantities for numerous syntheses.

Beginning syntheses were completed with resorcinol, catechol, and phenol. Due to previous results with these types of resins, there was a quick advance to the synthesis of a chelating resin incorporating 8-hydroxyquinolinol [10]. Again, due to a general lack of success and the added

complexities of the ion imprinting process as applied, a leap was made to polymer-based resins with carboxylic acid functionalities.

The pKa value for phenol is near 10 [11] and that of carboxylic acid is about 5 [12], which would foreshadow faster kinetics in the pH range suitable for the actinides. Following an initial polymer-based resin synthesis by way of a radical polymerization method, the process was repeated while incorporating an ion imprinting technique with the uranyl ion.

After a uranyl-imprinted resin was successfully produced, the process was modified for application to other elements. The second imprinted, or templated, resin was produced based on the Th(IV) ion. Along with the uranyl-templated resin, many tests were run regarding the properties of the resins, including: proton exchange capacity (PEC), loading capacity, kinetics, thermodynamic properties, and batch extraction competition studies.

The results of the batch extraction competition studies indicated that there may be some binding sites present in the resin which were not involved in the ion imprinting process, thereby providing some "random" binding sites. Although these so-called random binding sites can increase the loading capacity of the resin, they decrease the selectivity of the resin, which is an undesirable side effect.

In an effort to curtail this decreased selectivity presented by the random binding sites, a new synthetic process was developed to remove the random binding sites. This synthesis was essentially a number of additional processing steps that were added onto the back end of the initial synthetic process. After production of the resin, but before the removal of the template metal, the random binding sites are changed from carboxylic acid groups with metal binding abilities into methyl groups, which have no effective binding ability.

A Np(V) imprinted resin was in parallel development, initially at the Actinide Research Facility in TA 48 at Los Alamos National Laboratory, and later reproduced in the Actinide Research Group's hot lab at MIT. Due to the difficulty in obtaining large quantities of Np, the synthesis was run only on a small scale and minimal characterization experiments were run.

A resin was also developed for application to Am(III) separations. Due to radioactivity concerns and possession limitations, the resin was imprinted with lanthanides that have similar ionic radii: Pr(III), Nd(III), and Sm(III). A series of experiments were run to evaluate which resin was best applied to Am(III) separations and compared with the behavior of Eu(III) and Gd(III) binding to the resins.

The results of these syntheses and experiments have achieved many of the project goals set at the start. The kinetics of the new resins are very fast, the method is solid-liquid extraction, the reactions are size-scalable, and the imprinting process has served to further solidify the efficiency of the resins.

3.1.3 Research task list

In order to accomplish the goals put forth in the project overview, a number of tasks had to be carried out. These tasks are listed below along with descriptions and specific objectives.

Task 1- Synthesis of Phenolic Resins: The first task of this thesis was to synthesize various phenolic-based resins in order to stretch the limits of the synthetic conditions and test the feasibility of applying the ion imprinting technique. A number of different types of resins were synthesized and the products were examined for experimental suitability. Ultimately it became obvious that the ion imprinting technique was not going to be compatible with the phenolic resin synthetic process, nor were any suitable resins produced for further experimentation, which led into task 2.

Task 2- Development of Ion Imprinting Capability with Uranyl: The second task of the project was to then develop a resin that was inherently compatible with the ion imprinting technique. This task purely focused on the application of this process to the uranyl ion, due to the ease of attainability, the obvious importance to the nuclear industry, and its chemical stability. The resin was then characterized via common values such as proton exchange capacity (PEC), kinetics, and thermodynamics. This resin was also evaluated for its ability to separate the uranyl ion from a mixture of other ions common in nuclear waste. All samples were analyzed for metal concentration via either inductively coupled atomic emission spectroscopy (ICP-AES) or inductively coupled mass spectrometry (ICP-MS). The PEC values were obtained via indirect titrations.

Task 3- Adaptation of Synthetic Route to Th(IV) Ions: The third task involved adapting the synthetic process developed in task 2 for use with Th(IV). After the successful development of the resins, both tasks 2 and 3 were extended to include characterization of the resins and experiments to

determine their efficacy. This resin was also evaluated for its ability to separate the Th(IV) ion from a mixture of other ions common in nuclear waste. All samples were analyzed for metal concentration via either ICP-AES or ICP-MS. The PEC values were obtained via indirect titrations.

Task 4- Adaptation of Ion Imprinting Synthesis to Np(V) Ion: The fourth task involved the further adaptation of the resin synthetic process to minor actinides, specifically Np. This task involved synthesizing a resin imprinted with Np(V) and obtaining proton exchange capacities.

Task 5- Development of Resin for Am(III) Separations: The fifth task involved the development of a resin for Am(III) separations. This task required the synthesis of three resins imprinted with Sm(III), Nd(III), and Pr(III) which were tested for efficacy with Eu(III), Gd(III), and Am(III). The lanthanide (Ln) samples were analyzed for metal concentration via ICP-AES and the Am(III) samples were analyzed for metal concentration via scintillation spectroscopy.

Task 6- Development of Methodology for Removal of Random Binding Sites: The sixth task was based on the results of tasks 2 and 3, and involved further modification of the resin synthesis developed in task 2 in order to further increase the efficacy of the resin. The goal of task 6 was to develop a process to remove any random binding sites present in the imprinted resins. These random binding sites are potential binding sites present in the resins which were not involved in the imprinting process. Titrations were also completed to obtain values for the proton exchange capacity.

3.2 Thesis Overview

This thesis contains the work undertaken by Karen Lynn Noyes in fulfillment of a Doctor of Science degree in Nuclear Chemical Engineering. The thesis topic is the synthesis of new resins for actinide separations. The research involved in this thesis included organic synthetic techniques, standard aqueous chemistry procedures, standard chemical analysis techniques including ICP-AES and IR spectroscopy, and characterization techniques such as EXAFS. In summary, the new resins produced for this thesis project have been proven effective for actinide separations. The application of a radical polymerization technique in conjunction with an ion imprinting technique has been forged as a new category of resins for actinide separations and can probably be further applied to other actinides with equal success.

This thesis is broken down into ten sections. Each section is listed below with a brief description of its contents.

- Section 1 is the thesis abstract with a short overview of the motivations and key findings from the thesis research.
- Section 2 is the thesis summary with a more detailed description of the main research activities, the results of those activities, and conclusions based on those findings.
- Section 3 is the introduction which includes material concerning the project objectives and introductory material on the subject matter of the thesis.
- Section 4 contains background materials within the area of thesis research in order to explain the relevant chemistry.
- Section 5 explains the workings of the relevant analytical techniques used for data analysis in the accomplishment of the tasks outlined in the project overview.
- Section 6 describes the work carried out in the investigations of phenolic-type functional resins and the limitations this imposed on the application of an ion imprinting technique.
- Section 7 details the first two syntheses carried out successfully with the ion imprinting technique. These syntheses used the U(VI) and Th(IV) ions and also describe all experiments carried out with the resins.
- Section 8 describes the application of the ion imprinting technique to a Np(V) ion imprinted resin and all experiments carried out on that resin.

- Section 9 details the production of a resin suitable for Am separations via imprinting three separate resins with Sm, Nd, and Pr, respectively. The section also includes the results of characterization experiments and resin experiments with Eu, Gd, and Am.
- Section 10 describes the modification of the original uranyl-imprinted resin synthesis in order to remove random binding sites to increase resin efficiency. The chapter also includes results from all relevant characterization experiments.
- Section 11 gathers together the conclusions from all previous chapters and states overall concluding remarks based on the entire scope of the project.

3.3 The Development of a Need for Actinide/Lanthanide Separations Processes

The current fuel cycle in the United States is known as a “once-through” fuel cycle, in which the uranium fuel is manufactured, used, and disposed of directly, i.e. without modification. Other countries, such as France, utilize the recycling philosophy and reprocess their spent fuel in order to separate out and reuse the fissile content in subsequent fuel production. Currently, given the increasing demands for energy, some countries are considering going even further with their fuel cycles. In some cases this means using both uranium and plutonium for subsequent energy production as MOX fuels or transmuting elements (such as Tc, I, and An) that would otherwise be waste in accelerators or light water reactors for energy production and waste minimization [13]. Three figures are included below in order to diagram potential routes for the fuel cycles mentioned previously.

Figure 3.1: Once-through fuel cycle.

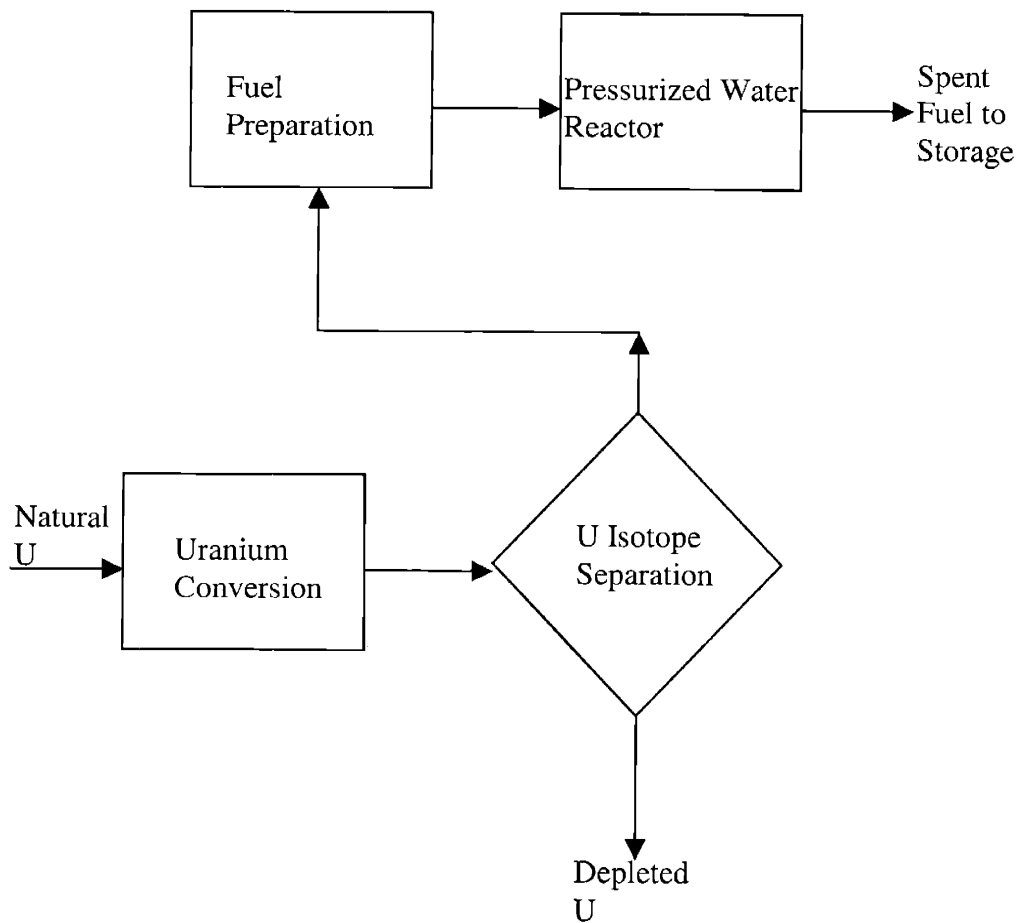


Figure 3.2: Fuel cycle with U reuse.

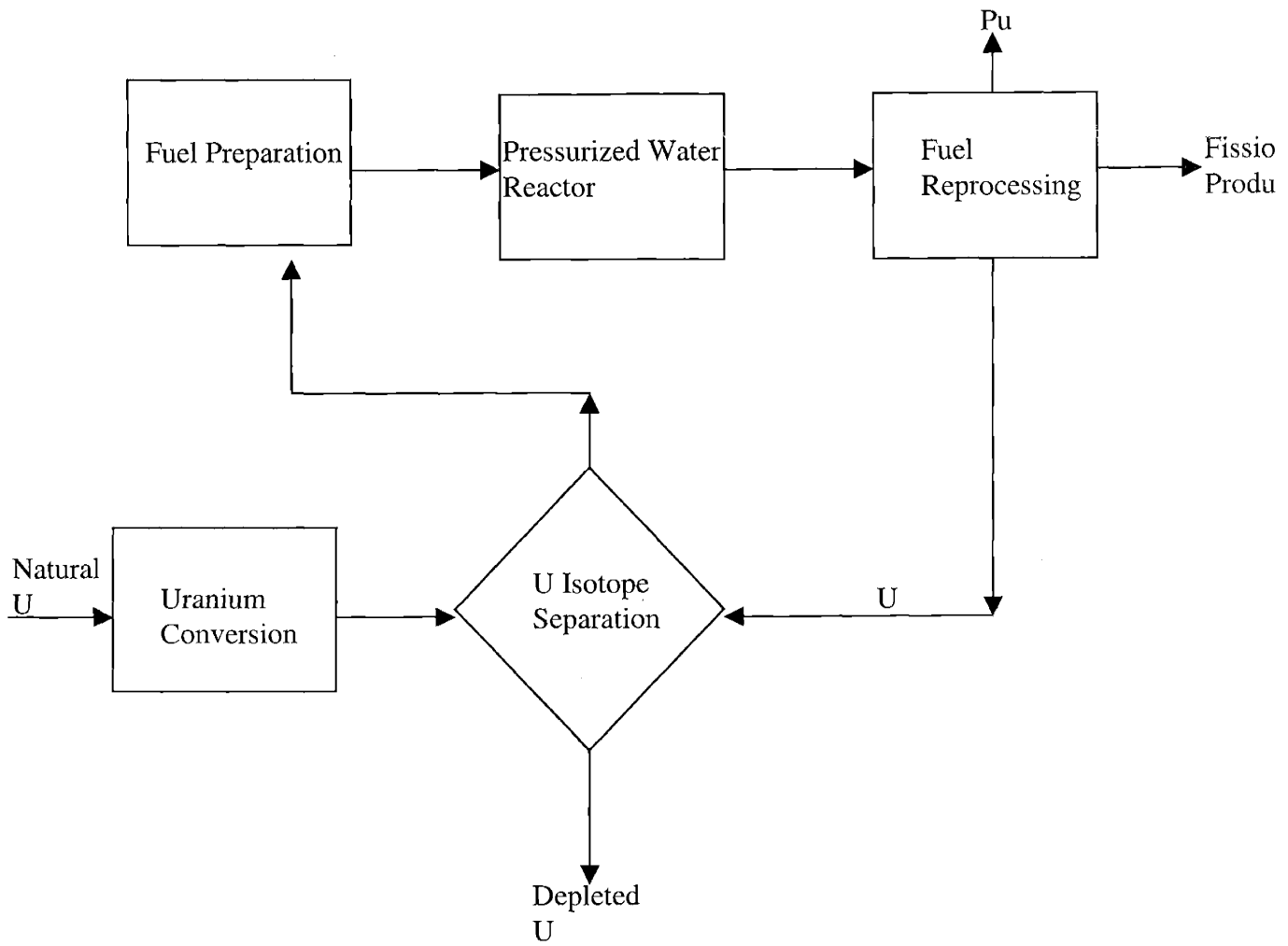
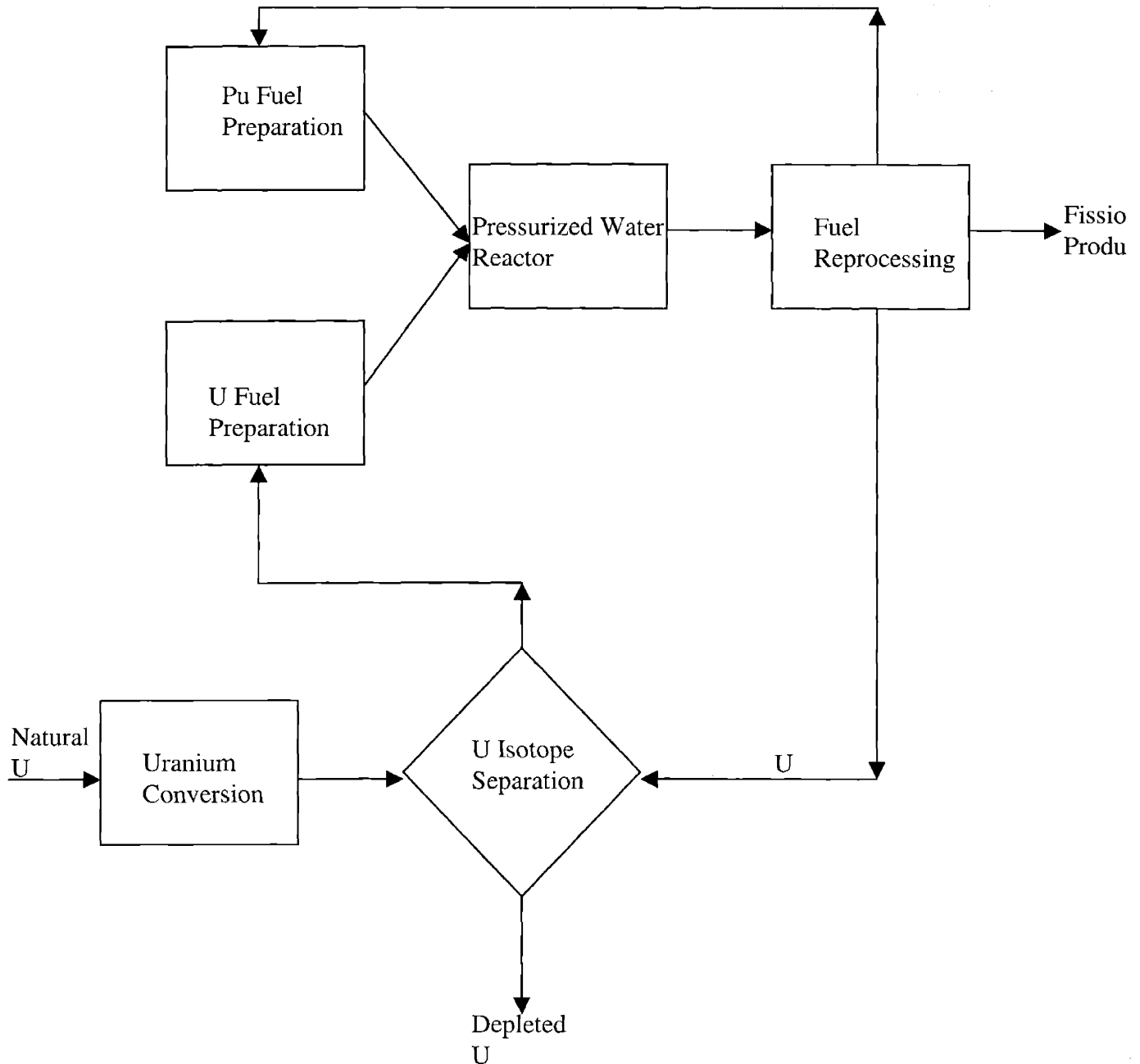


Figure 3.3: Fuel cycle with U and Pu reuse.

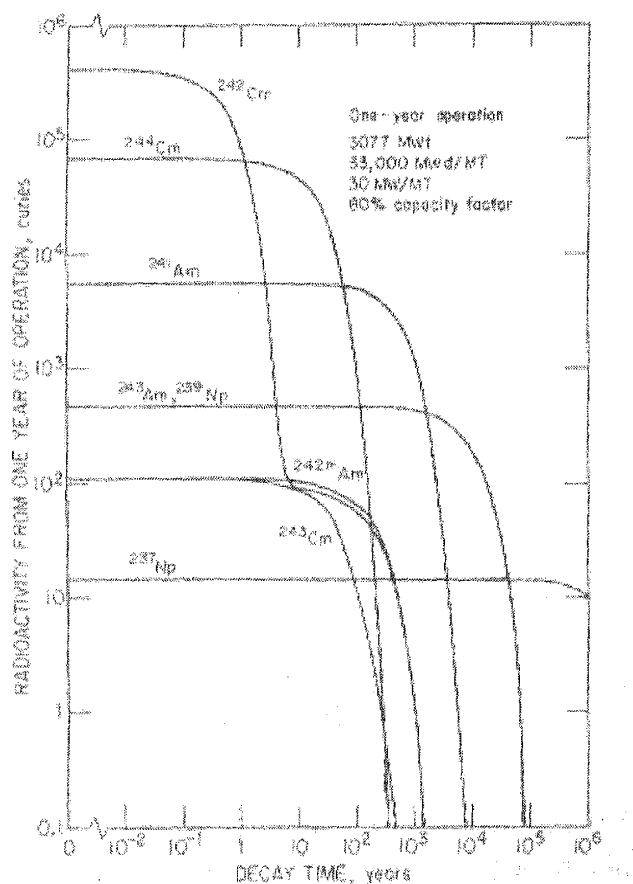


One can see that all fuel cycles, with the exception of the “once-through” cycle, require some type of reprocessing, particularly actinide/lanthanide separation technology. This is an art that has been lost to the passing of time in the United States. Actinide separation capabilities did exist in the past in the U.S., but have essentially been scrapped with the end of the Cold War. Due to the nature of the industrial needs during the development of actinide separations

processes, they are mainly designed to solely to separate actinides, largely U and Pu, from fission products. In the past, separations for actinides were really designed not as strictly actinide separations, but as a means of Pu production for weapons [17]. Recent desires for actinide separations aim more to separate actinides from fission products either for subsequent transmutation into stable or less radioactive species or for disposal in specially tailored waste forms [14].

In the case of transmutation, the actinides must be separated from all other elements, particularly the lanthanides [15]. With respect to long-term geological disposal, the minor actinides ^{241}Am and ^{237}Np are of prime concern because they will provide the largest portion of the radiotoxicity inventory after about 1000 years and, additionally, Np is of a concern from a mobility standpoint. This can be seen below in **Figure 3.4**.

Figure 3.4: Radioactivity of Np, Am, and Cm as a function of time.



Transmutation is being considered as a waste disposal option because of the inherent advantages of decreasing the long-term dose from radioactive waste. Generally, the fission

products decay off relatively quickly, with many of the highly active isotopes largely decayed after 100 years and essentially gone after 1000 years. However, the actinides are largely long-lived and provide a few particular concerns: long half lives imply that actinides provide all long-term dose, ^{239}Pu is a relatively large component as well as a proliferation risk, and ^{237}Np is both long-lived and mobile in the environment selected by the United States for a geological repository, Yucca Mountain.

3.4 Actinide Separations: A Brief History

The quest for efficient actinide separations began with the nuclear arms race during World War II. The discovery of Pu by Glenn Seaborg and the subsequent production of that element for use in nuclear weapons necessitated the development of separations processes. Initial separations procedures were most useful on a bench-scale because they were developed expressly for that purpose in order to produce Pu amounts suitable for chemical studies. This first method of separation is a precipitation method; subsequent methods include liquid-liquid extraction, solid-liquid extraction, volatility processes, and pyroprocesses.

The initial separations processes, which were precipitation methods, were typified by what has become known as the bismuth phosphate process [16]. This process made use of the solubility chemistry of Pu and Bi, since they will coprecipitate as tetra-phosphates [17]. This method also makes use of the numerous oxidation states of both U and Pu, utilizing the solubility of U(VI) and insolubility of Pu(IV). An initial starting solution of U and Pu is electrochemically modified such that it then contains U(VI) and Pu(IV), rather than a potential mixture of oxidation states.

Once in the tetravalent state, Pu will precipitate upon complexation with phosphate. After this point, the Pu can be further purified by a cyclic process in which the Pu is alternately oxidized back to the hexavalent state and reduced to the tetravalent state again. For these purposes, the reducer of choice was NaNO_2 , while the oxidant of choice was Na_3BiO_3 [17]. The impressive successes of this process include: a direct scale-up from bench-top to industrial scale (10^8 increase), production of hundreds of kilos of Pu at 99.9% purity, and 97% chemical yield (the decontamination factor from fission products was greater than 10^7) [17].

However, in spite of these obvious successes and advantages, the bismuth phosphate process had some drawbacks as well. The main problems were that it recovered only Pu and that it required batch operation, due to the nature of the chemical processes involved. After some

experimentation, the first liquid-liquid solvent extraction processes were developed. Some of the first advantages over the bismuth phosphate process included the ability to extract other elements in addition to Pu and the ability to remotely operate a facility, a key concern when processing high radioactive irradiated fuel.

Initial solvent extraction processes utilized methyl isobutyl ketone (MIBK or hexone) as the extractant, which removed both U and Pu from the same oxidizing streams used in the bismuth phosphate process [17]. Hexone is able to extract hexavalent U and Pu into the organic phase as AnO_2^{2+} , where An is an actinide, by forming bonds with these An(VI) nitrates:



where MIBK represents hexone. This hexone-based process became known as the REDOX process [17]. Pu was back-extracted into the aqueous phase with a dilute nitric acid solution containing a salting agent and a strong reductant, usually Fe(II), which reduced Pu without reducing U. U was later extracted into a dilute nitric acid solution. The major disadvantage of this process was that contact with nitric acid slowly degraded the hexone [17].

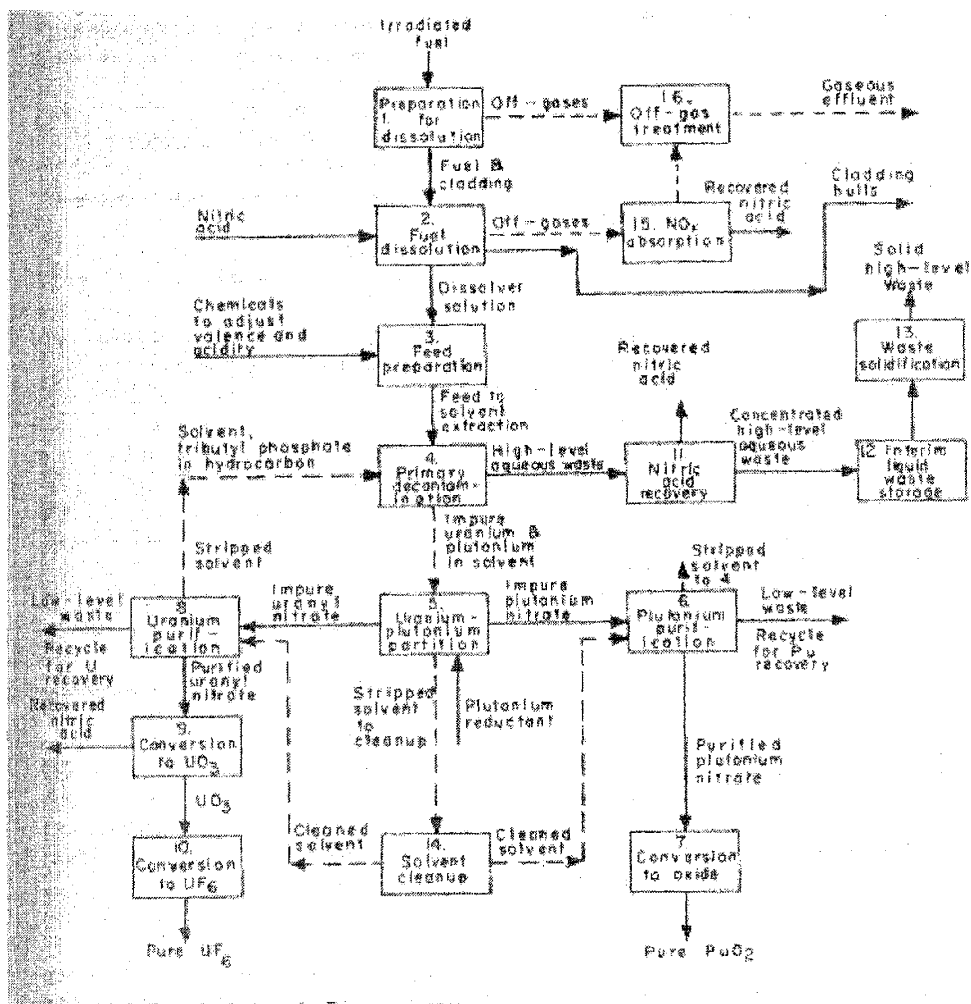
This led to the development of what has become known as the PUREX process, the current world-wide industrial standard for actinide, particularly U and Pu, separations. The PUREX process is very similar to the REDOX process, with the major difference being that PUREX utilizes tributyl phosphate (TBP) as the organic complexant. The first industrial scale plant using the PUREX process was opened in November 1954 in Aiken, South Carolina, and then later replaced the REDOX process at Hanford, Washington, in January, 1956. The significant advantages of PUREX over REDOX are: waste volumes are much lower, TBP is less volatile than hexone, TBP is more stable against nitric acid, and operating costs are lower [18].

In order for the Plutonium-Uranium Extraction (PUREX) process to work properly, the plutonium and uranium must be present in solution as nitrates, so the solids, usually spent fuel, are dissolved in nitric acid. Uranium dissolves as hexavalent uranyl (UO_2^{2+}), plutonium as a mixture of tetravalent and hexavalent (Pu^{4+} , PuO_2^{2+}), and neptunium as a mixture of inextractable pentavalent and extractable hexavalent (NpO_2^+ , NpO_2^{2+}) [18]. Next, Pu is reduced to the tetravalent, or more extractable, state with the addition of hydroxylamine (N_2O_4) [18].

Once the aqueous solution is prepared, it can be contacted with the organic phase, usually 30% TBP in kerosene, in order to carry out the extraction [17]. When contacted, the TBP forms complexes with the UO_2^{2+} and Pu^{4+} , with some NpO_2^{2+} contamination, which are then soluble in

the organic phase [17]. The U and Pu can be separately removed from the organic phase with the reduction of Pu to the trivalent state and then back-extraction into 6 M HNO₃. Following removal of the Pu, the U can be extracted into dilute HNO₃ [17]. The higher actinides and fission products remain behind in the original aqueous solution, thus providing three output streams: waste (fission products, higher minor actinides), U, and Pu. A diagram of the industrial PUREX process is included below as Figure 3.5.

Figure 3.5: Flow chart of PUREX process.



Further work has been done on some modifications to the PUREX process for use in more modern fuel cycles, which might include partitioning and transmutation. These new separations processes tend to be very similar to the PUREX process with the addition of a few steps in order to separate the trivalent actinides from the trivalent lanthanides, which is very important for any partitioning and transmutation process. The first modification involves the change of the organic

complexant from TBP to a combination of TBP and octyl(phenyl)-N,N-diisobutylcarbamoylmethylphosphine oxide (CMPO), as 0.25 M CMPO, 0.75 M TBP in C_2Cl_4 [19]. The Am can be back-extracted from the organic solution with 0.05 M HNO_3 [19].

In summary of the various separations techniques, a table from *Reprocessing and Recycling* is reproduced below as Table 3.1.

Table 3.1: Summary of separations processes [taken from: 20].

Name of Process	Input Fuels	Principle of Separation	Stage of Development	Ability to extract Pu	Affiliation of work	Remarks
AQUEOUS PROCESSES						
Solvent extraction						
Butex	UO ₂ Oxide fuels	Solvent extraction	Lab studies	Yes	Union Carbide Nuclear Co.	Process for recovery and decontamination of Pu from irradiated U. Recovery of uranium is accomplished, but decontamination is not adequate to permit direct handling.
Chelation	UO ₂	Solvent extraction	Lab studies	Yes	UC Berkeley Rad. Lab.	Pu recovery and decontamination from dissolver solutions and redox wastes.
Halex	UO ₂ Oxide fuels	Solvent extraction	Lab studies	Yes	Argonne	Identical to purex, except that CCl ₄ used as diluent for TBP.
Purex	Metallic, UO ₂	Solvent extraction	Commercial	Yes	Oak Ridge Nat. Lab.	Extensively employed commercially; bulk of R & D effort spent on this. Good separation of U & Pu. Good decontamination.
Redox	Metallic, UO ₂	Solvent extraction	Pilot plant	Yes	Oak Ridge Nat. Lab.	Superseded by purex.
Thorex	Th, ThO ₂	Solvent extraction	Pilot plant	---	Oak Ridge Nat. Lab.	Solvent extraction process for Th fuels; high decontamination factor achieved.
Ion exchanger						
Ion exchange	Metallic U, UO ₂ , Pu, PuO ₂	Adsorption- desorption	Commercial possible	Yes	Oak Ridge Nat. Lab.	Alternate process in 1942-44 at Hanford for Pu production. Used primarily as tail-end to purex, etc, for further purification and concentration of U-235, U-233, Th, Pu, etc.
Photochemistry						
Photochemical induced separation	Any type that fits Purex	Selective oxidation or reduction	Conceptual	Yes	Brookhaven	Still in conceptual stage, viewed as modification to purex tail end to permit almost complete separation of actinides.
Electrolysis						
Flurex	Metallic, oxides	Electrolytic (aqueous)	Lab studies	Possible, with great modification	Hanford	Designed for U recovery from NH ₄ UF ₅ .
Precipitation						
Bismuth phosphate precipitation	Metallic U, Pu	Precipitation	Military purpose plant	Yes	Hanford	Basically for separation of Pu from U, & fission products. This has been expanded for recovery of other fission products individually.
PYROPROCESSES-PYROPHYSICAL						
Fractional distillation						
Airox	UO ₂	Volatility	Lab studies	Not possible	Atomics International	Low decontamination, rapid recycle; remote refabrication needed, suitable only for UO ₂ fuels.

Name of Process	Input Fuels	Principle of Separation	Stage of Development	Ability to extract Pu	Affiliation of work	Remarks
Deboer	Metallic U, U alloy	Volatility	Lab Studies	No	Knolls Atomic	Decontamination from all long-lived fission products except Zr by formation of UI_2 . By selective condensation of UI_4 , U & Zr can be separated slowly.
Fluoride volatility	UO_2 , PuO_2 alloys, Metallic U, UC	Volatility	Pilot plant	PuF_6 extraction possible. High purity.	Argonne	Along with chloride & bromide volatility, this method has been the subject of much research. More activity in France & USSR than in USA in recent years.
Molten salt-fluoride volatility	Metallic U of U-alloy	Volatility & sorption-desorption	Lab studies	Difficult	Oak Ridge Nat. Lab.	For recovering decontaminated U from U-Al fuels with Al cladding.
Nitrofluor	Alloys, UO_2	Volatility	Lab studies	PuF_6 extracted together with some fission products; Pu distillation possible.	Brookhaven	Non-aqueous fluoride volatility U, Pu separation & purification; kilogram amounts of fuel have been tested and studied.
Carbox	UC	Separation only of volatile fission products	Lab studies	Pu cannot be removed	Atomics International	Specially developed for UC fuels. Low decontamination recycling. Only volatile fission products removed by separation.
Fractional crystallization						
Hermex	U, U alloy, Th	Fractional crystallization with solvent	Lab studies	No	Oak Ridge Nat. Lab.	Suitable for metallic U, low decontamination.
Hydride separation	Metallic U	Sieving	Lab studies	Pu-rich phase can be separated. Very low purity	Ames & Oak Ridge	Poor separation, only lab studies. Kinetic rates expected to be very slow since processing will probably be in the solid state.
Pyrozinc	Metallic U	Fractional crystallization	Lab studies	No	Argonne	Suitable for metallic fuels; Pu not separated. For U recycling only.
Zone melting	Metallic U	Fractional crystallization	Lab Studies	Not possible	Argonne	Very slow; applicable only for the production of small quantities of high-purity metals for laboratory purposes.

Name of Process	Input Fuels	Principle of Separation	Stage of Development	Ability to extract Pu	Affiliation of work	Remarks
Liquid-liquid partitioning						
Ag extraction of Pu & fission products	Metallic U	Liquid-liquid partitioning	Lab studies	Low extraction ability for Pu contamination.	Ames, Iowa	Low decontamination. Separation of Pu improves with addition of gold. Economic feasibility not expected for large scale separation.
Buffer method	Metallic U, U alloys	Liquid-liquid partitioning	Lab studies	Doubtful	Brookhaven	Designed to separate U and other fission products. Possible to modify to remove Pu from fission products.
Fused salt-liquid metal	U-233 Th	Liquid-liquid partitioning	Lab studies	---	Ames, Iowa	For reprocessing of U-233 Th fuels, separating U-233 from Th.
Mg extraction of Pu from molten U	Metallic U or U alloy	Liquid-liquid partitioning	Lab studies	Process designed for Pu extraction. Purity of product low.	Atomics Int'l	Suitable for metallic fuels, low decontamination for recycling. Only lab study reported.
Salt transport process	UO ₂ , PuO ₂	Liquid-liquid partitioning	Lab studies	Pu separable	Argonne	High decontamination developed for LMFBR but could be applied possibly to other fuel types with suitable modification.
Liquid-solid extraction						
DAP	Metallic U, Pu; U, Pu alloys	Liquid-solid separation	Lab studies	Possible, but low purity	Dow Chemical Co.	Dow aluminium pyro-metallurgical process. U is dissolved in molten Al and precipitated as UAl ₃ . Separate step required for Pu recovery. Applicability to oxide and carbide fuels doubtful.
Tin nitride	Metallic, UO ₂ , UC	Liquid-solid separation	Lab studies	Possible	Stanford	Lab studies only, suitable for in-situ reprocessing of reactor fuels. Separate U-Pu from fission products.
PYROPROCESSES--PYROCHEMICAL						
Electrochemical						
Electro-refining	Metallic U or mixed salt	Electro-chemical (pyro)	Lab studies	PuCl ₃ removed as vapour	Knolls Atomic Power Lab.	Only lab studies, though work not followed up in the US. Current research in the USSR quite extensive. Not suitable for ceramic fuels and carbon coated fuels.
Molten salt electrolysis	UC	Electrolysis	Lab studies	Pu stays in salt	Atomics Int'l	Application of molten salt to reprocessing of UC fuels.
Salt cycle process	UO ₂ , UO ₂ -PuO ₂	Electrolysis	Pilot plant	PuO ₂ crystals deposited	Battelle Memorial	Research began in 1956; lab and pilot plant studies have been done.
Cyclic oxidation reduction						
Nitride-carbide cycle	UC	Oxidation-reduction	Lab studies	No	Atomics Int'l	For processing of UC fuels only. Low decontamination pyro-chemical method. High Pu losses.
Selective oxidation						
Melt refining	Metallic U	Volatility & selective oxidation	Pilot plant	Pu not removed	Argonne Nat. Lab.	No U-Pu separation, decontamination by volatilization or oxidative-slagging. Experimental processing done at EBR-II for few years. Remote fabrication of fuel rods carried out successfully.

3.5 References

1. U.S. Department of Energy, Office of Nuclear Energy, Science, and Technology. *Report to Congress on Advanced Fuel Cycle Initiative: The Future Path for Advanced Spent Fuel Treatment and Transmutation Research*. January 2003.
2. G. Cote, Hydrometallurgy of strategic metals, *Solvent Extr. Ion Exch.*, (2000), **18**, 703-727
3. G. Wulff, A. Sarhan, *Angew. Chem. Int. Ed. Eng.*, 1972, **11**, 341 ; R. Arshady, K. Mosbach, *Makromol. Chem.*, 1981, **182**, 687-692
4. a) A. Sarhan, G. Wulff, *Makromol. Chem.*, 1982, **183**, 85-92 ; b) G. Wulff, J. Haarer, *Makromol. Chem.*, 1991, **192**, 1329-1338
5. M. Kempe, K. Mosbach, *J. Chromatogr. A*, 1995, **694**, 3-13
6. a) B. Sellergren, M. Lepistö, K. Mosbach, *J. Am. Chem. Soc.*, 1988, **110**, 5853-5860 ; b) D. Spivak, M.A. Gilmore, K.J. Shea, *J. Am. Chem. Soc.*, 1997, **119**, 4388-4393
7. K. Uezu, M. Yoshida, M. Goto, S. Furusaki, *Chemtech*, 1999, 12-18
8. Saunders, G., Foxon, S., Walton, P., Joyce, M., and Port, S.: A Selective Uranium Extraction Agent Prepared by Polymer Imprinting. *Chem Commun.* 2000, **4**, 273-274.
9. Kazuba, J.P., Runde, W.H.: The Aqueous Geochemistry of Neptunium: Dynamic Control of Soluble Concentrations with Applications to Nuclear Waste Disposal. *Env. Sci. Tech.* 33, 4427-4433 (1999)
10. Draye, M.; Czerwinski, K. R.; Favre-Reguillon, A.; Foos, J.; Guy, A.; Lemaire, M. *Separation Science and Technology*, 35(8), 1117-1132 (2000).
11. http://www.chem.ubc.ca/courseware/233/5-5_pka.pdf
12. <http://www.chem.ucalgary.ca/courses/351/Carey/Ch19/ch19-1.html>
13. Laidler, J.J. *J. Nucl. Mat. Mgmt.*, 2002, 36-38.
14. Aoki, S. *Progress in Nucl. Energy*, 2002, 343-348.
15. Mukaiyama, T., Takano, H., Ogawa, T., Takizuka, T., and Mizumoto, M. *Progress in Nucl. Energy*, 2002, 403-413.
16. Hoffman, Darleane. *Advances in Plutonium Chemistry, 1967-2000*. American Nuclear Society: 2002.
17. Choppin, G.R. *Chem. Sep. Tech. And Related Meth. Of Nucl. Waste Mang.*, 1999, 1-16.
18. Benedict, M., Pigford, T., and Levi, H.W.: *Nuclear Chemical Engineering*, Second edition. McGraw-Hill: 1981.
19. Manthur, J.N., Murali, M.S, and Nash, K.L. *Solv. Extr. Ion Exch.*, 2001, 357-390.
20. Selvaduray, G., Goldstein, M.K., and Anderson, R.N. *Reprocessing and Recycling*, 1978, 35-40.

IV. Background

The information in this section is background information which should make the project, in terms of direction and approach, easier to grasp for those not in actinide chemistry or separations. Other historical aspects, such as past actinide separation schemes are included in chapter 3. Basic chemistry and technique information is included in this chapter.

4.1 Physico-Chemical Properties of the Actinides and Lanthanides

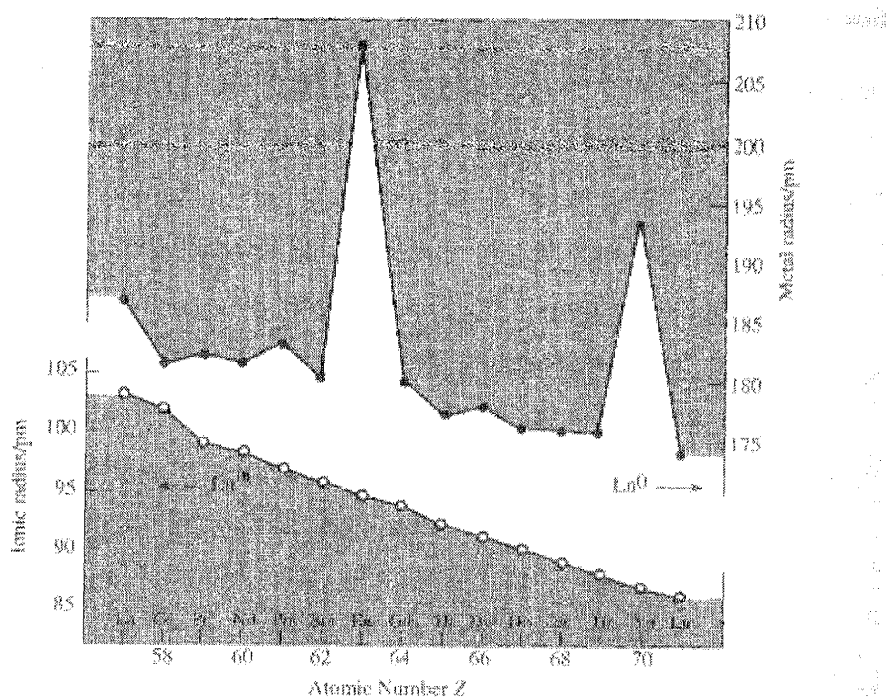
The lanthanides and actinides have some of the most complex chemical properties, due to their multiple oxidation states and the unique presence of partially filled *f* orbitals. This section will give some very basic background information on the lanthanides and actinides, since their properties are so integral to their chemistry and the work in this thesis.

4.1.1 The Lanthanides

The lanthanide series contains the elements $_{57}\text{La}$ to $_{71}\text{Lu}$, 14 elements in all; the lanthanide series is located at the bottom of the periodic table as the top row of the island below the main table [1]. The chemistry of the lanthanides, Ln, is so similar that they were mistakenly thought of as pure when mixtures were present. The number of elements in the Ln series was not conclusively determined until 1913, when H.G.J. Moseley's work on atomic numbers came to the conclusion; before that point hundreds of claims were put in for the discovery of new Ln elements [2].

The electronic configurations of the Ln elements are generally understood to be: $[\text{Xe}]4f^n5d^06s^2$, with the exception of Ce (the 5d orbital is occupied), Gd (stability due to a half-filled 4f), and Lu (the 4f shell is filled) [2]. This complexity in the electronic shell configuration only seems to effect the solution chemistry of Ce, as the other Ln elements mainly exhibit the trivalent state in solution. Another interesting aspect of the Ln elements is known as the "lanthanide contraction," in which the ionic radii of Ce to Lu steadily decrease, seen below in Figure 4.1 [2].

Figure 4.1: Elemental and +3 ionic radii for lanthanide series [2].



The lanthanide contraction becomes very important from a solution chemistry standpoint. The size reduction of the radii across the Ln series makes separation possible, but the small difference in size (and identical charge) makes it extremely difficult. Near Ho the contraction becomes so pronounced that radii are comparable with those of Y (a much lighter element) [2]. This explains the initial confusion as to the identification of what would become the Ln elements, as well as mistaken purities of samples.

The Ln mainly exhibit the trivalent state in solution, with radii so large that any bonding is generally ionic in nature, with a preference for hard-sphere donors [2]. Coordination chemistry tends to be more complex than that of the d-elements and complexes tend to involve high coordination numbers, often with ill-defined stereochemistries [2]. Due to these properties, it is often easiest and most effective to remove Ln from solution with chelating ligands [2]. Lower coordination numbers can only be achieved with very large ligands, and even then the lowest value is 6 (very uncommon). Ln coordination numbers are generally 7, 8, or 9 [2].

As mentioned previously, the most common oxidation state of the Ln is the trivalent state, but a few other oxidation states are possible in solution. Ce(IV) is well-known to exist in solution and is often used as a homolog for Pu(IV); Ce(IV) is also a strong

oxidant. Due to inherent electronic stabilities, Eu(II) can also exist in aqueous solution, however it is a strong reducer. These are really the only possible oxidation states in solution, thus restricting the aqueous redox chemistry of Ln.

4.1.2 The Actinides

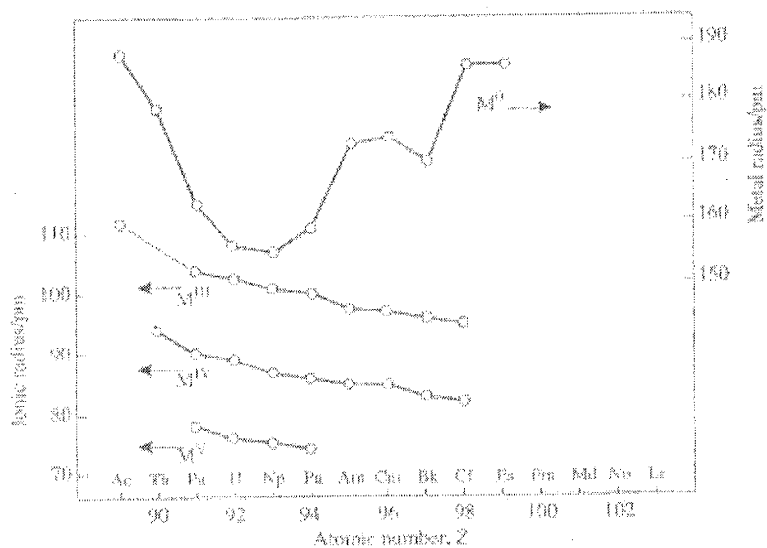
The actinide series encompasses the group of 14 elements from $_{89}\text{Ac}$ to $_{103}\text{Lr}$ and can be found on the periodic table located at the very bottom of it all [1]. They are analogous to the Ln in the sense that they begin filling the 5f orbital, where the Ln begin filling the 4f orbital. Before 1940, only the naturally occurring actinides, An, had been discovered (Th, Pa, U); the remaining An are all artificially produced. Thus, the first notable property of the An is their radioactivity. The level of radioactivity increases with increasing atomic mass, which is easily seen in that the only naturally occurring An are the lightest elements in the series.

The concept of “bulk” properties is not applicable to all of the An, as they are often only present in very small amounts synthesized in various nuclear reactions. Other problems with determining the chemistry of the actinides include their (often) high levels of radioactivity and very limited availability (due to the methods of production and imbedded difficulties in the separation from other An or Ln). Even when sufficient quantities of the elements can be obtained for chemical analysis, decays products can build up fast enough to interfere with experiments.

The solid properties of the An elements is complex, with all elements except for Cf having more than one crystalline form and Pu having six [2]. Solution chemistry of the An is also complex, with most of the An elements having more than one oxidation state. The stability of the oxidation states increases from +3 to +6. It has been conclusively shown that an “actinide contraction” also exists and is very similar to the Ln contraction [2].

The An contraction characterizes the steady decrease in ionic radius of a given oxidation state across the An series as atomic number increases. The An contraction is very similar to the Ln contraction, especially with respect to the trivalent state [2]. This trend can be observed on Figure 4.2 included below:

Figure 4.2: Actinide radii for elemental, +3, +4, and +5 [2].



Detailed chemical knowledge of the An is generally restricted to Th, U, and Pu, due to their extensive use in civilian and military industries. The radioactive nature of the An is both a blessing and a curse, from a chemical standpoint. High levels of radioactivity (generally manifested as a half-life of less than 20 years) cause instabilities in oxidation states in solution (and in extreme cases can also degrade ligands present in solution). The radioactivity of certain isotopes can also be used advantageously as tracers, so that only small amounts of highly radioactive sources are used to easily detect other isotopes of the same element with much lower levels of radioactivity.

The An can exhibit many different oxidation states in solution, with the most stable oxidation state decreasing as atomic number increases. The potential oxidation states are shown below in Table 4.1, with the most stable oxidation states shown in bold.

Table 4.1: Oxidation states of An elements [3].

Species present in H ₂ O	Th	Pa	U	Np	Pu	Am	Cm	Bk	Cf	Es	Fm	Md	No	Lr
M ²⁺	-	-	-	-	-	(2)	-	-	(2)	(2)	2	2	2	-
M ³⁺	3	(3)	3	3	3	3	3	3	3	3	3	3	3	3
M ⁴⁺	4	4	4	4	4	4	4	4	(4)	-	-	-	-	-
MO ₂ ⁺	-	5	5	5	5	5	-	-	-	-	-	-	-	-
MO ₂ ²⁺	-	-	6	6	6	6	-	-	-	-	-	-	-	-
MO ₅ ³⁻	-	-	-	7	7	-	-	-	-	-	-	-	-	-

Thus, the chemistry of An is very complex and varies throughout the series; many of the An are also very similar chemically to the Ln, particularly Am and Cm, both important for potential tiered nuclear fuel cycles.

4.2 The Origin of Actinide/Lanthanide Separations

Actinide/lanthanide inter- and intra-group separations are among the most difficult chemical separations, and may become necessary in future fuel cycles. Chemical separation techniques have been key to the nuclear since its dawn. Separations were required in order to manufacture both weapons and fuel, for both military and civilian enterprises. Since the lanthanides are fission products and Pu for weapons use is produced in nuclear reactors, the Pu is produced side-by-side with lanthanides.

Some lanthanides have high neutron absorption cross-sections, thereby making them nuclear reaction “poisons,” and their removal necessary to retain the integrity of the reaction. Given that future fuel cycles propose making use of transmutation techniques, which utilize a neutron source in order to lower the overall radioactivity of waste and/or produce power, there is a definite need for fast, efficient actinide/lanthanide separations.

Past fuel cycles or military uses mainly focused on the partitioning of U and Pu. Their separation from the lanthanides is easily achieved by exploiting the extractability of the higher oxidation states of these particular actinides. Future fuel cycles will also require the partitioning of Am and Cm, which are trivalent actinides and therefore chemical homologs for the trivalent lanthanides. Am and Cm will need to be separated from the

trivalent lanthanides in order to produce targets or blanket fuel pins which are free of neutron poisons such as Gd [4].

4.3 The Inherent Difficulties in Actinide/Lanthanide Separations

Due to the chemical properties of the actinides and lanthanides, as detailed in section 4.1, the chemistry of the trivalent An and Ln is extremely similar. Thus, since they have both the same charge (+3) and very similar ionic radii, standard separation schemes, normally based on charge or significant size differences, are not useful for An/Ln separations. With respect to successful separations, ion exchange and solvent extraction have proven most useful for these difficult separations [4].

4.4 Principles of Molecular and Ion Imprinting

The concept of molecular imprinting is, on the surface, a very simple idea: first the template metal (or target molecule, depending on the application—see section 4.5) is bound by a functional group, second the target complex is cross-linked to a backbone, and lastly, following the end of the synthesis, the target ion or molecular is removed from the matrix [5, 6]. After removal of the template molecule or ion, a cavity remains behind which has a specific size and shape based on the original target material. This cavity provides for superior recognition based on spatial features and bonding preferences, so that the target can be successfully and efficiently separated from a mixture or chemical species [7]. This can be seen below in Figure 4.3.

Figure 4.3: Schematic representation of the molecular imprinting technique [7].

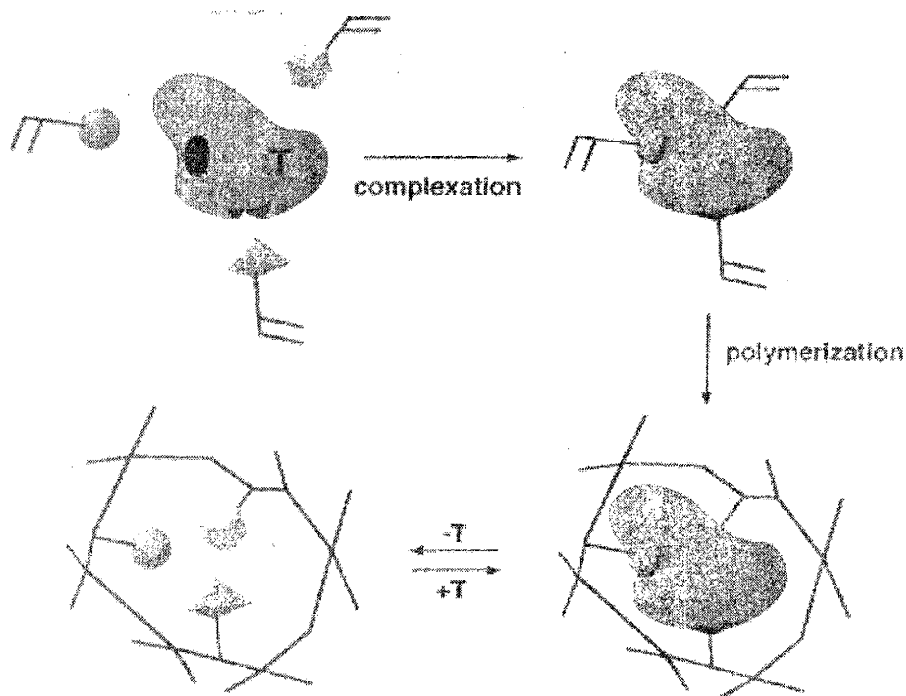


Figure 4.3 Schematic representation of the molecular imprinting technique

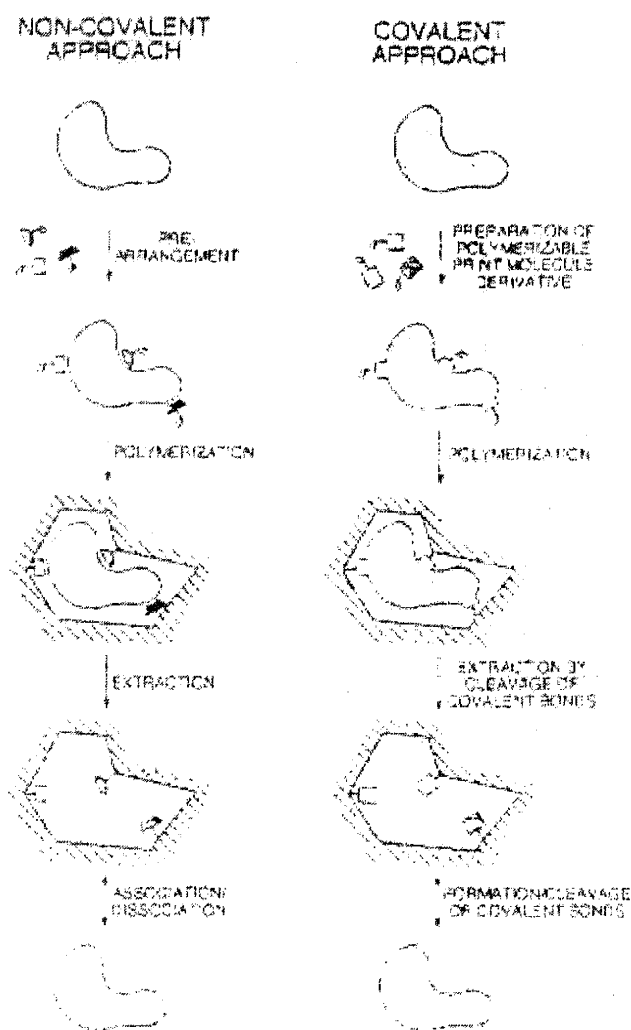
The molecular imprinting technique was originally developed for use with large molecules and molecular ions, so the practice is well established for those uses, however the application to metal ions has been much more recent and the research is not as robust in that particular application, but is being developed rapidly [8]. Molecular imprinting has been applied to the reaction of recognition sites for small organic molecules, inorganic ions, and even biological molecules, including application to the separation of optical isomers [7]. The most important features of the imprinted polymers are that the shape and stability of the complex are directly dependant on the metal ion (or original starting molecule) [9].

When Linus Pauling postulated a mechanism for the formation of antibodies in the 1940s, the concept of molecular imprinting was born [10]. Most current interest was spurred by the Wulff and Sarhan paper published in 1972, which deals with artificial antibodies [11]. This builds an interesting bridge of knowledge and synthetic techniques between biochemistry and organic chemistry. Work in the area of molecular imprinting was broadened with the entries of Mosbach, et. al., as they introduced the second type of

molecular imprinting: non-covalent bonding; previous approaches had utilized covalent bonding interactions [12].

The former approach, known as the non-covalent method, the synthesis relies on hydrogen bonding, electrostatic interactions, and metal ion coordination [7]. The quality of the artificial binding site improves with the number of non-covalent types of bonding present; due to the nature of these types of interactions, they are generally enhanced when the reaction is run in highly polar solvents, such as chloroform or toluene [8]. One of the most common ligands used in this process is methacrylic acid; since non-covalent interactions are, by definition weak, at least a four-fold excess of the ligand should be used [7, 13]. This large excess of ligand may result in the formation of binding sites with a large variation in affinities [7]. Once successful non-covalent bonding has been established between the ligand and target (usually peptides, nucleotides, saccharides, drugs, herbicides, or inorganic ions), a polymerization reaction is initiated and the polymer matrix is formed around the template species [10]. Once the polymer has been formed, the template molecule or ion can be largely removed under relatively mild conditions, and the polymer is then able to re-bind its target at complementary sites [10]. The polymerization step involves the addition of a cross-linking agent, which can effect the affinity of the final product; one of the most common cross-linking agents is ethyleneglycol dimethacrylate [7]. A schematic diagramming the non-covalent vs. the covalent approach is included below.

Figure 4.4: Schematic of non-covalent vs. covalent approaches of molecular/ion imprinting techniques [10].



The latter, or covalent, types of polymers generally consist of a template-monomer complex that is formed by reversible covalent bonding, which is then incorporated into the polymer matrix during a polymerization process [7]. The most common types of bonding are formed with either esters of carboxylic/boronic acids, ketals, or imines (Schiff bases) [10]. The problem with the covalent bonding type of molecular imprinting is that it is not very flexible in terms of the ligand functionality and template species, thereby reducing the versatility of the approach because of the constraints applied to the synthetic route and the number of potential template targets [7, 10]. The advantages of the covalent bonding technique are that the polymer products tend to be more easily analyzed, the template metal is easily removed via acid catalysis, and the template metal

can be rebound by exposing the solid, insoluble polymer to an aqueous solution containing the target molecule [7, 10].

Amongst the covalent types of polymers utilizing the molecular imprinting method, there is yet another division in the methodologies applied in the synthetic process. The first method is a cross-linking of linear chain polymers carrying metal-binding groups with bifunctional reagent reacted in the presence of metal ions [5]. The second method is a preparation of metal ion-complexing monomers that are polymerized with matrix-forming monomers in the presence of a metal ion [5]. Both of these methods have some inherent common problems: grinding and sieving is necessary before use; grinding causes partial destruction of the imprinted binding sites; some residual metal ions may remain in the polymer product; and there are major difficulties in handling water-soluble biologically important organic molecules as template targets [5]. Thus, in an effort to resolve these issues, a third method was developed. The third method is known as surface imprinting, and can be carried out with an aqueous-organic interface and is mainly used for biological applications [5].

4.5 Applications and Advantages of Molecular and Ion Imprinting

Molecular and ion imprinted polymers have been used in a variety of analytical applications. As the applications are so numerous and widespread, a number will be discussed in detail, with a table at the end of the section summarizing a number of uses and applications. Following the discussion of the applications of molecular and ion imprinting, some information will be included concerning the advantages of molecular and ion imprinted products.

Imprinted polymers can be used for the chromatographic separations of molecular species. This mainly involves the use of a molecular-imprinted polymer in a stationary phase that is used in high performance liquid chromatography (HPLC) [7]. Similarly, imprinted polymers can also be used for the selective sorption of molecular or ionic species. Tests have mainly been concerned with solid-liquid batch-type sorption experiments with molecular or ion imprinted polymer products, as appropriate [7, 8].

Imprinted polymer membranes have also been manufactured for the selective transport of molecular species. This application is still in the developmental stages, but provides a means for the selective permeation of chemical species through a membrane [7].

Imprinted polymers have also been used in ion selective electrodes, and have been shown to possess high affinities for their target ions, such as uranyl ions [7, 8]. Sensors involving templated polymers have also been produced, largely for detecting molecules such as glucose, but can also be applied to optical sensors and sensors are being developed for the nerve gas sarin [7].

Other uses of molecular or ion imprinted polymers include artificial antibodies in drug and pesticide analysis, as well as for use as artificial enzymes. Further uses are shown below in Table 4.2.

Table 4.2: Molecularly imprinted polymers and their potential areas of applications [10].

Class	Compound	Approach	Application
Drugs	Timolol	Non-covalent	Chiral separation
	Theophylline	Non-covalent	immunoassay
	diazepam	Non-covalent	immunoassay
	morphine	Non-covalent	immunoassay
	naproxen	Non-covalent	Chiral separation
	ephedrine	Non-covalent	Chiral separation
	pentamidine	Non-covalent	separation
hormones	enkephalin	Non-covalent	immunoassay
pesticides	atrazine	Non-covalent	Immunoassay/ separation
proteins	transferrin	covalent	separation
	RNase A	Non-covalent	separation
	urease	Non-covalent	separation
Amino acids	Amino acid derivatives	Non-covalent	Chiral separation
	Dansyl-Phe-OH	Non-covalent	sensor
Peptides	Ac-Trp-Phe-OMe	Non-covalent	Chiral separation
	Phe-Gly-anilide	Non-covalent	Chiral separation
	Boc-Phe-Gly-OEt	Non-covalent	Chiral separation
	Cbz-Ala-Ala-OMe	Non-covalent	Chiral separation
	Cbz-Ala-Gly-Phe-OMe	Non-covalent	Chiral separation
Carbohydrates	Galactose-derivatives	Non-covalent	Separation, separation/immunoassay
		covalent	Chiral separation
	Glucose-derivatives	Non-covalent	Separation/immunoassay
	Fucose-derivatives	Non-covalent	Separation/immunoassay
	Fructose-derivatives	covalent	Chiral separation
	Mannose-derivatives	covalent	Chiral separation
Co-enzymes	Pyridoxyl-derivative	Non-covalent	catalysis
Nucleotides	NAD ⁺	covalent	separation
Nucleotide	9-ethyladenine	Non-covalent	separation

bases			
Steroids	Steroid ketones cholesterol	covalent covalent	Directed synthesis separation
Miscellaneous	Bis-imidazoles	Metal coordination	separation
	diaminoanthraquinone	Non-covalent	separation
	Mandelic acid	Non-covalent covalent	Chiral separation Chiral separation
	Phenyl succinic acid	Non-covalent	Chiral separation
Dyes	Safranin O	Non-covalent	separation
	Rhodanile blue	Non-covalent	separation
		Metal coordination	sensor
Metal ions	Ca ²⁺	Metal coordination	sensor
	Cu ²⁺	Metal coordination	separation

There are many advantages to using molecular or ion imprinted polymers, which are summarized below in X. Essentially, the materials are robust and are highly selective for their target molecules or ions.

Table 4.2: Some characteristics of molecular or ion imprinted polymers [10].

Feature	Characteristics
Physical stability	Resistant against mechanical stress, high pressures and elevated temperature
Chemical stability	Resistant against acids, bases, various organic solvents and metal ions
Storage endurance	>8 months without loss of performance
Capacity	0.1-1 mg imprint molecule/g polymer
Imprint memory	Repeated use >100 times without reduction
Recovery yield	>99%
Binding strength	mM range (determined by chromatography)
	mM range (determined by radioligand assay)

4.6 References for Section IV

1. Overview of the Actinide and lanthanide (the f) elements by G. Seaborg, *Radiochemica Acta* 61, 115-122 (1993).
2. Greenwood, N.N., and Earnshaw, A. *Chemistry of the Elements*. Butterworth Heinemann: Woburn, 1997.
3. Seaborg, G.T., and Loveland, W.D. *The Elements Beyond Uranium*. John Wiley & Sons: New York, 1990.
4. Nash, K.L. *Solvent Extr. and Ion Exch.*, 1993, 729-768.
5. Tsukagoshi, K., Murata, M., and Maeda, M. *Techniques and Instrumentation in Analytical Chemistry*, 2001, p. 245-269.
6. Fish, Richard H. "Metal Ion Templated Polymers" from *Molecular and Ionic Recognition with Imprinted Polymers*, Bartsch, R.A. and Maeda, M., ed. Published by the American Chemical Society: Washington, D.C., 1998, p. 238-250.
7. Bartsch, R.A. and Maeda, M. "Molecular and Ionic Recognition with Imprinted Polymers: A Brief Overview" from *Molecular and Ionic Recognition with Imprinted Polymers*, Bartsch, R.A. and Maeda, M., ed. Published by the American Chemical Society: Washington, D.C., 1998, p. 1-8.
8. Zeng, X., Bzhelyansky, A., Bae, S.Y., Jenkins, A.L., and Murray, G.M. "Templated Polymers for the Selective Sequestering and Sensing of Metal Ions" from *Molecular and Ionic Recognition with Imprinted Polymers*, Bartsch, R.A. and Maeda, M., ed. Published by the American Chemical Society: Washington, D.C., 1998, p. 218-237.
9. Nishide, H., Deguchi, J., and Tsuchida, E. *Chemistry Letters*, 1976, 169-174.
10. Mosbach, K., and Ramström, O. *Biotechnology*, 1996, 163-170.
11. Wulff, G. and Sarhan, A. *Angew. Chem., Int. Ed. Engl.*, 1972, 341.
12. Andersson, L., Sellergren, B., and Mosbach, K. *Tetrahedron Lett.*, 1984, 5211.
13. Kuchen, W., and Schram, J. *Angew. Chem. Int. Ed. Engl.*, 1988, 1695-1697.

Figure 5.2: Detail of basic ICP-AES configuration.

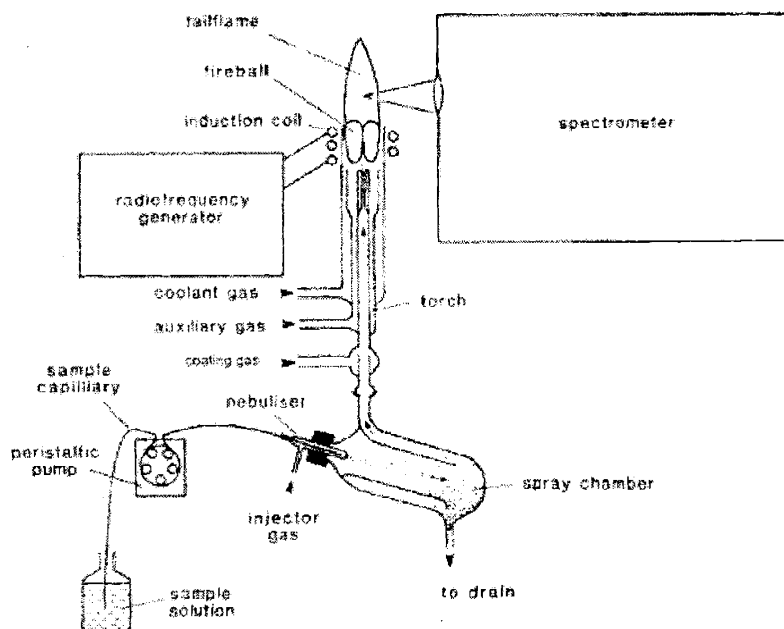
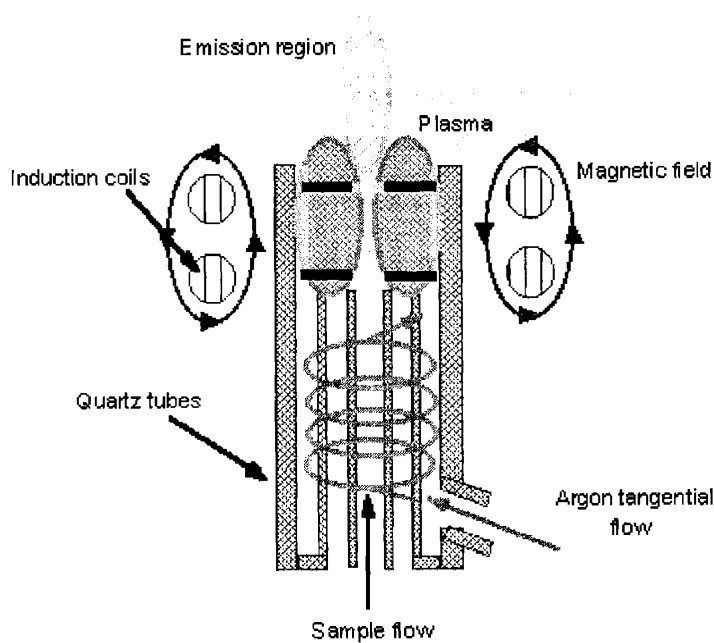


Figure 5.3: ICP-AES plasma torch operation.



This sample analysis technique cannot tell an absolute concentration due to uncertainties in the nebulizer efficiency, optical efficiency, and other aspects of the system. A relative concentration can be determined by calibrating the system each time with known standards in order to determine the concentration in the samples. Standard concentrations can range from the

V. Analytical Techniques

The analytical techniques to be discussed in this section are those that were used for sample analyses in this thesis. These include inductively coupled atomic emission spectroscopy (ICP-AES), inductively coupled mass spectrometry (ICP-MS), synchrotron techniques (as applied for XAS data collection and analysis), Fourier transform infrared spectroscopy (FTIR), and scintillation spectroscopy.

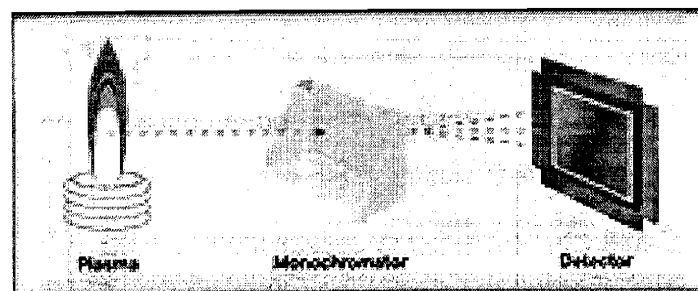
5.1 ICP-AES

Metal ion concentrations for the lanthanides, thorium, and uranium were determined via inductively coupled plasma atomic emission spectroscopy (ICP-AES). The principles behind this analytical technique as well as the sample preparation, standard preparation, and data analysis are described in this section.

5.1.1 Principles of ICP-AES

The principle behind ICP-AES is that a plasma is generated by an igniting device consisting of an oscillating electromagnetic field established by a high frequency coil wrapped around a quartz torch. The oscillating field causes argon atoms to collide, transferring energy to other argon atoms, which become ionized and cause further collisions. This process continues until the plasma reaches a steady state. Aqueous samples are introduced into the system via a peristaltic pump, which pumps the sample through a nebulizer. The nebulizer creates a fine aerosol mist. Particles that are small enough to be excited by the plasma are carried away by argon gas into the plasma. Once in the plasma, sample atoms collide with the rapidly moving plasma atoms and become excited. These excited atoms eventually relax to a lower energy state and emit characteristic photons. A spectrometer, set to measure a specific characteristic energy, measures the intensity of the emitted photons [1]. Figure 5.1 and Figure 5.2 show the basic arrangement of an ICP-AES. The operation of the plasma torch is depicted in Figure 5.3.

Figure 5.1: ICP-AES basic arrangement.



lower detection limit to just below the saturation point of the machine. A linear regression fit of the data from the standards is then used to determine the concentration of each unknown sample.

The best way to lower the detection limit of the system is to increase the efficiency of the nebulizer. A standard pneumatic nebulizer has an efficiency of around 1%-3%, while an ultrasonic nebulizer can have an efficiency as much as 15 times as high. In addition, samples should be slightly acidified in order to minimize sorption to the surface of tubes and glassware in the instrument, which can increase the background and therefore the detection limit of the machine.

5.1.2 Standard Preparation

The method of standard preparation and type of standard used for ICP-AES calibration can effect the quality of the data and is therefore very important. The most important aspect of standard preparation is to match the standard matrix to the sample matrix. This is to account for any interferences the matrix may cause with the optical line of interest. In order to account for any optical interference that sodium in the torch may cause, all standards were prepared in identical 2 vol% HNO₃ solutions. It is also important to create a large enough range of standards to cover the expected range of sample concentrations, so that a good calibration curve can be created in the correct region. This is especially important when determining concentrations near the detection limit of the instrument, since most curve fitting programs will preferentially weight the curve to the higher concentration data.

Initial analysis showed that sample concentrations ranged from below the detection limit of the instrument to approximately 10 µmol/L. Standards were prepared ranging from 0.1 µmol/L to 100 µmol/L by diluting Aldrich 970 µg/L (4.18 mmol/L) Th, U, or Sm atomic absorption standard solution, as appropriate, with 2 vol% HNO₃ to match the sample matrix. The standards were then diluted to 2 vol% HNO₃ using the appropriate amount of 15.56 M reagent grade nitric acid, also to match the sample matrix, as well as to limit sample plating in the poly lines and glassware. In addition, a 2 vol% HNO₃ standard was prepared in the same manner and used as a "matrix blank" in order to determine the background count rate of the instrument. This standard was chosen because it was well below the detection limit of the machine and consisted of the same matrix as the samples and the standards.

5.1.3 Procedure

The standard startup procedure for the Spectro Analytical Instruments Spectroflame ICP-AES was followed each time the instrument was used. A minimum warm-up time of 15 minutes was allowed while flushing the instrument with purified water at each startup. The sequential optics were then reprofiled in order to accommodate any changes in instrument operation parameters since the last use. Detection parameters for all elements were set up in the same manner, with the thorium case included here as an example for reference. Two thorium emission lines were available for use. The sample analysis method was set up to look at both lines simultaneously, but the 401.913 nm line was always preferentially used for data analysis due to its larger intensity and lower detection limit. The 283.730 nm line was mainly used to check that the ICP-AES was working properly. After reprofiling the optics, the location of the actual thorium peak was checked against the machine determined location using the strongest standard in order to assure that the optics were properly calibrated. The location of the thorium peaks did not move at any time.

The instrument was flushed with 5 vol% nitric acid after the peak location check in order to remove any lingering thorium from the system. The background was then checked against the initial background to ensure that the system was clean. All poly tubes were replaced periodically to ensure the data was not affected by thorium plating on the tubing. In addition, the spray chamber and torch were cleaned by soaking in a 5 vol% hydrochloric acid bath for several hours followed by a thorough rinsing in purified water every month.

Once the lines were sufficiently clean, the standards were run in order of increasing concentration to create a calibration curve. A matrix background was taken before the first (lowest concentration) standard. After the final (highest concentration) standard was analyzed, the system was again flushed with 5 vol% nitric acid until the background returned to the initial level. This was double checked by running another matrix background for comparison to the previous one. Samples were then run in order of lowest estimated concentration to highest. A two minute 5 vol% nitric flush was performed between each sample in order to limit plating. Nitric backgrounds were taken periodically for comparison. Every ten samples, a blank matrix background was taken to further ensure that sorption of metals, particularly thorium, to the instrument surfaces was not interfering with the data.

Following each ICP use, the instrument was shut down using the Spectro procedure. The instrument was flushed with purified water for a minimum of ten minutes before the torch was turned off. The system was then allowed to cool for another five to ten minutes and then turned off.

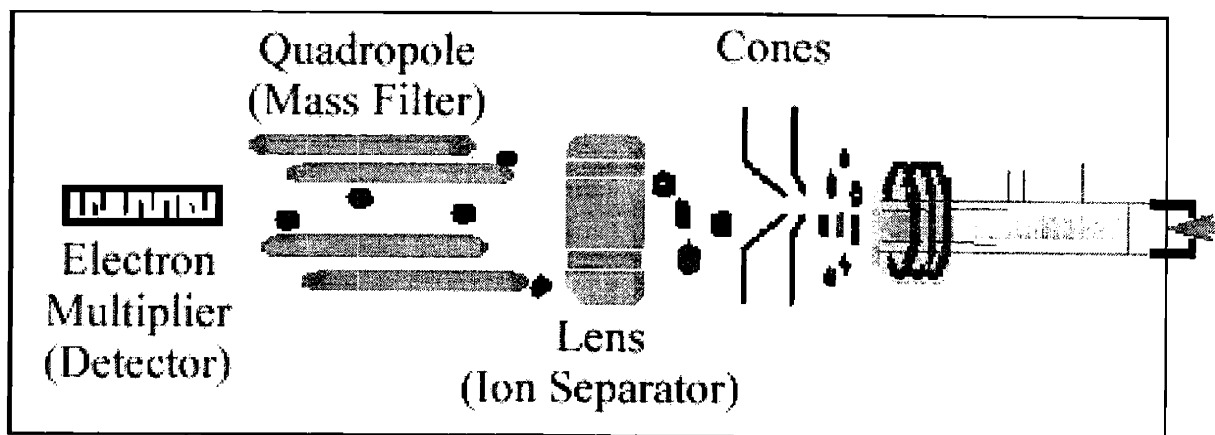
5.2 ICP-MS

Metal ion concentrations from the uranium and thorium resin competition experiments, as detailed in section VII, were analyzed via inductively coupled plasma mass spectrometry (ICP-MS). The change in analysis methods was made due the detection limits of the ICP-AES for some metals involved in the experiments.

5.2.1 Principles of ICP-MS

In plasma mass spectroscopy, the inductively coupled argon plasma (ICP) is once again used as an excitation source for the elements of interest. However, in contrast to ICP atomic emission spectroscopy, the plasma in ICP-MS is used to generate ions that are then introduced to the mass spectrometer and focused by a cone. These ions are then separated by the “a” lens (ion separator). The ions change trajectory when they enter the quadropole magnetic field (mass filter), and are collected according to their mass to charge ratios in electron multiplier cup detectors. The constituents of the unknown sample can then be identified and measured by the detectors. ICP-MS offers extremely high sensitivity for many elements and can also be successfully applied to a wide range of elements. **Figure 5.4** shows the basic components of an ICP-MS system. Detection limits of ICP-MS systems can be from one to four orders of magnitude lower or more than their ICP-AES counterparts.

Figure 5.4: Major components of an ICP-MS.



Like ICP-AES, the ICP-MS technique is used to determine relative concentrations. Known standards must be used to calibrate the ICP data and determine actual concentrations.

5.2.2 Sample Preparation

All samples were prepared for analysis by ICP-MS by filtering and then diluting the original sample with 2 vol% HNO₃ and the addition of an internal standard, in order to guard against detector drift and inaccuracies. All U samples contained 10 ppb Th as the internal standard, all Th samples contained 10 ppb U as the internal standard, and all samples containing both Th and U contained 10 ppb of ²⁰⁹Bi as the internal standard. A typical total sample volume was 5 mL after dilution.

5.2.3 Standard Preparation

Standards were prepared in 2 vol% HNO₃ with either Th or U at concentrations of 1 ppb (4.3 nmol/L), 5 ppb, 10 ppb, 50 ppb, 100 ppb, and 250 ppb (1.1 μmol/L). A blank sample was also created, which was a solution of 2 vol% HNO₃ in order to account for any background effects from the sample matrix. An initial calibration curve was created using the standards prior to running any samples. In addition, each standard solution was spiked with an internal standard to protect against detector drift. All Th standards contained 10 ppb of U; all U standards contained 10 ppb of Th, and all standards that contained both Th and U were spiked with 10 ppb of ²⁰⁹Bi. The blank solutions contained the same internal standard as the corresponding standard solutions for the experiment and/or data collection run in progress. All standard solutions and internal standards were diluted from PlasmaCal standard solution from SCP Science. Each solution contained 1000 μg/mL of Th, U, or Bi.

5.2.4 Procedure

The standard startup procedure for the ICP-MS was used every time it was used for data collection. The liquid argon tank was turned on and set at 80-90 psi; if the tank was not new, the pressure building knob was opened. Both water chillers were turned on 10 minutes before the plasma was lit, in order to ensure adequate cooling upon operation. The large chiller was set at 13°C and the small one at 0°C. Inside the ICP hood, the torch box coolant supply and return valves were turned completely on so that the coolant could reach the plasma. The ICP-MS was put into operate mode by clicking the appropriate button on the computer screen. The gasses then purged the nebulizer, the plasma lit, and the vacuum pump for the expansion chamber turned on to pump out the chamber and bring the machine into operate mode. This often needed

to be attempted more than once before it was successfully completed. After the plasma was successfully lit, the peristaltic pump was switched on.

The ICP was equilibrated for a minimum of 30 seconds in order to increase the stability of all measurements. At the end of this period, a tuning solution was run through the ICP in order to maximize the detection and sensitivity for the target metal of interest (this process was normally focused on U). The tuning process finely adjusts the position of the ICP torch box, which contains the plasma torch, in order to maximize sensitivity and minimize instabilities. Before the start of all data collection runs, a series of 10 quick measurements were taken from a tuning solution in order to check the stability and error of measurements. When the error was acceptably low (<2%), data collection was started; samples were run in sets of no more than 20 per run.

Samples were injected with the aid of a peristaltic pump at the rate of 1 mL/minute and manually changed. Between each sample, a wash of 2 vol% HNO₃ was run for 60 seconds between all samples and standards in order to clean out the sample lines and ensure that there was no cross-contamination of samples. Throughout the sample run, a standard of 10 ppb of appropriate elemental composition for the current experiment was run through as a check to guard against detector drift and inaccuracies. Each sample was counted three times and the error was taken as the variance between these measurements. Data analysis was done with Excel and Origin.

At the end of sample collection runs, the machine was switched into the “vacuum ready” state or, in very rare cases, off. The same procedures for start-up were run in reverse. When left in the vacuum ready state, the vacuum pump for the analyzer chamber remained on unless the machine was switched to the “off” state. Following the operational status change of the instrument, the peristaltic pump was turned off. The ICP hood was opened and the torch box coolant supply and return valves were turned off. The small water chiller and the argon tank (including the “pressure building” valve) were turned off. The temperature setting of the large chiller was increased in order to prevent condensation formation inside the ICP hood and torch box if the laboratory temperature was elevated.

5.3 Synchrotron Techniques

A synchrotron was used as a source of intense, high energy X-rays in order to probe the average local structure of some Sm-, Th-, and U-bearing samples. Extended X-ray absorption

fine structure (EXAFS) is an ideal method for probing the local structure of actinide and lanthanide bearing materials because of their high atomic masses. X-ray absorption near edge structure (XANES) is a non-destructive method for the confirmation of oxidation states of heavy metals within various matrices. Here, X-ray absorption spectroscopy (XAS), which includes both EXAFS and XANES, was used to confirm oxidation states, suspected structures of the resins, and to examine the binding of the metals to the resins.

5.3.1 Principles of Synchrotron Techniques

The analytical technique of Extended X-ray Absorption Fine Structure (EXAFS) is based on the variation of the absorption coefficient of an element as a function of X-ray photon energy that occurs after each absorption edge of an element and extends for up to 1500 eV further. Through careful analysis of the oscillating segment of the spectrum after the edge, information relating to the coordination environment of a central excited atom can be obtained.

EXAFS samples are commonly analyzed with the aid of a synchrotron and related radiation detection equipment. The synchrotron is used as a high intensity source of X-rays with a broad spectral range of energies. A sample picture of a typical synchrotron is included below as Figure 5.5. The X-ray energies are tunable and filterable such that a small, specific range of energies appropriate for analysis of the element of interest. In general, samples are arranged such that the X-rays initially pass through the sample of interest and then pass through a standard for reference. Detection equipment then records either the X-ray transmission or, in cases of low concentrations, the fluorescence. A sample diagram of a typical sample analysis setup is shown below in Figure 5.6.

Figure 5.5: Typical synchrotron setup.

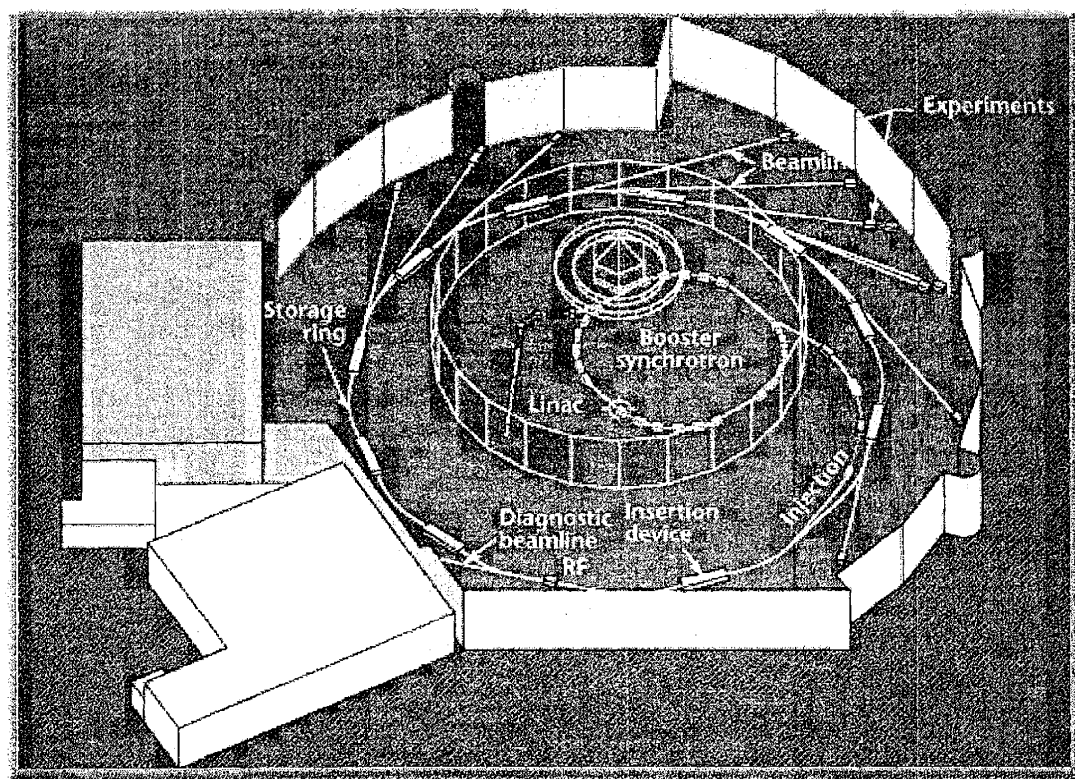
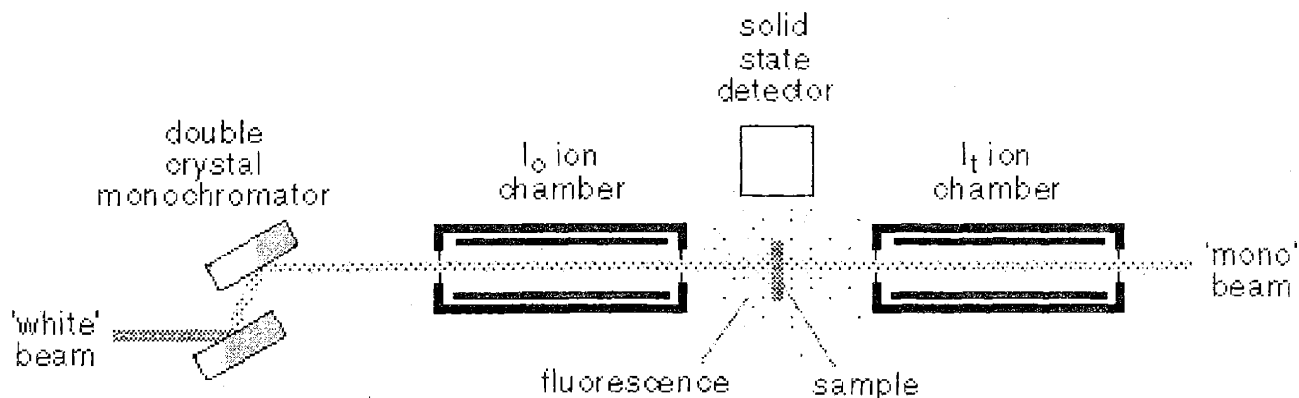


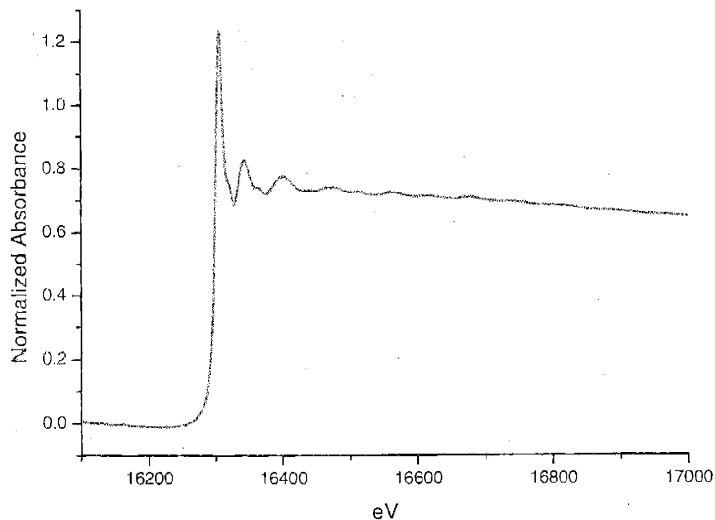
Figure 5.6: Typical EXAFS sample analysis setup.



X-rays can be absorbed by atoms in molecules. Generally, the proportion of X-rays absorbed (the absorption coefficient) will decrease as their energy increases, but at certain energies, specific to each element, a sudden increase in the amount of energy absorbed is observed. These energies are known as absorption edges. The energies correspond to the ejection of an electron from the atom (*i.e.* ionization). The increase in absorption at the edge occurs when the energy of the incident X-rays is equal to the threshold energy necessary to eject an electron. Spectra

containing only these edge jumps are known as X-ray absorption near edge spectra (XANES), a sample of which is shown below in Figure 5.7.

Figure 5.7: Sample XANES (“edge”) spectra.



Simple models of X-ray absorption predict a gradual monotonic decrease in the absorption coefficient with increasing energy away from the absorption edge. Such behavior is observed in spectra of isolated atoms, like noble gases, but for atoms either in a molecule or a condensed phase, the presence of other atoms around the absorber causes oscillations in the absorption coefficient near the edge. These oscillations in the post edge region arise from the back-scattering of the emitted electron wave off neighboring atoms and so the structure of the post edge region of the X-ray absorption spectrum is related to the radial distribution of atoms in the sample. Hence, by analyzing this spectrum (the frequency and amplitude of the oscillations), information about the local environment of the absorbing element can be derived [2]. A sample EXAFS spectra is included below as Figure 5.8 and Figure 5.9.

Figure 5.8: Sample k^3 weighted EXAFS oscillation spectrum.

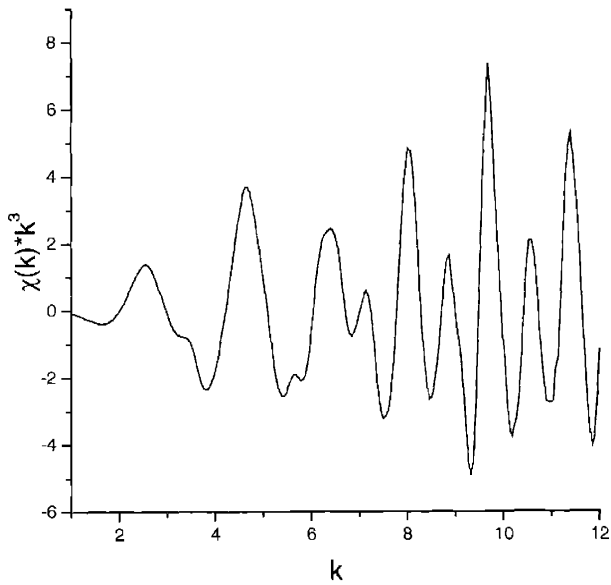
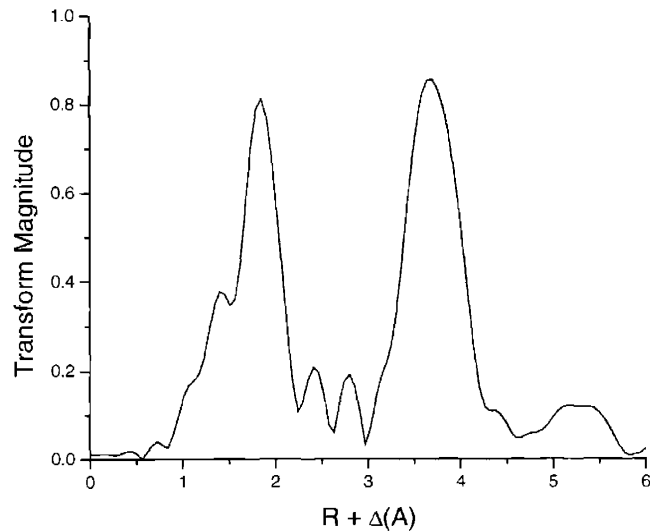


Figure 5.9: An example of a Fourier transformed EXAFS spectrum.



For the purposes of these analyses, both XANES and EXAFS spectra were recorded. The XANES spectra correspond to the region before (to the left of) the edge jump through the beginning of the EXAFS oscillations, which can be up to 40 eV about the edge. The absolute position of this edge in the XANES spectra corresponded to the oxidation state of the element of

interest, which can be confirmed by the presence of a standard. The XANES spectra also contained information on vacant orbitals, electron configuration, and site symmetry.

EXAFS spectra are taken from the region of data above, or to the right, of the edge jump. This region is produced by photoelectrons from the interaction of the X-rays with the metals of interest (hence the technique is not useful for elements with low atomic numbers). These back-scattering photoelectrons then effect the further interaction of the X-rays with the sample and these changes are detected. Information from the EXAFS spectra was used to determine the atomic number, distance, and coordination of the nearest neighbors.

5.3.2 Sample Preparation

Two kinds of resins were prepared, “non-released” resin and reabsorbed resin, for EXAFS analysis. Small samples of ion-imprinted resins were withheld from the template removal step and were prepared as “non-released” samples. For the “reabsorbed” samples, 0.05g of resin was shaken for 20 min. with the target metal (concentrations of 200 % of the PEC) in 4 M HNO₃. After filtration, the resin is washed with water and put in a 65°C oven until dry.

A 50mg sample of the metal bound resin complex was mixed with an appropriate amount of Bio-Beads and ground to a fine powder with a mortar and pestle. An aluminum window manufactured for our particular XAS setup was filled with the mixture, sealed with Kapton tape, triply contained in heat-sealed plastic bags, and was then ready for analysis.

5.3.3 Standard Preparation

Oxide standards of U(IV) and Th(IV) were available for use at the Stanford Synchrotron Radiation Laboratory. A Sm(III) oxide standard was prepared in the lab for use on the synchrotron beam line. To make the Sm(III) standard, 100 mL of NH₄OH was added to 30 g of oxalic acid dissolved in 200 mL of hot water. Next, 15 g of Sm(III) nitrate was dissolved in 100 mL of hot water, which was slightly acidified with nitric acid. The resulting precipitate was washed several times with water and acetone, then put in a 70°C oven until dry. The heat of the oven was then increased to 150°C for 12 h, and the solid was calcinated at 700°C for 1 h to produce the oxide reference.

A 50 mg sample of the oxide reference was mixed with an appropriate amount of Bio-Beads and ground to a fine powder with a mortar and pestle. An aluminum window manufactured for our particular XAS setup was filled with the mixture, sealed with Kapton tape, triply contained in heat-sealed plastic bags, and was then ready for analysis.

5.3.4 Procedure

EXAFS and XANES data for Sm(III) were collected at the Stanford Synchrotron Radiation Laboratory. One transmission spectra was taken for each sample due to time constraints. Samples were scanned on the Sm K-edge. Samples were scanned to $k=12$. A Sm metal standard was used to calibrate the Sm scans. The EXAFS analysis was performed using EXAFSPAK, Atoms, and FEFF. Phase and amplitude functions were calculated using FEFF.

5.4 Spectroscopy

Two spectroscopic techniques were used for sample analysis: Fourier transform infrared (FTIR) and liquid scintillation spectroscopy. The FTIR spectroscopy was used for analysis of some U- and non-templated resins, as well as some U-templated resins which were bound to U. Liquid scintillation spectroscopy was used for metal concentration analysis of both Np and Am due to their radioactive alpha emissions. Due to the small quantities of Np and Am used in experiments, as well as the inability to analyze them by traditional methods of solution concentration quantification, this was an ideal method.

5.4.1 FTIR Spectroscopy

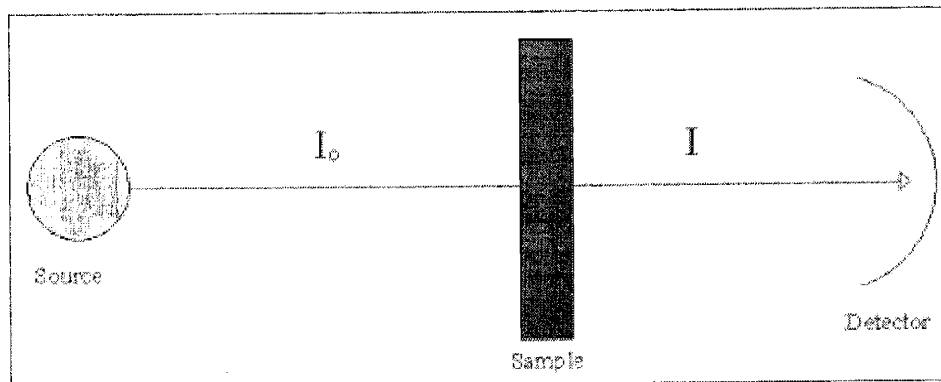
FTIR spectroscopy is a well-known and widely used technique for the qualification of organic samples. FTIR spectroscopy can be used to probe for the presence of various organic functional groups or to compare bound ligands with unbound ligands. In this case, FTIR spectroscopy was used to compare the following: unbound non-templated resin, unbound U-templated resin, and U-bound U-templated resin.

5.4.1.1 Principles of FTIR Spectroscopy

Since samples were analyzed via transmission FTIR spectroscopy for this work, only transmission FTIR will be discussed. This is the most simple and basic type of the infrared spectroscopic sampling techniques. Essentially, infrared radiation is passed through a sample and the transmitted radiation is measured. The spectra obtained are representative of the whole of the sampled area and localized properties can quite easily be lost in the bulk properties. It is generally only useful for thin ($<10 \mu\text{m}$) samples or when looking at weak bands, such as

overtone, in thicker samples. Often sample preparation such as the manufacture of KBr discs or Nujol (mineral oil) mull preparation is necessary which can be time consuming and difficult to reproduce. A very basic diagram of an IR spectroscopy setup is shown below in Figure 5.10.

Figure 5.10: Basic diagram of FTIR spectroscopy setup.



The IR transmittance is analyzed via the following equation:

$$T = \frac{I}{I_0} = \exp(-\alpha l)$$

where T is the transmittance, I is the transmitted intensity, I_0 is the initial intensity, α is the absorption coefficient, and l is the thickness of the sample. The incident light is produced by a source, the proper wavelengths are selected by a monochromator, and a slit selects the group of waves that actually passes through the sample. The light that is transmitted through the sample is detected and converted to electronic signals for analysis [3].

5.4.1.2 Sample Preparation

For analysis, 0.01 g of the appropriate resin sample was combined with 0.10 g of KBr and this mixture was thoroughly ground together with a mortar and pestle. This mixture was then added to a 13 mm die and pressed to form a pellet for analysis. Pellets were then placed in an appropriate sample holder and inserted into the FTIR spectrometer for analysis.

5.4.1.3 Standard Preparation

A standard, per se, was not used. Rather the library of data from the FTIR spectroscopy program was used in order to examine and analyze any peaks present. Since peaks are well-known and defined, no standards are necessary. However, a blank sample containing only KBr was also pressed in order to quantify the background levels of the detector. A sample containing only KBr and UNO_3 was also prepared, in order to calibrate the positions of any peaks due to U.

5.4.1.4 Procedure

First a background spectrum of the standard KBr only pellet was taken. Following this, a reference spectrum for U was taken from the KBr/ UNO_3 pellet. After this, sample pellets were sequentially analyzed and compared. Samples were analyzed for interesting peaks and the appropriate markers were added to the spectra printouts.

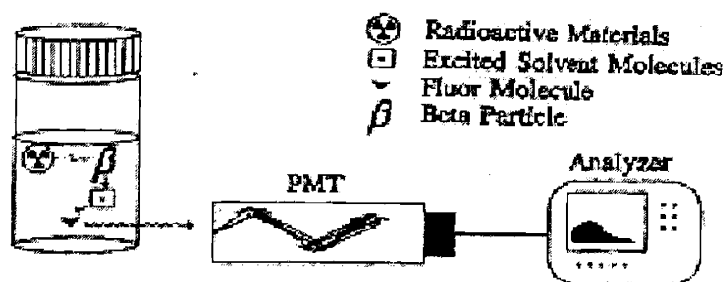
5.4.2 Alpha Scintillation Spectroscopy

The Packard Tri-Carb 2900TR scintillation counter used by the Actinide Research Group is able to distinguish and detect both α and β emissions. Due to this, it is an ideal analysis method for the detection and quantification of low quantities of radionuclides such as Np and Am.

5.4.2.1 Principles of Liquid Scintillation Spectroscopy

Liquid Scintillation Counting is based on the adding of a solvent to the radioactive material, forming a chemical medium capable of converting the kinetic energy of nuclear emissions into light energy. Figure 5. 11 provides a schematic illustration of the way the emitted radiation interacts with the solution leading to a count recorded by the system.

Figure 5. 11: Liquid scintillation counting.



The technique used in this study was Alpha Scintillation Spectroscopy. The radioactive material emits α particles in a radioactive decay. The kinetic energy of the particle is absorbed by the solution in heat, ionization and excitation. Some of the α energy is absorbed by solvent molecules making them excited. The excited solvent molecules can transfer energy to themselves, or to the solute, a fluor. When the excited orbital electrons of the solvent molecule return to the ground state, a radiation results, in this case a photon of UV light. The UV light is absorbed by solute molecules, fluor, which emit blue light flashes upon return to ground state. The total number of photons from the excited fluor molecules constitutes the scintillation.

The blue light flashes hit the photo cathode of the photo multiplier tube (PMT). The photons are transferred as electric energy and an output signal is obtained which is proportional to the total intensity of the scintillation. After being analyzed, the spectrum can provide information about the energy of the radiation or the amount of radioactive material in solution [4].

5.4.2.2 Sample Preparation

For analysis, experiment appropriate 100 μL samples were taken the original samples for analysis. These samples were added to scintillation vials and combined with 10 mL of Packard Ultima Gold AB scintillation fluid. These samples were then ready for analysis in the scintillation counter.

5.4.2.3 Standard Preparation

The scintillation counter was calibrated with a NIST –traceable standard.

5.4.2.4 Procedure

The apparatus used was a Packard Tri-Carb 2900TR scintillation counter. A calibration of the spectroscope with known concentrations was necessary. For the analysis, 100 μL samples were examined and counted in triplicate. The standard deviation of the three samples was used as the error.

5.5 References for Section V

1. Gill, Robin, *Modern Analytical Geochemistry*, Longman Singapore Publishers, LTD, Singapore, Indonesia 1997 pp. 41-60
2. <http://xray.chm.bris.ac.uk:8000/research/exafs.html>
3. <http://www.chem.orst.edu/ch361-464/ch362/irinstrs.htm>
4. <http://www.uwm.edu/Dept/EHSRM/RAD/HANDOUT.pdf>

VI. Phenolic Resin Syntheses

6.1 Introduction

Throughout the history of the nuclear industry, there has been both a need and a desire for effective solid-liquid extraction methods. Although the solid-liquid extraction methods have mainly been used on a bench-top or lab scale, their potential used on a larger scale has become particularly attractive. If made from only C, N, O, and H, resins are completely incinerable. Therefore, after they are spent, the resins can be burned in order to help reduce waste and lower the volume of radioactive waste that separations contribute to a potential repository.

Previous work in the area of resin synthesis for actinide/lanthanide separations has already been performed using phenolic-type resins, but the molecular imprinting technique had not yet been used [1]. Given other successes with molecular and ion imprinting techniques, this work seeks to incorporate the advantages of ion imprinting in order to create a more efficient resin [2]. Since there are many types of phenolic resins, maybe types were synthesized, including a chelating resin.

6.2 Background

Many resins have been created which make use of a phenol-type functional group to bind the metals of interest. These have included resorcinol, catechol, phenol, and 8-quinolinol as functional groups. Some of these resins have been modified to include soft donors in the backbone in order to create a higher binding affinity for the target An and Ln metals. None of these resins have been made with the application of an ion imprinting technique.

Given the harsh pH (basic) conditions of these types of resin syntheses, it may not be possible to keep the target ion in solution during resin production because of hydrolysis, which is required by the ion imprinting technique. Work undertaken in this section seeks to investigate the limits of synthetic conditions for phenolic resins and possible compatibility with ion imprinting techniques. Experiments were limited to syntheses of the resin products.

6.3 Experimental

This section includes the synthetic routes and protocols, as well as descriptions of all modifications made to those processes. All observations concerning the syntheses will be described in detail in section 6.4.

6.3.1 Materials

6.3.1.1 Chemicals and Reagents

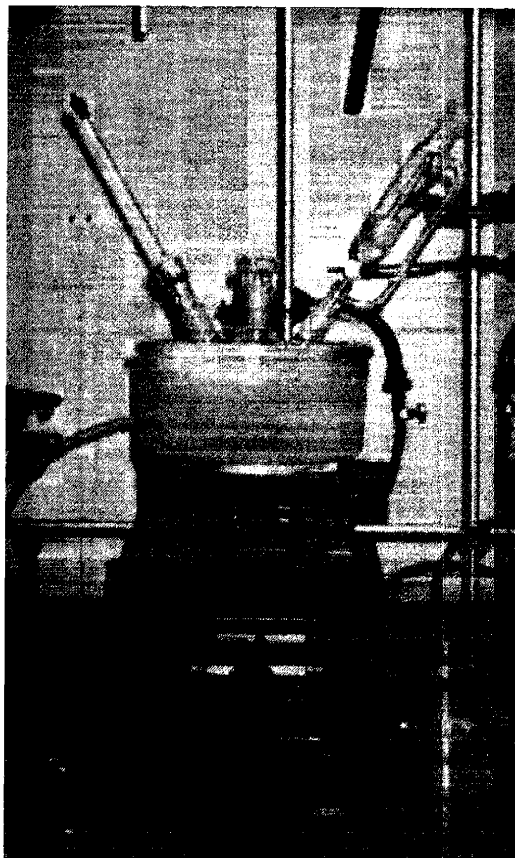
Formaldehyde, catechol, quinolinol, and phenol were obtained from Acros Organic and used without further purification. Resorcinol and iminodiacetic acid were obtained from Sigma-Aldrich and used without further purification.

6.3.2 Resin Syntheses

6.3.2.1 Resorcinol Resin

First 5.97 g (14.9 mmol) of NaOH pellets were dissolved in 75 mL of deionized water in a round-bottom three-neck flask. Next 11.01 g (100 mmol) of resorcinol ($C_6H_6O_2$) was added and the flask was packed with ice to cool to 0 °C. When the proper temperature was achieved, 19 mL (628.2 mmol) of formaldehyde (CH_2O) was slowly added while stirring. The solution was left to stir and react for 30 minutes, then transferred to an air oven at 100 °C in a beaker for curing for three days. After curing, the resin was then ground and used as a reference for other resorcinol-based resins. A typical setup for the phenolic type resin synthetic setups is included below as Figure 6.1.

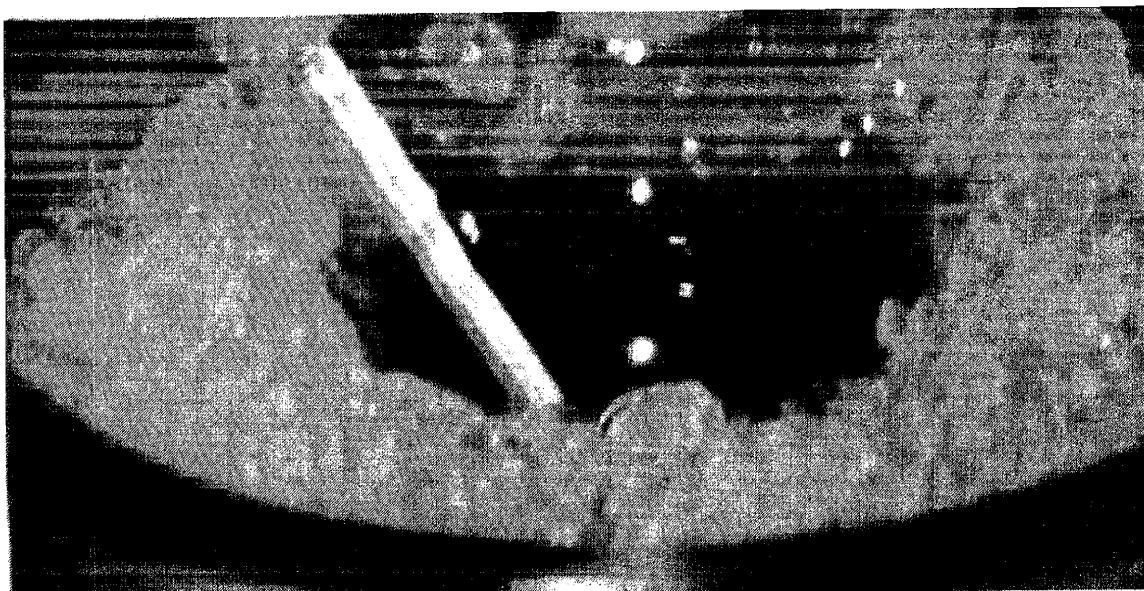
Figure 6.1: Basic setup for phenolic type resin synthesis.



6.3.2.2 Catechol Resin

Initially 5.96 g (14.9 mmol) of NaOH pellets were dissolved in 75 mL of deionized water in a round-bottom three-neck flask. Following this dissolution, 11.01 g (100 mmol) of catechol ($C_6H_6O_2$) was added; the vessel was then packed with ice. When the temperature reached 0 °C, 19 mL (628.2 mmol) of formaldehyde (CH_2O) was very slowly added while stirring in order to maintain the temperature. At the end of the addition, the mixture was left to react for 30 minutes while stirring. At this point, the solution was transferred to a beaker and placed in a 100 °C air oven for three days for curing. After curing was complete, the resin was cooled, ground, and thereafter used as a reference as a normal catechol-based resin sample. A photo of the catechol synthesis is included below as Figure 6.2 so that the deep olive green color can be observed.

Figure 6.2: Closeup of catechol synthesis after packing with ice and addition of all reagents.



6.3.2.3 Modifications to Catechol Synthesis

A second group of catechol syntheses were run; the batch was split into four groups for further experimentation. The initial batch of resin, before splitting, is detailed as follows: 30.02 g (750.5 mmol) of NaOH was combined with 375 mL of deionized water, then 55.05 g (500 mmol) catechol, and finally 100 mL (3.46 mol) of formaldehyde was added at 0 °C while stirring. This mixture was left stirring overnight.

After stirring overnight, the batch was split into four sections. One section was left untouched and had a normal pH of about 10. The second batch was adjusted to pH 1, the third was a small batch adjusted to pH 7, and the fourth was a large batch adjusted to pH 7. All of these samples were then transferred to a 100 °C air oven for heat curing for three days, followed by cooling and grinding.

6.3.2.4 8-Quinolinol Resin Synthesis

An initial solution containing 16.70 g (115 mmol) of 8-quinolinol (C_9H_7NO), 4.16 g (104 mmol) of NaOH, and 75 mL of deionized water. A 21.5 mL sample (288 mmol) of formaldehyde (CH_2O) was slowly added to this mixture, then allowed to stir for 1 hour. Next, 12.66 g (115 mmol) of resorcinol was dissolved in 17 mL of 6 M NaOH with 58 mL of deionized water, then added to the reaction vessel. Finally, 21.5 mL (288 mmol) of formaldehyde was very slowly added to the reaction vessel. A deep red gel slowly formed at room temperature. After 1 hour the mixture was split in half. One section was unmodified and

remained at a pH of about 9.5; the other half was adjusted to pH 7. The unmodified portion of the resin was then transferred to a 100 °C air oven for curing for three days.

6.3.2.5 Cross-linked Resorcinol Resin Synthesis

Reactants consisting of 13.3 g (100 mmol) of iminodiacetic acid ($C_4H_7NO_4$) and 13.47 g (122.3 mmol) of resorcinol ($C_6H_6O_2$) were combined with 75 mL of deionized water. A solution of 6 M NaOH was added until the reactants had dissolved, at about pH 7.5. This mixture was then split into two parts. The first, unmodified portion, was combined with 50 mL (1.73 mol) of formaldehyde and then transferred to a 100 °C air oven for curing for three days. The second portion was adjusted to pH 9, followed by the addition of 50 mL (1.73 mol) of formaldehyde and transferred to a 100 °C air oven for curing for 3 days. After curing, the resins were ground.

6.3.2.6 Phenol Resin Synthesis

To begin the reaction, 20 g (212.5 mmol) of phenol (C_6H_6O) was combined with a solution of 10.88 g (272 mmol) NaOH pellets and 136 mL of deionized water. Following dissolution, 40.5 mL (540 mmol) of formaldehyde was slowly added at 0 °C; the reaction was stirred for 4 hours at room temperature, the pH was adjusted to 7.5 with HCl, and then split into two batches. The first batch was unmodified and was directly transferred to a 100 °C air oven for curing for three days. The second batch was combined with 5.02 g (10 mmol) of $UO_2(NO_3)_2$ and then transferred to a 100 °C air oven for curing for three days. The resins were then ground.

6.3.2.7 Cross-linked Phenol Resin Synthesis

Reactants consisting of 20 g (210 mmol) of phenol, 2.80 g (21 mmol) of iminodiacetic acid, 1.8 g (45 mmol), and 22.5 mL of deionized water. The vessel was then packed with ice and 15 mL (200 mmol) of formaldehyde was added at 0 °C while stirring. This reaction was stirred at room temperature for 4 hours and then the pH was adjusted to 7.5, and then split into two portions. The first section was then transferred directly to a 100 °C air oven for curing for three days. The second portion was combined with 5.02 g (10 mmol) of $UO_2(NO_3)_2$ and transferred to a 100 °C oven for curing for three days.

6.4 Results and Discussion

The resorcinol resin, unmodified, yielded a pinkish-purplish powder, while the catechol resin, unmodified, yielded a dark, almost black powder. The results of the modifications to the catechol resin are as follows, and can also be seen in Table 6.1. The pH 1 resin, post-curing, was a single solid mass with a light-colored film over the normal dark mass. The small batch of

pH 7 resin was present in a number of pieces, but exhibited a similar film-type coating like that on the pH 1 sample. The larger pH 7 sample was a single mass, and while it did not contain a film, it did have a number light-colored portions that resembled barnacles. These “growths” were mainly present on the beaker, not on the resin. The pH 10 sample, which was left unmodified, was in a number of chunks and was dark colored and matte. These resins were then ground and sieved to a particle size of 200-800 μm .

Table 6.1: Summary of results for resorcinol and catechol resins.

Resin Type	Modification Status	Result
Resorcinol	None	Pinkish-purplish powder
Catechol	None	Nearly black powder
	pH 1	Single mass with film
	pH 7 (small batch)	Small pieces with film
	pH 7 (large batch)	Single mass with “barnacles”
	pH 10	Large chunks

The quinolinol resin was split into two parts, labeled A and B. Portion B was left unmodified and was observed, post-curing, as a number of pieces which was dark colored and shiny, almost like glass. Section A, pre-curing, was to be adjusted to a pH value of 7, but upon the addition of a few drops of acid, a yellow precipitate immediately formed no matter how dilute the added acid added. For this reason, the quinolinol A resin was discarded before curing. This seems to indicate that ion imprinting will not be possible, at least for this type of chelating resin. These resins were then ground and sieved to a particle size of 200-800 μm .

The cross-linked resorcinol resin had also been split into two portions, C and D. The first section, C, was left unmodified and was observed as a chunky, shiny deep red formation. The other, modified portion D, was very similar with an orange tinge; both sections looked very glass-like. At this point both C and D were ground. Sample C became a safety orange powder while D became a similar powder with a red tinge. Section C was then sieved to a 200-800 μm particle size and added to a solution of 1 M NaOH to test for cross-linking; C indeed was successfully cross-linked, as it did not dissolve in the solution. Section D was then sieved to a

200-800 μm particle size and then added to a 1 M NaOH solution; D did not dissolve either, indicating successful cross-linking.

All of the above resins, post-grinding and sieving, were then washed according to the following procedure. The resins were washed with water until run-off was clear, washed with 1 M HCl, washed with water until neutral, washed with 1 M NaOH, washed with water until neutral, washed with 1 M HCl, washed with water until neutral, washed with 1 M NaOH, and washed with water until neutral. After washing/conditioning as above, the resins were placed in a 100°C air oven to dry. IR spectra were attempted, but failed due to the hardness of the resins and the weakness of the mortar and pestles available in the lab. Although the resins could be ground with a coffee grinder to achieve powders, these powders could not be subsequently ground more finely with a mortar and pestle for use in IR pellets.

The phenolic resin, which had been split into parts E and F, in order to run an actual test of ion imprinting was removed from the curing oven. Part E was not imprinted or modified in any way and was observed as a number of cloudy white chunks. Part F was attempted as an ion imprinted resin and was observed as a number of deep red chunks, likely a successful ion imprinting foray, as evidenced by the color change, which indicates that the uranium has been incorporated into the reaction. The resins were then ground and sieved to a particle size of between 200 and 800 μm . Following grinding and sieving, the resins were then washed and conditioned. The same procedure was used as above on the non-imprinted resins, with the following modification: the first step for imprinted resins was to add 1 M HCl, let stand for 15 minutes, then filter off, in order to remove the uranium. Following the washing, the resins were placed in a 100 °C air oven for drying.

The phenolic cross-linked resin was also split into two portions, G and H, to test the feasibility of ion imprinting with cross-linking. Section G was left unmodified and unimprinted; upon removal from the curing oven, it was observed as transparent tan chunks. Portion H was attempted with ion imprinting and was observed as a deep red mass with yellow edges. In order to accomplish grinding and sieving, the beaker containing section H had to be broken to remove the resin. After the breakage, the resins were then ground and sieved to a particle size of 200-800 μm . These resins were then washed, conditioned, and dried in the same manner as the non-cross-linked phenolic resin.

Table 6.2: Summary of results for remainder of resin syntheses.

Resin Type	Modification Status	Result(s)
Quinolinol A	pH 7	(discarded before curing)
Quinolinol B	none	Dark shiny pieces
Cross-linked Resorcinol C	none	Deep red chunks; successful cross-linking
Cross-linked Resorcinol D	pH 9	Deep red chunks with orange tinge; successful cross-linking
Phenol E	none	Cloudy white chunks
Phenol F	Ion imprint attempt	Deep red chunks
Cross-linked Phenol G	none	Transparent tan chunks
Cross-linked Phenol H	Ion imprint attempt	Deep red mass with yellow film

6.5 Conclusions

This work has shown that ion imprinting is very difficult to accomplish on phenolic-based resins while maintaining the integrity of the resin. Due to the chemistry of uranium, or actinides in general, the syntheses require large pH modifications (from very basic to at least mildly acidic) in order to create an environment suitable for uranium, or actinide, dissolution. Since the ion imprinting technique requires that the target ion be present in solution while the resin is formed, this step is crucial to the successful production of an ion imprinted resin.

In general, the only potential success in this task was the production of a phenol imprinted resin, which is very limiting and may not be applicable with further modifications, such as adding soft donors to the back bone or adding chelators. Given these severe limitations, ion imprinting is not deemed to be a compatible technique with phenolic-type resin syntheses. Other types of resin syntheses could show more promise for this technique and are investigated throughout the remainder of this thesis, as well as by other researchers for use with other, lighter metals.

6.6 References for Section VI

1. Draye, M.; Favre-Reguillon, A.; Wruck, D.; Foos, J.; Guy, A.; Czerwinski, K. **Removal of ^{243}Am with phenol-based resins.** *Separation Science and Technology* (2001), 36(5 & 6), 899-909; Draye, M.; Czerwinski, K. R.; Favre-Reguillon, A.; Foos, J.; Guy, A.; Lemaire, M. **Selective separation of lanthanides with phenolic resins: extraction behavior and thermal stability.** *Separation Science and Technology* (2000), 35(8), 1117-1132.
2. Kuchen, W., and Schram, J. *Angew. Chem. Int. Ed. Engl.*, 1988, 1695-1697.

VII. Synthesis and Evaluation of Uranium and Thorium Imprinted Resins

Ion exchange resins with carboxylic acid functional groups were synthesized based on the templating method to complex either UO_2^{2+} or Th^{4+} from aqueous solutions. The nitrate salt of the target metal ion was dissolved in CH_2Cl_2 , while the resin was created around the ions to provide a unique structure based upon each metal. These resins were synthesized by a radical polymerization method, producing a reusable organic solid. The resins were qualified by obtaining values for their proton exchange capacities and data to define their complexation kinetics. Proton exchange capacities were determined using an indirect titration and were found to be 6.40 meq/g for the uranium-based resin and 4.61 meq/g for the thorium-based resin. Data for the resins' kinetics were obtained at pH 1.0, 2.5, 4.0, and 5.5. Results show that the templated resin rapidly removed the target actinides from aqueous solution under experimental conditions. Once loaded with metal, the ions can easily be removed with 5 M HNO_3 and reused. Competition experiments were also run with strontium, europium, thorium, and uranium at pH values of 1, 2, 3, 4, 5, and 6. Some EXAFS data is also included for uranium-resin complexes.

7.1 Introduction

Organic based ion selective resins have some similar attributes: ease of synthesis, high metal ion complexation ability, and flexibility for different nuclear waste management applications. For most chelating polymers, the ligand is deemed to be of primary importance for the interaction with the targeted metal ion. The role of the polymer matrix is usually ignored. The concept of molecular-imprinted polymers was developed more than 20 years ago [1] and shows a potential for applications in analytical chemistry [2-4]. The technique of molecular imprinting can be used for the production of selective ion exchange resins. Both simple organic compounds and polymers have been created using these methods in order to separate lanthanides [5] and actinides [6]. The more traditional simple organic compounds utilized functional groups such as phenols, resorcinol, and catechol. The problems with these previous resins include slow kinetics and difficulty with creating a molecularly imprinted product. This led to the investigation of templated resins with carboxylic functional groups.

A uranium selective polymer has yielded promising results and was used as the synthetic basis for the work described in this paper [6]. This paper examines the creation and qualification of a new polymer-based thorium selective resin and a similar uranium selective resin. The

separation of uranium from other metals has been used by the nuclear industry, mainly for fuel production and the handling of waste streams. Thorium is an important element in advanced nuclear fuels and therefore a desire to separate it from other metals was seen. In addition the synthesis of a Th selective resin can prove the methodology for template synthesis using higher valent metal ions.

With the success of the uranium-imprinted resin synthesis given below, a modified synthetic route was developed in order to create a thorium-imprinted resin. The final, successful process is also outlined below. The proton exchange capacity of the synthesized templated resins were determined. The interaction of U and Th with their respective templated resin as a first step towards competitive reactions was investigated.

7.2 Experimental

7.2.1 Materials

7.2.1.1 Chemicals and Reagents

Methacrylic acid, triethylamine, ethylene glycol dimethacrylate, and azobisisobutyronitrile (AIBN) were obtained from Aldrich and used without further purification. Dichloromethane, U(VI) nitrate, and Th(IV) nitrate were obtained from Alfa Aesar and used without further purification.

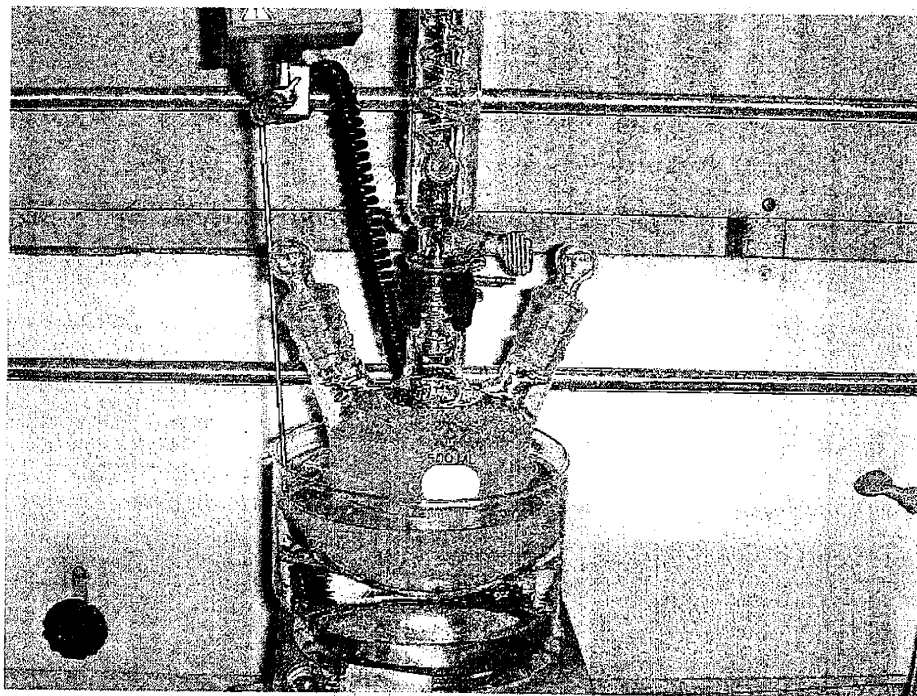
7.2.1.2 Uranium Resin Synthesis

A three-neck round-bottom flask was prepared for the synthesis by the addition of 450 mL of dichloromethane (CH_2Cl_2), a magnetic stir bar, reflux, stoppers, and placement in a room temperature oil bath. The reaction was set up by adding 1.36 g of methacrylic acid ($\text{C}_4\text{H}_6\text{O}_2$) to the dichloromethane, stirring to dissolve, and then adding 3.45 g of uranyl nitrate ($\text{UO}_2(\text{NO}_3)_2 \cdot 6\text{H}_2\text{O}$). In order to solvate the uranyl nitrate and minimize the presence of solids, tri-ethylamine ($\text{C}_6\text{H}_{15}\text{N}$) was added dropwise to the solution. A total of 4.5 mL of tri-ethylamine was added, forming a yellow solution indicative of uranyl. For comparison, an analogous random polymer can be produced by withholding the metal and tri-ethylamine.

A temperature-controlled oil bath was set to 40 °C to give some additional assistance with the dissolution of the uranium for of 2 hours; a picture of the reaction at this stage is included below as Figure 7.1. Following this, 11.72 g of ethylene glycol dimethacrylate ($\text{C}_{10}\text{H}_{14}\text{O}_4$) was added to this solution along with 1.36 g of Azo(bis)IsoButylNitrile (AIBN) ($\text{C}_8\text{H}_{12}\text{N}_4$). To initiate and

sustain the reaction, the oil bath temperature was increased to 60°C and was left to react overnight.

Figure 7.1: Uranyl resin synthesis before polymerization.



The polymer created in this synthetic process was obtained by evaporating the remaining dichloromethane with a Rotavap. The flask containing the product and solvent was cooled in an ice bath while the solvent was boiled under vacuum. Once the resin was dry, the solid was ground and sieved to a particle size between 63 and 125 μm . Next, a 5 M nitric acid solution was added to the yellow polymer and the mixture was sonicated for 15 minutes to unload the resin. Finally, the solution was filtered with 0.22 μm filters under vacuum, and washed with water until neutral. The solid that was obtained from the filter was transferred to a beaker. Ethanol was used to rinse the filter. The polymer-ethanol mixture was placed in a 60°C oven until thoroughly dry (1-2 days). The resin was then used in experiments.

7.2.1.3 Thorium Resin synthesis

The process used to produce a thorium-imprinted resin is similar to that described above to produce uranyl-imprinted resins. First 1.56 g of methacrylic acid is added to about 450 mL of dichloromethane, making a clear solution in a three-necked round-bottom flask with reflux. Next, the thorium used to create the molecular imprint was added in the form of 3.23 g of thorium nitrate ($\text{Th}(\text{NO}_3)_4 \cdot 4\text{H}_2\text{O}$). The methacrylic acid then complexes the thorium ions to form

the basis of the template, eventually becoming the resin functional groups. Tri-ethylamine was added dropwise to the above solution, until about 4.5 mL had been added via a syringe. This small amount is necessary to produce a soluble template complex for further reactions.

After replacing the stoppers in the necks of the flask, the entire solution was heated to 60 °C in a temperature-controlled oil bath while being stirred with a magnetic stir bar. Within approximately 10 minutes the thorium nitrate was completely dissolved, forming a clear solution. Lastly, 11.80 g of ethylene glycol dimethacrylate and 1.44 g of Azo(bis)IsoButylNitrile were added to the solution made above. The ethylene glycol dimethacrylate served as the cross-linking agent and the AIBN was used to thermally initiate the radical polymerization of the reaction. After these final additions, the flask was again sealed against the atmosphere and the temperature of the oil bath was increased to 80 °C and left to react overnight. A photograph of the thorium resin reaction at completion is included below as Figure 7.2.

Figure 7.2: Thorium resin at reaction completion.

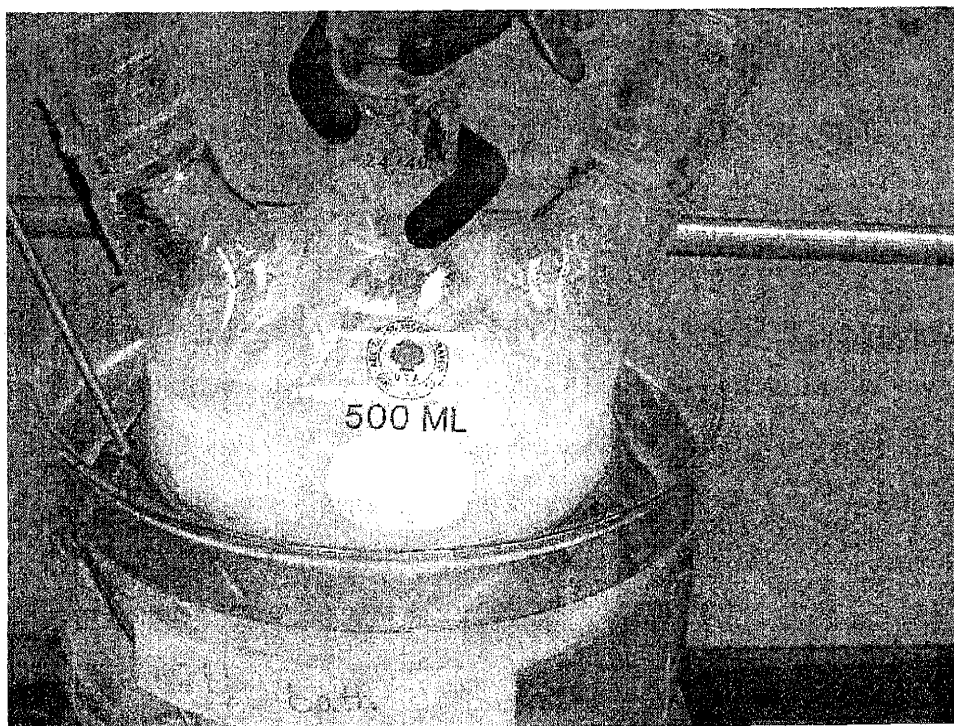
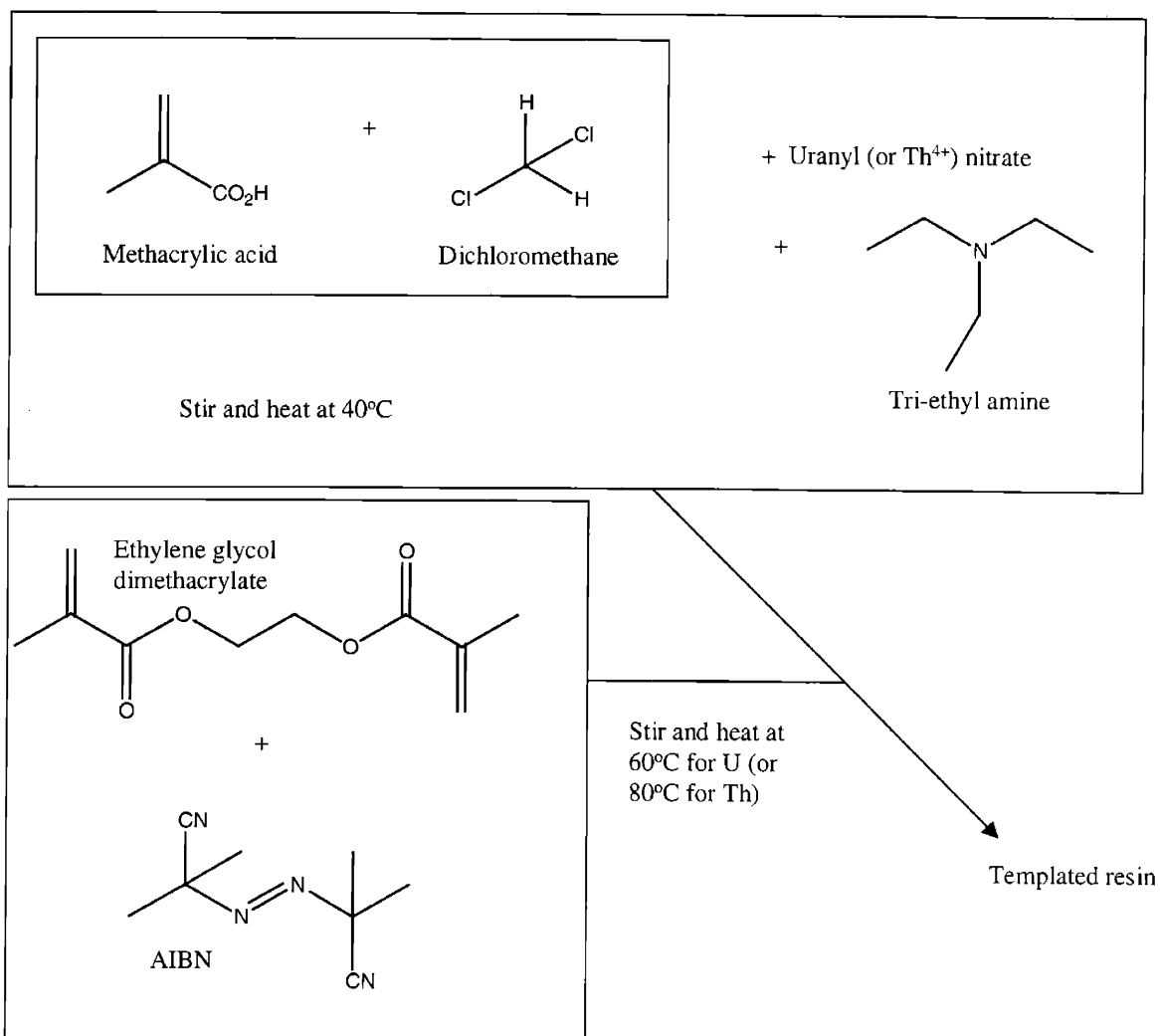


Figure 7.3: Synthesis of Uranium and Thorium Imprinted Resins.



The solid polymer created in the synthesis was obtained by evaporating the original solvent with a Rotavap. The flask containing the polymer and solvent was cooled in an ice bath while the remaining dichloromethane was boiled under vacuum. Once the resin was dry, the solid was ground and sieved to a particle size between 63 and 125 μm . Next, a 5 M nitric acid solution was added to the white dry polymer and the mixture was sonicated for 15 minutes to unload the resin. Finally, the solution was filtered with 0.22 μm filters, under vacuum, and washed with water until neutral. The solid that was obtained from the filter was transferred to a beaker; ethanol was used to rinse the filter. The polymer-ethanol mixture was placed in a 60 °C oven until thoroughly dry (1-2 days). The resin was then used in experiments.

7.2.2 Analytical Section

7.2.2.1 Titration Experiments

Solutions, as prepared below, were titrated with a 736 GP Titrino from Metrohm after equilibration under Ar atmosphere for 1 hour. The titration parameters were 0.15 mL additions of 0.10 M HCl every 10 minutes to total 30 mL of solution, with the endpoint of the titration used to calculate the PEC of the resins.

7.2.2.2 FTIR

FTIR (Fourier Transform Infrared Spectroscopy) spectra were taken of imprinted resin samples that were: bound to U (having never been released after templating), bound to U (after being released and resorbed), or not bound to U (having been released). Transmission data was collected from 0 - 4000 cm^{-1} with a Perkin-Elmer FTIR system.

7.2.2.3 EXAFS

EXAFS and XANES data were collected at the Stanford Synchrotron Radiation Laboratory. One transmission spectra was taken for each sample due to time constraints. Samples were scanned on the Sm K-edge. Samples were scanned to $k=12$. A Sm metal standard was used to calibrate the Sm scans. EXAFS analysis was performed using EXAFSPAK, Atoms, and FEFF. Phase and amplitude functions were calculated using FEFF.

7.2.2.4 ICP-AES

Some U and Th, and all Sr and Eu concentrations were determined using a Spectro D ICP system from Spectro Analytical Instruments. Calibrations were made via detection of standard solutions obtained from SCP Science.

7.2.2.5 ICP-MS

Some U and Th concentration were determined using a VG Plasma Quad system from Fisons Instruments. Calibrations were made via detection of spiked standard solution obtained from SCP science (see chapter 5 for details on preparation and detection).

7.2.3 Resin Characterization

7.2.3.1 Determination of Proton Exchange Capacities (PEC)

Samples of each resin weighing about 0.1 g were used to obtain proton exchange capacity measurements. The PECs were calculated via indirect titrations of 0.1 M NaOH with 0.1 M HCl. The resin samples were combined with 50 mL of a solution of 0.1 M NaOH with 5% NaCl.

These mixtures were shaken overnight so that they could equilibrate and then centrifuged and filtered to remove each resin.

The resulting solutions were then titrated with the aid of a computerized titrator manufactured by Metrohm. Titration parameters were as follows: a volume of 10 mL of solution, an initial equilibration under argon atmosphere for one hour, and 0.15 mL additions of 0.1 M HCl every 10 minutes. The endpoints of these titrations were then used to calculate the proton exchange capacities of the resins.

7.2.3.2 FTIR Sample Preparation

Samples were prepared using 0.10 g of KBr and 0.01 g of dry resin, ground, and pressed into 13 mm pellets. Spectra from the three samples one bound to U, having never been released after templating; one bound to U, after being released and resorbed; and one not bound to U, since it was released, were compared to a spectra collected in an identical manner for a uranium nitrate sample.

7.2.3.3 EXAFS Sample Preparation

Small samples of the uranyl-imprinted resin were withheld from the template removal step and were prepared as “U-loaded U-imprinted resin” samples. For the “U/Th-loaded unimprinted resin” samples, 0.05 g of an analogous unimprinted resin (made as the imprinted resins, except both the template metal and the triethylamine were withheld) was combined with 20 mL of 0.4 M HNO₃. Then, either thorium or uranium was added at concentrations of 200% of the PEC for each resin and the mixtures were shaken for 20 minutes. The resins were filtered and washed with water, then put in 65 °C oven until dry.

A 50 mg sample of the metal bound resins were each mixed with Bio-Beads® and ground to a fine powder. An aluminum window was filled with the mixture, sealed with Kapton tape, triply contained in heat-sealed plastic bags, and were then ready for analysis.

7.2.4 Th and U Sorption to Resins

Kinetic experiments were run at pH values of 1.0, 2.5, 4.0, and 5.5. Samples of 0.05 g of each of the uranium- or thorium-imprinted resins were combined with 17-18 mM uranyl nitrate or 7.2-8.2 mM thorium nitrate, respectively, in a total solution volume of 20 mL. Aliquots of 50 µL were taken according to the following sampling schedule: every hour for the first four hours, every two hours for the next eight hours, every four hours for the following 24 hours, every 6 hours for the next 12 hours, and finally every 12 hours for the last 24 hours.

Aliquots were then diluted for analysis in a series of additions of 2% HNO₃ for metal ion concentration determination via ICP-MS.

7.2.5 Competition Experiments with Resins

For these experiments, representative ions of nuclear waste streams were used as competing ions in order to evaluate the selectivity of the resin. Approximately 0.025 g of resin was equilibrated with a solution containing equal concentrations of UO₂²⁺, Sr²⁺, Eu³⁺, and Th⁴⁺ nitrate salts. Samples were prepared at solution pH values of 1, 2.5, and 4. The concentrations of all of the competing metal ions were 0.0076 M. Each metal was also allowed to interact with the uranium-imprinted resin individually.

A second, identical study was conducted with an analogous random, non-templated polymer. Similar studies were also performed with the Th⁴⁺ templated and non-templated resins.

7.3 Results and Discussion

7.3.1 Proton exchange capacities

From the titration experiments, values of 4.61 meq/g of dry resin for the thorium resin and 6.40 meq/g of dry resin for the uranium resin were obtained. If metal ion charge neutralization is assumed upon sorption, then the molar sorption capacities for the resins need to be normalized to the metal ion charge. For uranyl, a maximum sorption of 3.20 mmoles/g of dry resin is expected with charge neutralization. With thorium, a lower concentration of 1.15 mmoles/g of dry resin is expected due to the higher charge of Th⁴⁺ and the lower proton exchange capacity of the resins. Since the experiments used 0.05 g of resin a theoretic maximum of 0.160 mmoles UO₂²⁺ and 0.0575 mmoles of Th⁴⁺ are expected to sorb. However, the values assume only charge neutralization. Partial hydrolysis of the metal ions will result in lower overall charge, hence sorption values above the theoretical limit.

7.3.2 Sorption Studies

The results from the kinetic studies showed the sorption reaction to be very rapid, with relatively stable metal ion solution concentrations over the sampling period of 3 hours to 190 hours. The average solution metal ion concentrations are given in Table 7.1 and Table 7.2. The concentrations involved, when compared with the appropriate proton exchange capacity, indicate the uranium- and thorium-imprinted resins are nearly saturated or over-saturated, respectively, with the target metal.

Table 7.1: Experimental data for the sorption of UO_2^{2+} on uranyl templated resin.

$V = 20 \text{ mL}, m = 0.05\text{g.}$

pH	$[\text{UO}_2^{2+}]_{\text{tot}} \text{ M}$	$[\text{UO}_2^{2+}]_{\text{solution}} \text{ M}$	moles U/g resin
1.0	1.69×10^{-2}	$1.04 \pm 0.11 \times 10^{-2}$	$2.60 \pm 0.28 \times 10^{-3}$
2.5	1.77×10^{-2}	$1.00 \pm 0.04 \times 10^{-2}$	$3.08 \pm 0.14 \times 10^{-3}$
4.0	1.84×10^{-2}	$9.85 \pm 0.48 \times 10^{-3}$	$3.42 \pm 0.17 \times 10^{-3}$
5.5	1.75×10^{-2}	$8.85 \pm 0.47 \times 10^{-3}$	$3.46 \pm 0.18 \times 10^{-3}$

Table 7.2: Experimental data for the sorption of the Th^{4+} on thorium templated resin.

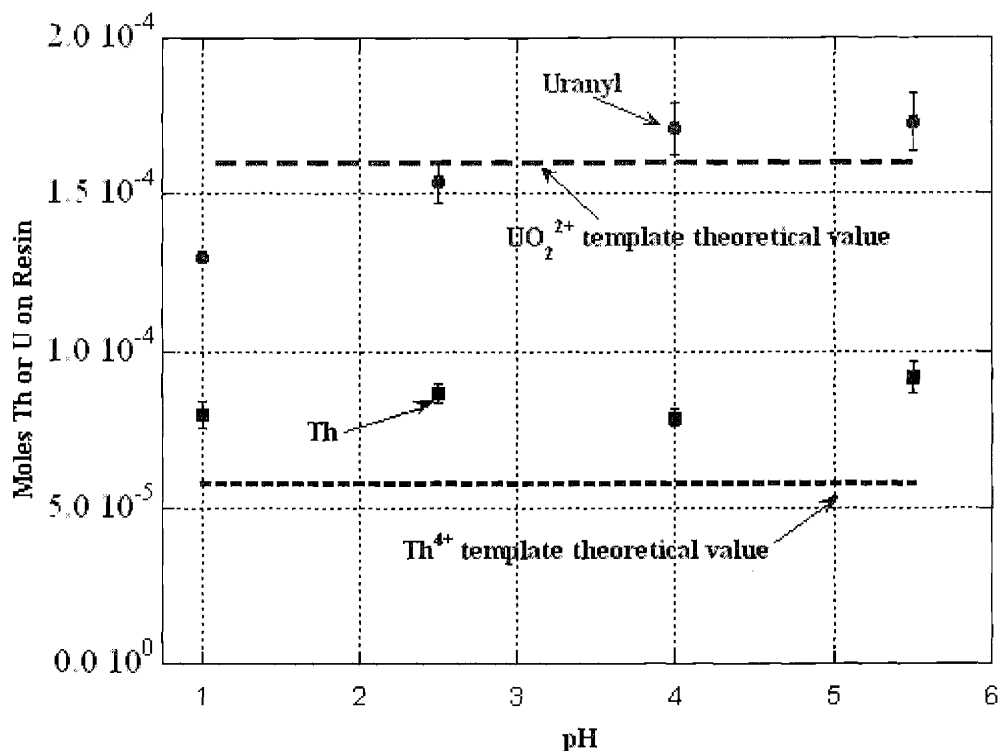
$V = 20 \text{ mL}, m = 0.05\text{g.}$

pH	$[\text{Th}^{4+}]_{\text{tot}} \text{ M}$	$[\text{Th}^{4+}]_{\text{solution}} \text{ M}$	moles Th/g resin
1.0	7.56×10^{-3}	$3.56 \pm 0.18 \times 10^{-3}$	$1.60 \pm 0.08 \times 10^{-3}$
2.5	8.21×10^{-3}	$3.88 \pm 0.14 \times 10^{-3}$	$1.73 \pm 0.06 \times 10^{-3}$
4.0	7.35×10^{-3}	$3.39 \pm 0.13 \times 10^{-3}$	$1.58 \pm 0.06 \times 10^{-3}$
5.5	8.28×10^{-3}	$3.69 \pm 0.20 \times 10^{-3}$	$1.83 \pm 0.10 \times 10^{-3}$

The uranium-imprinted polymer was observed to exhibit an average experimental metal sorption value over all pH values of 0.00303 ± 0.00013 moles per gram of resin. This is only slightly lower than the theoretical value of 0.00320 moles/g obtained via the proton exchange capacity (Figure 7.4). Another notable aspect is that the highest ion exchange capacities are obtained at the pH values of 4.0 and 5.5; this may be a bit misleading, since there was some precipitate present at pH 5.5.

The thorium-imprinted resin showed even more promise under the experimental conditions. The kinetics experiment performed in this case yielded an average ion exchange capacity over all four experimental pH values of 0.0200 ± 0.0002 moles of Th^{4+} per gram of resin. This is actually higher than the theoretical value of 0.00115 moles per gram of resin. In this case it appears as though the complex speciation of thorium increases binding to the resin due to the formation of hydrolysis species.

Figure 7.4: Experimental and theoretical sorption values for uranium and thorium sorption to uranium- and thorium-imprinted resins. The plot shows the results of PEC experiments as well as the binding results seen in tables 7.1 and 7.2.



7.3.3 Competition Experiments with Resins

The imprinted resins consistently exhibited an affinity for their target metal ions over both strontium and europium. Surprisingly the greatest competition was between thorium and uranium for binding sites. As expected, there was a variance in the selectivity with the variance in pH values. The best selectivity results were obtained at the higher pH values, pH 5 for uranium and pH 6 for thorium. Although the thorium-imprinted resin was binding thorium at 93% of theoretical capacity at its peak efficacy, the uranium-imprinted resin was only binding uranium at 37% of theoretical capacity at its peak efficacy. The results are shown below in Figure 7.5 and Figure 7.6.

Figure 7.5: Selectivity results for uranium-imprinted resin vs. pH.

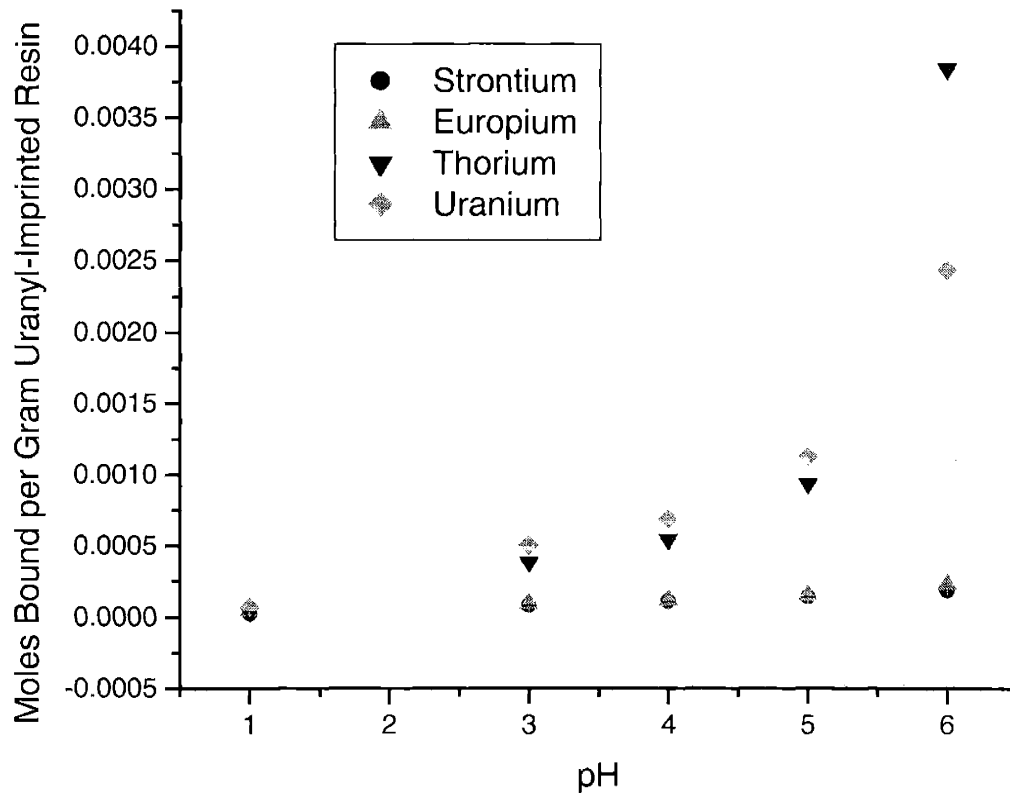
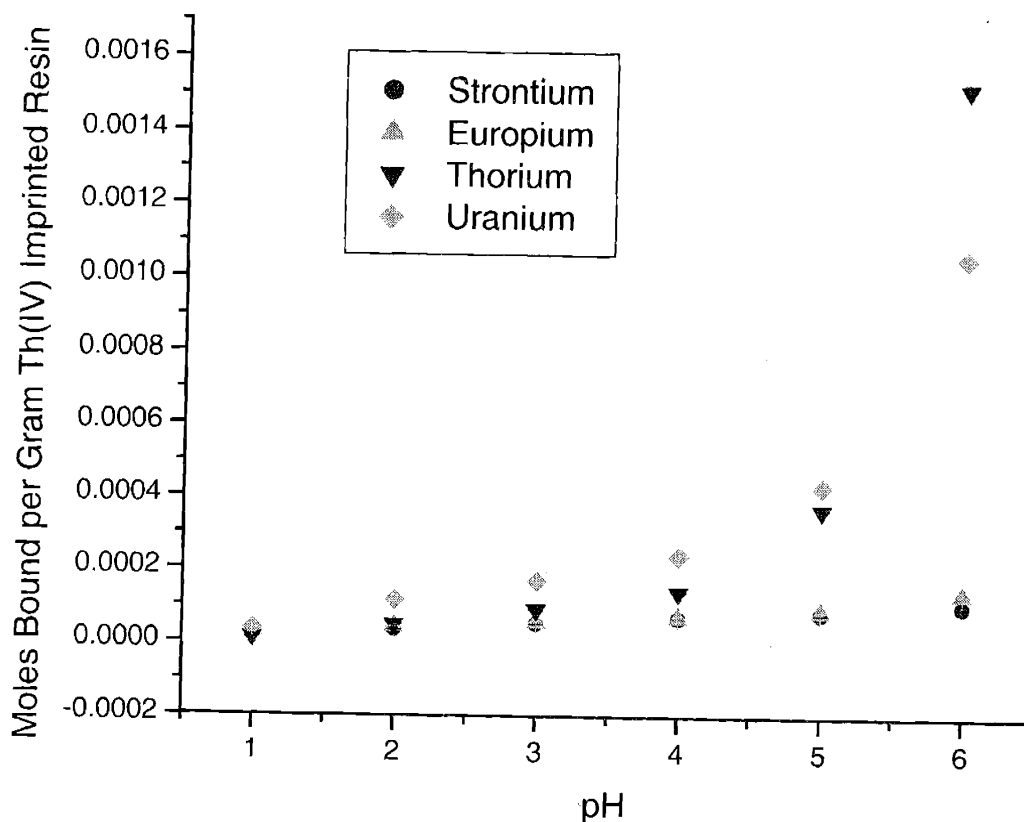


Figure 7.6: Selectivity results for thorium-imprinted resin vs. pH.

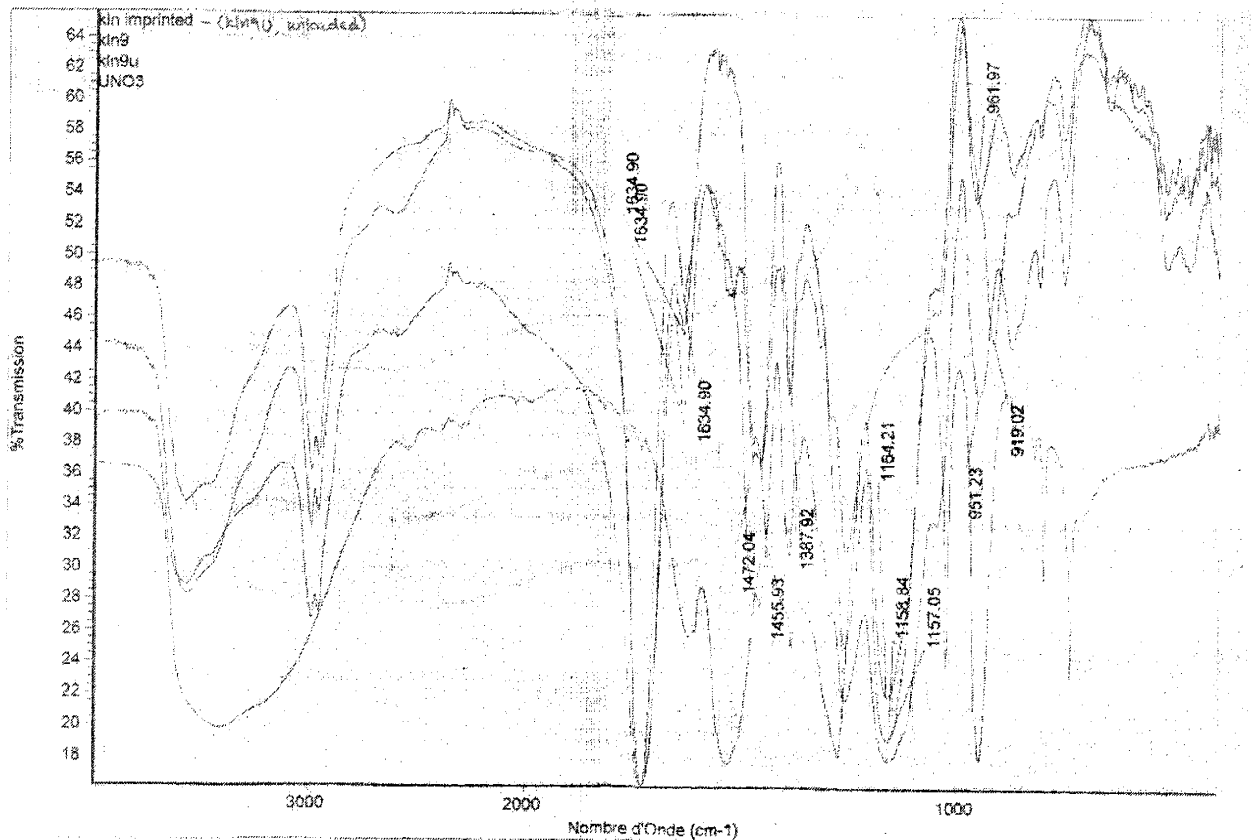


As shown above in Figure 7.5 and Figure 7.6, the strongest competition for the target metal ions uranium and thorium are thorium and uranium, respectively. At peak effectiveness, uranium is bound at 3.04 mmol/g resin and thorium is bound at 1.64 mmol/g resin. Both resins are more efficient for thorium extraction, but the uranium-imprinted resin is more efficient for uranium sorption than the thorium-imprinted one.

7.3.4 Uranium FTIR Results

The FTIR spectra yielded some interesting results. The resin was slightly modified by processing and the resin is clearly observed as bound to uranium. In fact, the results likely indicate that there is incomplete removal of uranyl during the template metal removal process, which may be further indicating potential binding problems. The spectra are included below as Figure 7.7.

Figure 7.7: FTIR spectra of uranium-imprinted resins and uranium nitrate.



7.3.5 Uranium EXAFS Results

The uranium EXAFS yielded some interesting results, the most mundane of which were that the uranium bound to both the imprinted and unimprinted resins was uranyl, or uranium(VI). The interesting finding was that the Th-loaded unimprinted resin contained uranium in the tetravalent state. This finding indicates that the laboratory source of thorium is likely contaminated with uranium(IV). The same diagram also indicates that the metals uranium and thorium are bound to O, as expected. These results are shown below in Figure 7.8, and a diagram of what a uranyl-imprinted resin complex might look like is also included as Figure 7.9.

Figure 7.8: Uranium L3 edge spectra for uranium and thorium loaded resins.

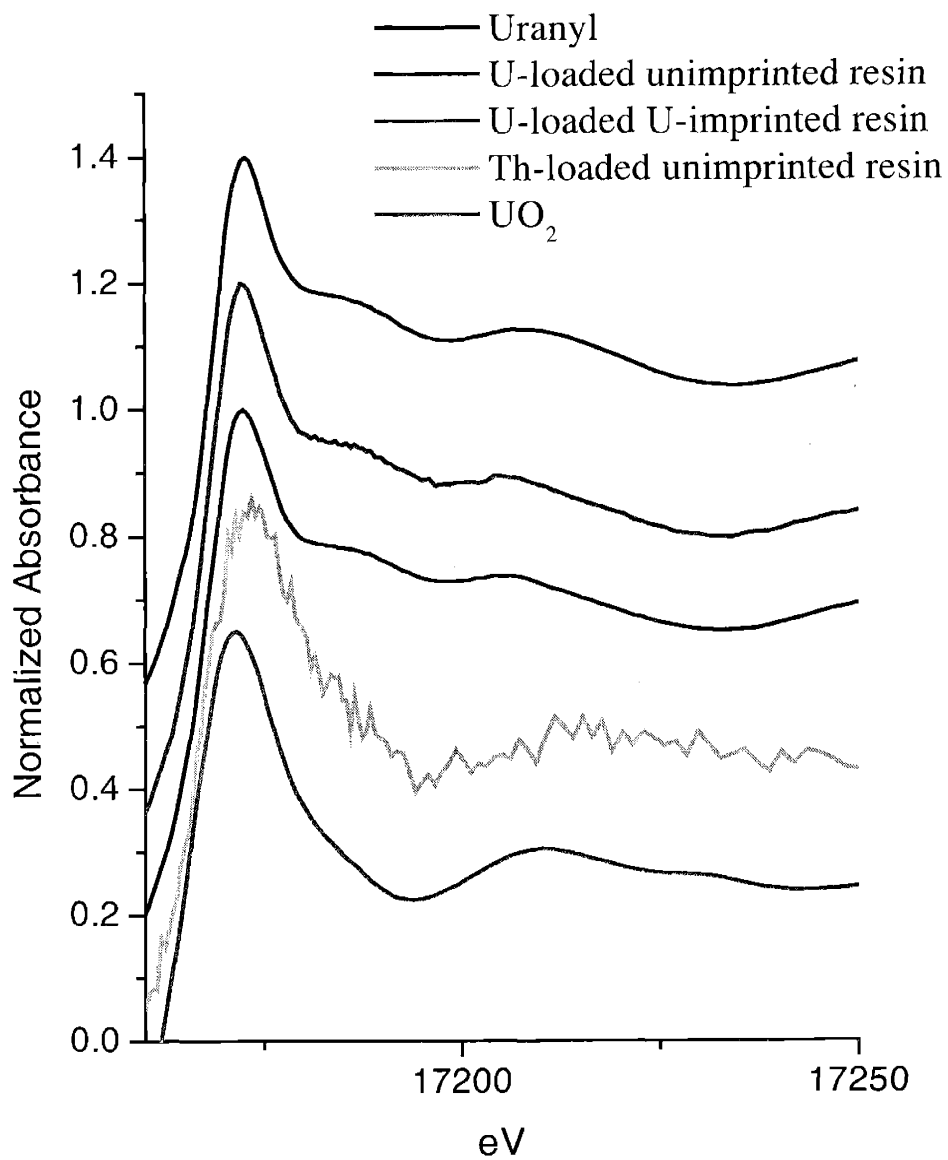
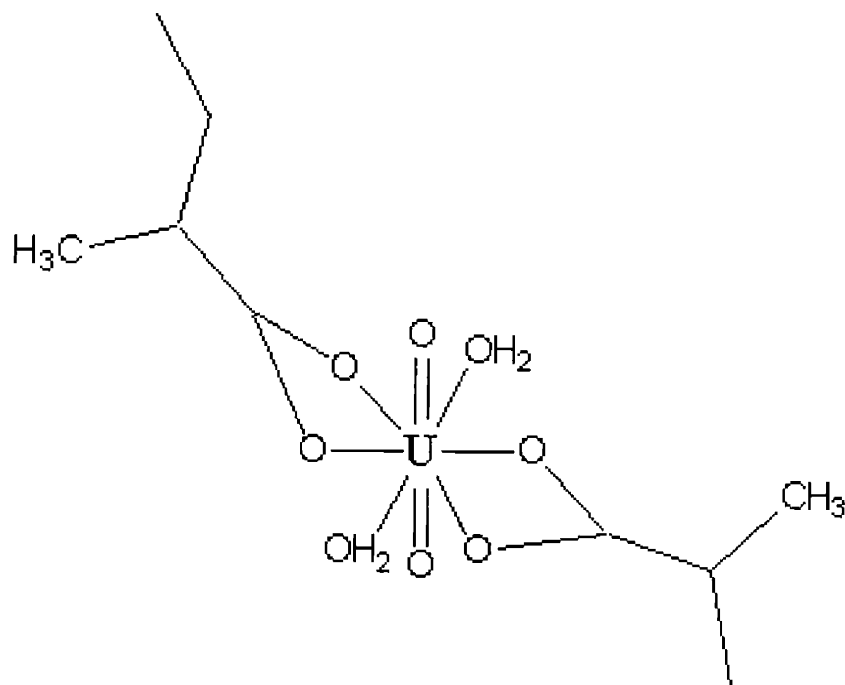
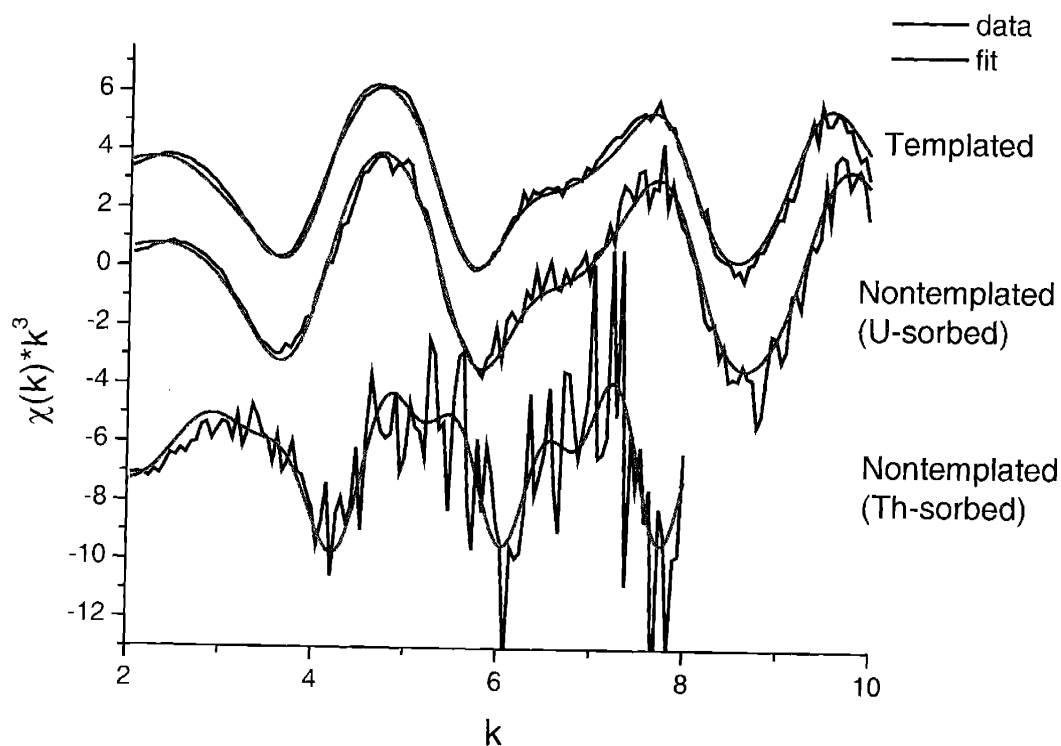


Figure 7.9: Diagram of uranyl-imprinted resin complex consistent with EXAFS data.



The EXAFS data also shows that while the uranyl-resin binding is similar, it is not identical for the imprinted and unimprinted resins. The same data also shows that the binding of uranium(IV) to the unimprinted resin is completely different from that of the uranyl binding. Both of these statements are represented below as Figure 7.10.

Figure 7.10: EXAFS data for uranium-resin binding characteristics.



7.4 Conclusions

These studies show that polymer-based resins templated with uranyl and thorium(IV) ions sorb their target metal ions. The ability of the resin to sorb the target metal ion while competing with metal ion of differing oxidation states yielded some unexpected results in that strong competition was coming from unexpected players, such as Th interfering with U binding on the U-imprinted resin. This may indicate that a fair amount of binding is occurring at random sites, or binding sites which were not produced via the imprinting process. A modification to the synthesis should be investigated in order to remove these random binding sites, which should further increase the selectivity of the resin.

The breakthrough of solutions containing the target metal in a resin column also must be determined in order to consider column feasibility. The syntheses of this study will also be used as a basis for templating higher actinides, such as neptunium and plutonium. One of the initial goals of this work was to produce a resin with rapid kinetics, and these experiments have indicated success. The values for the metal binding indicate charge neutralization, which is

confirmed with the EXAFS data. The reusability of the resin also remains to be proven, and will be investigated in another experiment.

7.5 Acknowledgements

Funding is provided by the Presidential Early Career Award for Science and Engineering with cooperation through the Glenn T. Seaborg Institute at Los Alamos National Laboratory. Additional funding was provided by Conservatoire National Des Arts et Metiers, Paris.

Part of this work was performed under the auspices of the U.S. Department of Energy (DOE) by the University of California Lawrence Livermore National Laboratory under Contract No. W-7405-Eng-48. This work was done (partially) at SSRL, which is operated by the Department of Energy, Division of Chemical Sciences.

7.6 References for section VII

1. G. Wulff, A. Sarhan, *Angew. Chem. Int. Ed. Eng.*, 1972, **11**, 341 ; R. Arshady, K. Mosbach, *Makromol. Chem.*, 1981, **182**, 687-692
2. a) A. Sarhan, G. Wulff, *Makromol. Chem.*, 1982, **183**, 85-92 ; b) G. Wulff, J. Haarer, *Makromol. Chem.*, 1991, **192**, 1329-1338
3. M. Kempe, K. Mosbach, *J. Chromatogr. A*, 1995, **694**, 3-13
4. a) B. Sellergren, M. Lepistö, K. Mosbach, *J. Am. Chem. Soc.*, 1988, **110**, 5853-5860 ; b) D. Spivak, M.A. Gilmore, K.J. Shea, *J. Am. Chem. Soc.*, 1997, **119**, 4388-4393
5. K. Uezu, M. Yoshida, M. Goto, S. Furusaki, *Chemtech*, 1999, 12-18
6. Saunders, G., Foxon, S., Walton, P., Joyce, M., and Port, S.: A Selective Uranium Extraction Agent Prepared by Polymer Imprinting. *Chem Commun.*2000, **4**, 273-274.

VIII. Neptunium Experiments

An ion exchange resin was created to complex NpO_2^+ from aqueous solutions. A chloride solution of the target metal ion (4 M HCl) was dried in the reaction vessel, then redissolved in CCl_2H_2 , while the resin was created around the ions in order to provide a unique structure based upon the metal. This resin was synthesized by a radical polymerization method, producing a reusable organic solid and is based upon the original work as seen in chapter 7. A new resin preparation process had to be developed to prepare this new type of resin (low volume, relatively high activity) for use in experiments. Once loaded with metal, the ions can easily be removed with 5 M HCl and reused.

8.1 Introduction

Currently there are proposals for the disposal, storage, and/or transmutation of some long-lived nuclear waste components, such as Np, which will require the development of separation schemes. This separation becomes particularly important if transmutation is to be considered, as Np must be separated from both other actinides and from fission products. Current separation schemes effectively leave Np dangling, since it tends to end up split between the “useful” U/Pu stream and the waste fission product/minor actinide stream, due to its multiple oxidation states and the different chemical behavior that each exhibits. For this reason, it is necessary to investigate minor actinide separations.

Previous work has shown the feasibility of ion-imprinting polymer-based resins for use in ion exchange type separations with metal ion recognition [1, chapter 7]. Other work has produced phenolic-based resins efficient for trivalent element separations, but almost no separation methods have specifically developed with Np in mind [2]. A uranyl-imprinted polymer resin has been synthesized successfully and used as the basis for templating a thorium ion imprinted resin [3,4]. This work concerns the development of an ion-imprinted resin for application to Np separations.

8.2 Background

The imprinting process generally requires the use of gram quantities of the target metal ion, which is difficult to accomplish when the target is Np(V), due to both radioactivity and the ability to procure necessary quantities. For these reasons, the

synthetic process was modified for use in very small quantities (roughly 250 times smaller than previous syntheses, seen in chapter 7, 9, or 10).

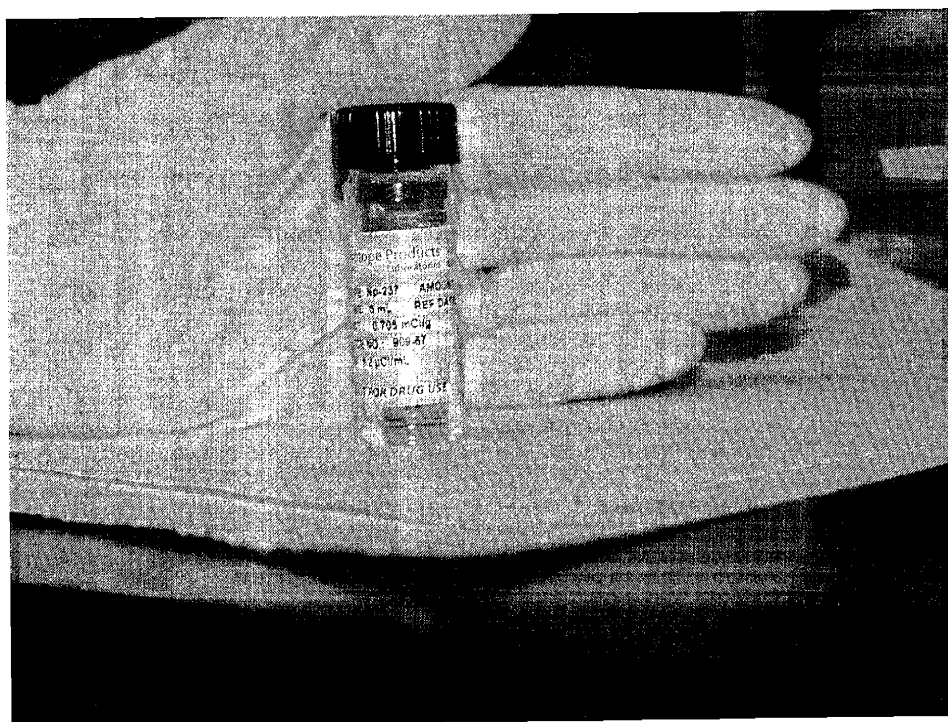
If there is a move toward transmutation, it is critical to separate Np from An and Ln in a coherent manner in order to control the amounts of Np present, an important aspect of both fuel production and criticality control. The experiments presented in this section intend to show that it is possible to produce an imprinted ion exchange resin for Np separations that could be used to control the flow of Np in output streams.

8.3 Experimental

8.3.1 Reagents

Methacrylic acid, triethylamine, ethylene glycol dimethacrylate, and azobisisobutyronitrile (AIBN) were obtained from Aldrich and used without further purification. Dichloromethane was obtained from Alfa Aesar and used without further purification. A solution of Np in 4 M HNO₃ containing 9.62×10^5 Bq (26 μ Ci) of ²³⁷Np with a total volume of 5 mL (1.92×10^5 Bq/mL; 5.2 μ Ci/mL) was obtained from Isotope Products. The Np solution was placed in the reaction vessel and thoroughly dried, then used in the synthesis. The neptunium, in initial form is shown below in Figure 8.1.

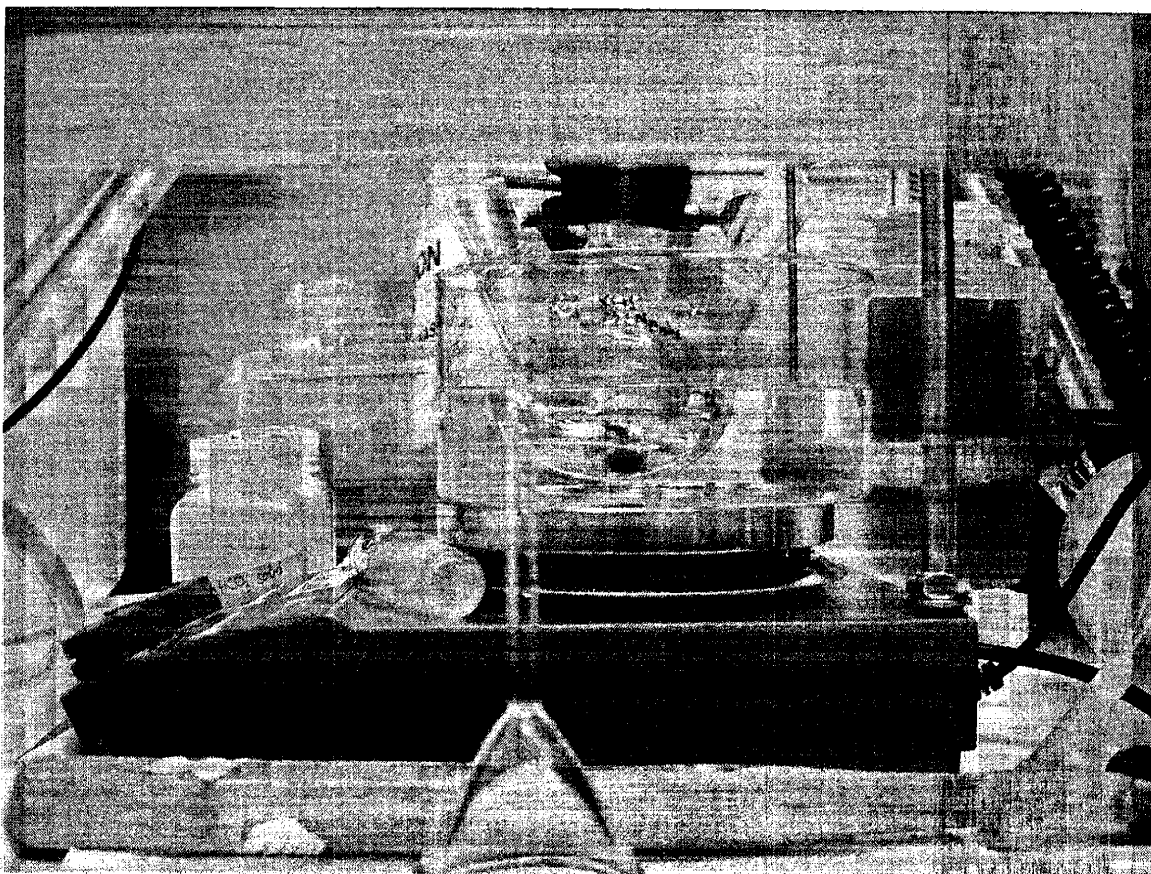
Figure 8.1: Neptunium, as received.



8.3.2 Resin Synthesis

A 26 μCi sample of ^{237}Np was initially dried in situ, while stirring, at 40°C until thoroughly dry. To this, dichloromethane (CCl_2H_2 , 11 mL) was added; this mixture was heated and stirred for four hours at 40°C . Next, methacrylic acid ($\text{C}_4\text{H}_6\text{O}_2$, 255.5 μmol , 22mg) was added with triethylamine ($\text{C}_6\text{H}_{15}\text{N}$, 789 μmol , 4.5 mL) drop-wise. This reaction mixture was stirred at 40°C for 12 hours under reflux in order to obtain a bright green solution and ensure complete dissolution of the Np. Ethylene glycol dimethacrylate ($\text{C}_{10}\text{H}_{14}\text{O}_4$, 1.62 mmol, 322mg) was added along with azobisisobutyronitrile (AIBN, $\text{C}_8\text{H}_{12}\text{N}_4$, 134 μmol , 22mg). The reaction mixture was heated to 70°C and kept at this temperature for six hours while stirring under reflux.

Figure 8.2: Picture of Np before dried.



After the reaction solution had cooled to room temperature, the solvent was separated from the resulting solid with MagnaNylon 5.0 μm nylon filters from Osmonics and vacuum aid. Once the dichloromethane was removed, residual organics were washed off with ethanol. Once the ethanol was filtered through, 5 mL of 4.2 M HCl was added and

agitated with a pipet in order to remove the Np from the resin. After a period of 15 minutes, the filtration was resumed under vacuum and the resulting Np in 4.2 M HCl was pulled through, leaving the imprinted, unbound resin on the filter membrane. After filtration and metal removal, the resin was then washed thoroughly with water until neutral and transferred to a 60°C air oven to cure for 2 days.

8.4 Results and Discussion

A resin was successfully imprinted with the NpO_2^+ ion for use in Np solid-liquid extractions. The resin was produced on a very small scale, but the process was fairly easily adapted to the volume limitations. The synthesis was also notably carried out while beginning with an aqueous reactant, which provided other synthetic difficulties that were successfully overcome. The reaction was also repeated twice on slightly different scales (roughly double the initial run described in section 8.3.2).

8.5 Conclusions

The successful imprinting of a resin with the Np(V) ion proves that it is possible to template both more radioactive metals and run the synthesis on very small scales. Other successes of the synthesis include starting with a wet (i.e. aqueous) target, which is notable since water easily and completely halts the radical synthesis involved in the formation of the imprinted resin. The resin preparation method was also altered in order to account for both the small amount of product and the radioactivity involved. All in all, this is a success which can be further applied to other elements in the future, such as Pu. Future work should include characterization of the resin and an examination of the thermodynamics of binding, as well as the effectiveness of the resin in competitive separation schemes.

8.6 References for Section VIII

1. H. Nishide, J. Deguchi, E. Tsuchida, *Chem. Lett.*, 1976, 169-174.
2. M. Draye, A. Favre-Reguillon, D. Wruck, J. Foos, A. Guy, K.R. Czerwinski, *Removal of ²⁴³Am with Phenol Based Resins*, *Sep. Sci. Technol.*, 2001, (36), 899-909.
3. G. Saunders, S. Foxon, P. Walton, M. Joyce, S. Port, *A Selective Uranium Extraction Agent Prepared by Polymer Imprinting*, *Chem. Commun.*, 2000, (4), 273-274.
4. K.L. Noyes, M. Draye, A. Favre-Reguillon, J. Foos, A. Guy, K.R. Czerwinski, *Synthesis and Evaluation of Uranium and Thorium Imprinted Resins*, MRS Fall 2001 Meeting Proceedings, Symposium JJ.

IX. Americium Separations

Molecular imprinting techniques have shown great promise for applications in chemical separations, including those involving lanthanides and actinides. This work examines the production of a selective resin for Am separations. Due to practical difficulties, resins were not imprinted with Am, rather 3 resins were created with each of Sm, Nd, and Pr as the template ions. An analogous “blank” or unimprinted resin was also created. The nitrate salt of the target metal ion was dissolved in CCl_2H_2 and the resin was created around the ions to provide a unique structure based upon each metal. These resins were synthesized by a radical polymerization method, producing a reusable organic solid. The resins were qualified by obtaining values for their proton exchange capacities and data to define their complexation thermodynamics. Proton exchange capacities were determined using an indirect titration and were found to be 10.08 meq/g for the Sm-imprinted resin, 7.25 meq/g for the Nd resin, and 7.14 meq/g for the Pr resin. Data for the resins’ thermodynamics were obtained at pH 1-7 in steps of 0.5 units. Results show that the templated resins rapidly removed the target actinide from aqueous solution under experimental conditions. Better separation results for Am, rather than Eu or Gd, were obtained with the Nd imprinted resin.

9.1 Introduction

Currently there are proposals for the disposal, storage, and/or transmutation of actinides such as Am, which will require the development of separation schemes. This separation becomes particularly important if transmutation is to be considered, as the trivalent lanthanides must be removed from the trivalent actinides in order to ensure neutronically favorable conditions. For this reason, it is necessary to investigate minor actinide separations.

Previous work has shown the feasibility of ion-imprinting polymer-based resins for use in ion exchange type separations with metal ion recognition [1]. Other work has produced phenolic-based resins that function well for Am-Eu separations, but exhibited slow kinetics and difficulties in the imprinting process [2]. A uranyl-imprinted polymer resin has been synthesized successfully and used as the basis for templating a thorium ion imprinted resin [3,4]. This work concerns the development of an ion-imprinted resin for application to Am separations.

9.2 Background

The imprinting process generally requires the use of gram quantities of the target metal ion, which is difficult to accomplish when the target is Am(III), due to both radioactivity and the

ability to procure necessary quantities. For these reasons, the lanthanides Sm(III), Pr(III), and Nd(III) were selected for use in the imprinting process because their ionic radii bracket that of Am(III) while being larger than that of Eu(III) and Gd(III), thus providing a close match based on size and charge.

If there is a move toward transmutation, it is critical to separate Am from Eu and Gd in order to maintain a good neutron economy. However, the use of the lanthanides as templates for a resin intended to target only Am could reduce the selectivity of the resin for Am. The experiments presented in this paper intend to show that the resins show an affinity for Am and future work will be dedicated to proving an affinity for Am over competing metal ions.

9.3 Experimental

9.3.1 Materials

9.3.1.1 Chemicals and Reagents

Methacrylic acid, triethylamine, ethylene glycol dimethacrylate, azobisisobutyronitrile (AIBN), Nd(III) nitrate, Sm(III) nitrate, and Pr(III) nitrate were obtained from Aldrich and used without further purification. Dichloromethane was obtained from Alfa Aesar and used without further purification.

9.3.1.2 Resin synthesis

The metal was added, while stirring, to a mixture of methacrylic acid ($C_4H_6O_2$, 15.80 mmol, 1.36 g) in dichloromethane (CCl_2H_2 , 450 mL) as a nitrate (6mmol: 2.7 g of Sm nitrate [$Sm(NO_3)_3 \cdot 6H_2O$]; 2.6 g of Nd nitrate [$Nd(NO_3)_3 \cdot 6H_2O$]; or 2.6 g of Pr nitrate [$Pr(NO_3)_3 \cdot 6H_2O$]) with triethylamine ($C_6H_{15}N$, 32.28 mmol, 4.5 mL) drop-wise. This reaction mixture was stirred at 40 °C for 2 hours under reflux. Ethylene glycol dimethacrylate ($C_{10}H_{14}O_4$, 59.13 mmol, 11.72 g) was added along with azobisisobutyronitrile (AIBN, $C_8H_{12}N_4$, 8.28 mmol, 1.36 g). The reaction mixture was heated to 60 °C and kept at this temperature overnight while stirring under reflux.

After evaporation, the resulting solid was ground and sieved to a particle size of 63-125 μm . To remove the template metal, 5 M nitric acid (30 mL) was added and the mixture was sonicated for 15 min. After filtration, the resin was then washed thoroughly with water until neutral, rinsed with ethanol, and kept at 60°C in an air oven to cure for 2 days. An analogous random polymer was synthesized using the same procedure, except the metal and triethylamine were withheld.

9.3.2 Analytical Section

9.3.2.1 Titration Experiments

Solutions, as prepared below, were titrated with a 736 GP Titrino from Metrohm after equilibration under Ar atmosphere for 1 hour. The titration parameters are 0.15 mL additions of 0.10 M HCl every 10 minutes to total 30 mL of solution, with the endpoint of the titration used to calculate the PEC of the resins.

9.3.2.2 EXAFS

EXAFS and XANES data were collected at the Stanford Synchrotron Radiation Laboratory. One transmission spectra was taken for each sample due to time constraints. Samples were scanned on the Sm K-edge. Samples were scanned to $k=12$. A Sm metal standard was used to calibrate the Sm scans. EXAFS analysis was performed using EXAFSPAK, Atoms, and FEFF. Phase and amplitude functions were calculated using FEFF.

9.3.2.3 ICP-AES

Lanthanide concentrations were determined using a Spectro D ICP system from Spectro Analytical Instruments. Calibrations were made via detection of standard solutions obtained from SCP Science.

9.3.2.4 Activity Measurements by scintillation counting

Am concentrations were determined using a Packard Tri-Carb 2900TR scintillation counter. Samples were prepared as 10 μL of sample in 10 mL of Packard Ultima Gold AB scintillation fluid.

9.3.3 Resin Characterization

9.3.3.1 PEC Experiments

For determination of the total proton exchange capacity, samples of 0.1 g resin were equilibrated for 12h with 50 mL of 0.1 M NaOH containing 5% NaCl solution while shaking. The amount of NaOH consumed in the $\text{H}^+ \rightarrow \text{Na}^+$ exchange was determined by titration of the remaining OH^- in the supernatant, after preliminary equilibration under Ar atmosphere, with 0.1 M HCl solution.

9.3.3.2 EXAFS Sample Preparation

The sample preparations differed slightly for the samples and the references. The procedures are detailed below.

9.3.3.2.1 Resin sample preparation

Two kinds of resins were prepared, non-released resin and reabsorbed resin, for EXAFS analysis. Small samples of ion-imprinted resins were withheld from the template removal step and were prepared as non-released samples. For the reabsorbed samples, 0.05 g of resin was shaken for 20 min. with the target metal (concentrations of 200 % of the PEC) in 4 M HNO₃. After filtration, the resin is washed with water and put in a 65 °C oven until dry.

9.3.3.2.2 Reference preparation

A 100 mL sample of NH₄OH was added to 30 g of oxalic acid dissolved in 200 mL of hot water. A 15 g sample of metal nitrate was dissolved in 100 mL of hot water, which was slightly acidified with nitric acid. The resulting precipitate was washed several times with water and acetone, then put in a 70 °C oven until dry. The heat of the oven was then increased to 150 °C for 12 h, and the solid was calcinated at 700 °C for 1 h to produce the oxide reference.

A 50mg sample of the oxide reference or of the metal bound resin was mixed with Bio-Beads and ground to a fine powder. An aluminum window was filled with the mixture, sealed with Kapton tape, triply contained in heat-sealed plastic bags, and was then ready for analysis.

9.3.4 Kinetics Studies

Samples of each the random, Sm-, Nd-, and Pr-imprinted resins were combined with Gd and Eu nitrate in a total solution volume of 20 mL. The metal concentrations were chosen as 150% of the resin PEC values and experiments were run at pH 4 for Gd and pH 5 for Eu, in order to enable good deprotonation while limiting hydrolysis.

Based on previous kinetics results for Th- and U-imprinted resins, the kinetics were assumed to be fast and equilibration was expected within 60 min. Thus, aliquots were taken at 1 min., 2.5 min., 5 min., 10 min., 20 min., 40 min., and 60 min., then diluted with 2 % HNO₃ for metal concentration determination via ICP-AES.

9.3.5 Sorption Studies

Three sets of experiments were run with 200% and 50% of theoretical loading for Eu(III) and Gd(III), with another set at 100 nM of Am(III). Each sample had a total volume of 20 mL and contained 50 mg of either the random, Sm-, Nd-, or Pr-imprinted resin. Each setup was repeated for the pH range 1-7 in steps of 0.5 units.

After adjusting the pH of each sample, the vials were shaken for 30 minutes in order to achieve equilibrium. Aliquots of 50 µL were taken and then diluted with 2% HNO₃ for

lanthanide concentration determination by ICP-AES. Am concentrations were determined by scintillation counting.

9.4 Results and discussion

9.4.1 PEC

The results of the PEC values are gathered below in **Table 9.1**. The table also includes the values for theoretical loading capacities, which assume charge neutralization of the metal upon complexation.

Table 9.1: Proton Exchange Capacities and theoretical sorption capacities of the resins.

	Random	Samarium	Neodymium	Praseodymium
PEC (meq/g)	9.20	10.08	7.25	7.14
Theoretical Metal(III) Sorption Capacity (mmol/g)	3.07	3.36	2.42	2.38

Table 9.1 shows that the proton exchange capacities obtained for the Nd- and Pr-templated resins are comparable but slightly lower than those obtained for the Sm-templated and random (non-templated) resins.

9.4.2 EXAFS Samples

Below in **Figure 9.1**, the left-most peaks are Sm-O bonds. The fits used placed a Sm-Sm bond at the next peak for the non-templated resin. The oscillations in the templated resins are most likely the result of multiple scattering from Sm-C bonds, indicating the Sm ions are bound within the resin. The second and third peaks show the contrast between the templated and non-templated structures.

Other results from the data fitting show that the non-templated resin could be a mixture of 6-coordinate and 8-coordinate arrangements (coordination number, N, of 6.6). The spectra indicate that the non-templated resin is fairly heterogeneous. Conversely, the templated resins are most likely 8-coordinate (non-released: N=7.8; reabsorbed: N=8). The lanthanide ion could indeed be coordinated by three bidentate functional groups and two water molecules, similar to results obtained for U [3].

The Sm-O bond lengths and coordination number are similar for both of the templated resins, non-released and reabsorbed, which shows that there is no significant difference in binding when

the resin is reloaded. The resin can thus be used, and then reused, without any degradation or change in the selectivity.

Figure 9.1: Fourier transforms and fits of EXAFS data.

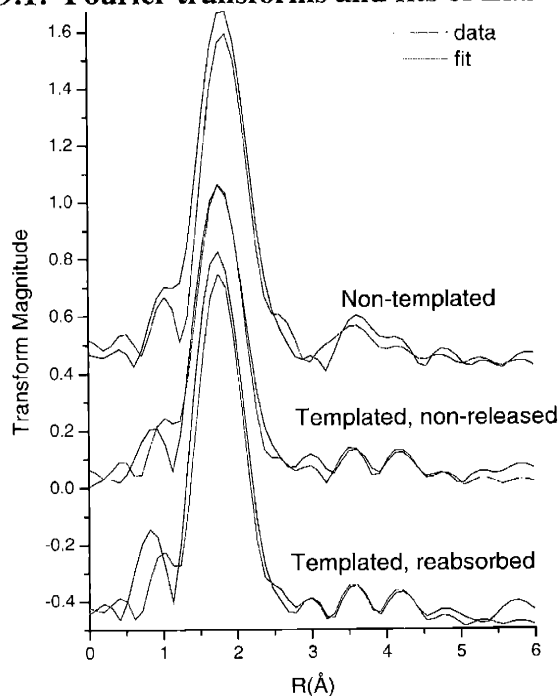
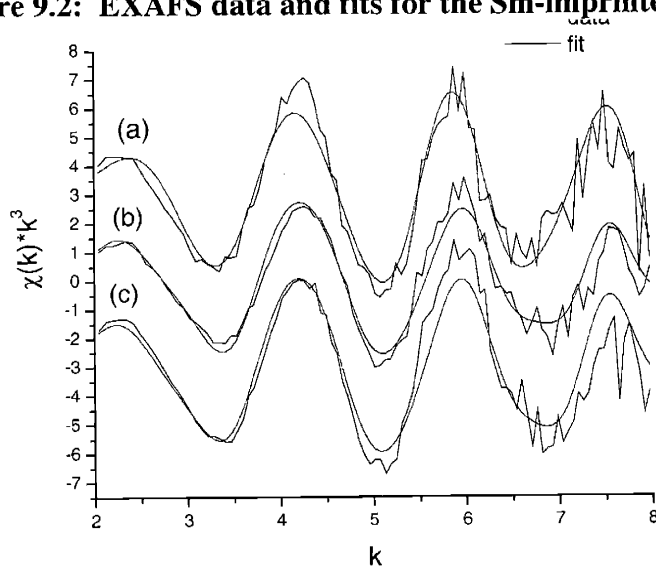


Figure 9.2 shows that the non-templated resin (a) is phase-shifted in comparison with the templated resins (b and c), indicating a longer Sm-O bond. This result, in conjunction with the results shown in **Figure 9.1**, means that the Sm-O bond is stronger for templated resin, probably due to the imprinting effect.

Figure 9.2: EXAFS data and fits for the Sm-imprinted resin.



The XANES (X-ray Absorption Near Edge Spectroscopy) data analyses show no shifts between peaks, indicating constant oxidation state. The Sm-O bond lengths are consistent with Sm(III)-O bonds.

9.4.3 Kinetics Studies

The results of the kinetics studies were uninteresting and were very similar to those for both the uranium and thorium resin experiments. Those results can be seen in chapter 8 of this document.

9.4.4 Sorption Studies

The saturation studies were used to determine the loading capacity of the resins, with the results listed below in **Table 9.2**. The results show similarities to the theoretical capacity obtained from the PEC experiments, with the Nd and Sm resins having greater than theoretical loading capacities. This can be expected, as the experimental capacities are still within the errors of the theoretical capacities.

Table 9.2: Loading capacities of the resins.

	Random	Samarium	Neodymium	Praseodymium
Theoretical capacity (mmol/g)	3.07 ± 0.23	3.36 ± 0.25	2.42 ± 0.18	2.38 ± 0.18
Experimental capacity (mmol/g)	3.03 ± 0.12	3.57 ± 0.14	$2.51 \pm .010$	2.31 ± 0.09

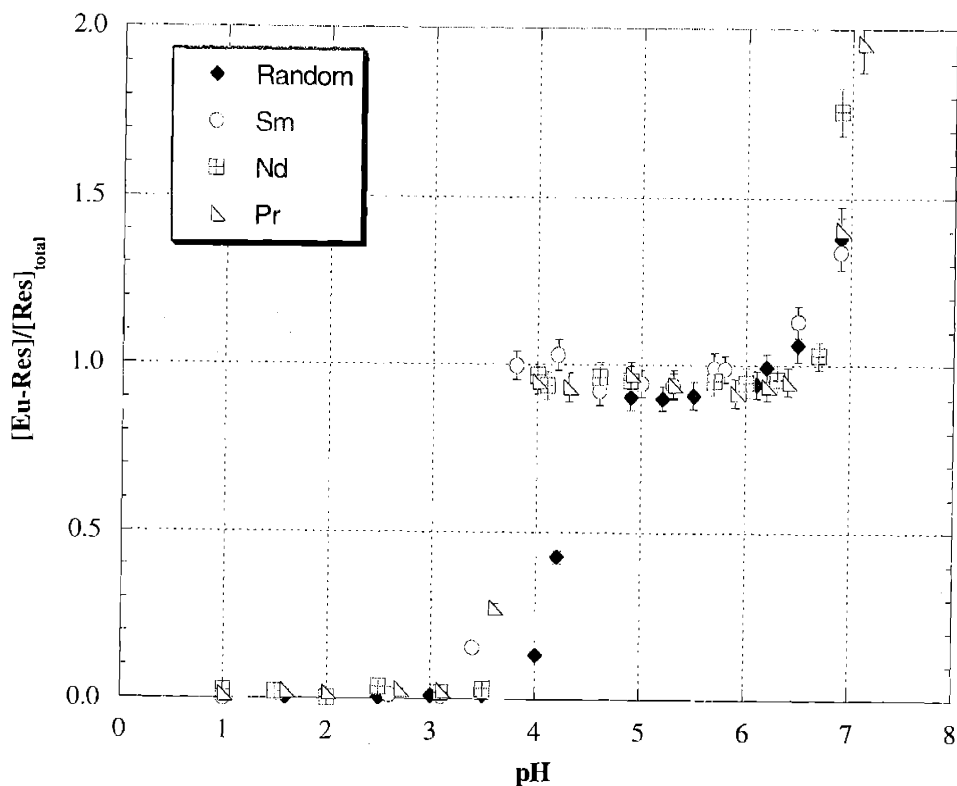
The theoretical loading capacities of the resins, as shown in , were calculated from the proton exchange capacity, as described earlier. The loading capacity values are taken from the results of the saturation experiments and indicate the maximum amount of target metal that can bind to the resin. The value for the loading capacity was determined by taking the minimum amount of the target metal remaining in solution and assuming that the rest had been bound to the resin, determining the number of moles bound to the resin, and then dividing that value by the mass of the resin used in the experiment, which yields a loading capacity in mol/g resin.

Sm-, Nd-, and Pr-templated resins were evaluated for Eu and Gd uptake. Their efficiencies were compared to those of the random, non-templated resin as a function of the pH. Quantities of note in the following figures include $[M-Res]$ and $[Res]_{total}$. The $[M-Res]$ value is the

concentration of the metal-resin complex. The $[\text{Res}]_{\text{total}}$ value is the concentration of resin, which is essentially the total concentration of binding sites available.

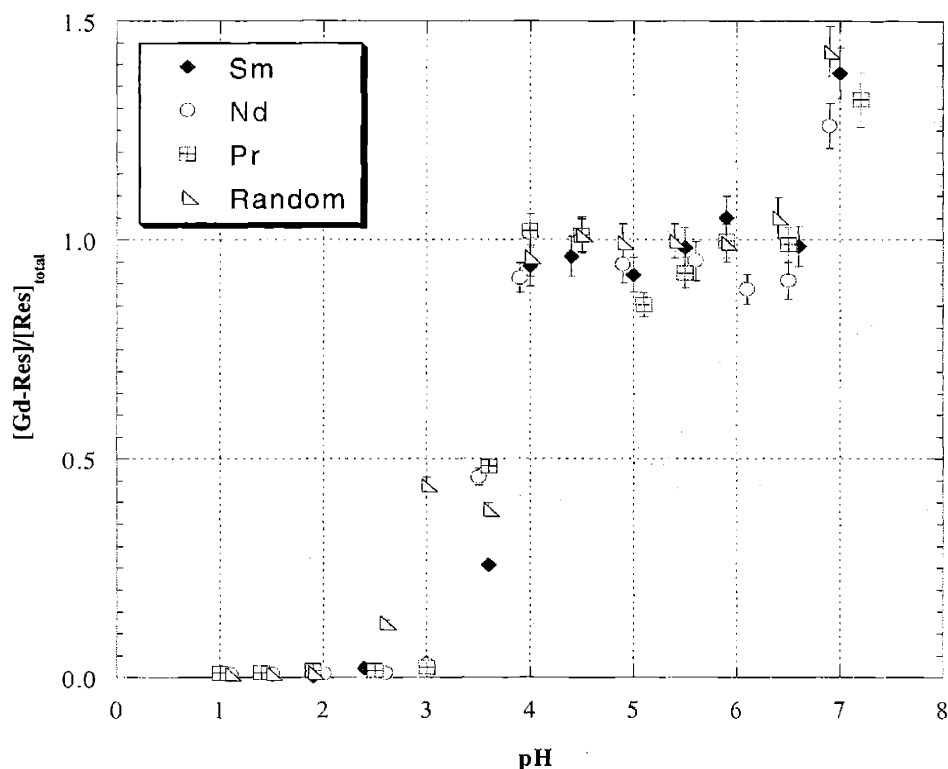
The remaining pH-dependant results show a clear influence of pH on the sorption capacities of the resins, with higher pH values showing higher binding to metal. The results for these experiments can be seen below in **Figure 9.3** and **Figure 9.4**. At the higher pH values, metal precipitation was observed.

Figure 9.3: Influence of pH on Eu-resin binding for Sm-, Nd-, Pr-, and non-templated resins at 200% of loading capacity.



As seen in **Figure 9.3**, there is no significant metal sorption by the resins until pH 4. As for the results for the various resins with Eu, there is no noticeable difference among them, with the small exception that the Pr- and Nd-templated resins seem to fare better than the others at pH 7.

Figure 9.4: Influence of pH on Gd-resin binding for Sm-, Nd-, Pr-, and non-templated resins at 200% of loading capacity.



As shown above in **Figure 9.4**, there is no significant binding of the metal by the resins until pH 3.5. This is likely due to the need for deprotonation of the carboxylic acid functional groups, as indicated by the pK_a value of carboxylic acid, which is about 4. With reference to Gd uptake, there is no noticeable preference shown by any of the resins, with the possible exception of the random.

Results from subsaturation experiments were used to calculate distribution coefficients, D_{ex} , for the resins and selectivity constants, K . The distribution coefficient is defined as:

$$D_{ex} = \frac{[M - Res]}{[M]_{free}}$$

Where $[M\text{-Res}]$ is the concentration of the metal-resin complex and $[M]_{\text{free}}$ is the concentration of free metal, which was determined by ICP-AES for Eu and Gd or by scintillation counting for Am. Values for $[M\text{-Res}]$ were calculated by subtracting the $[M]_{\text{free}}$ value from the $[M]_{\text{total}}$, which was the original total metal concentration. Results are shown below in **Figure 9.5**, **Figure 9.6**, and **Figure 9.7**.

Figure 9.5: D_{ex} values for Eu vs. pH at 200% of loading capacity.

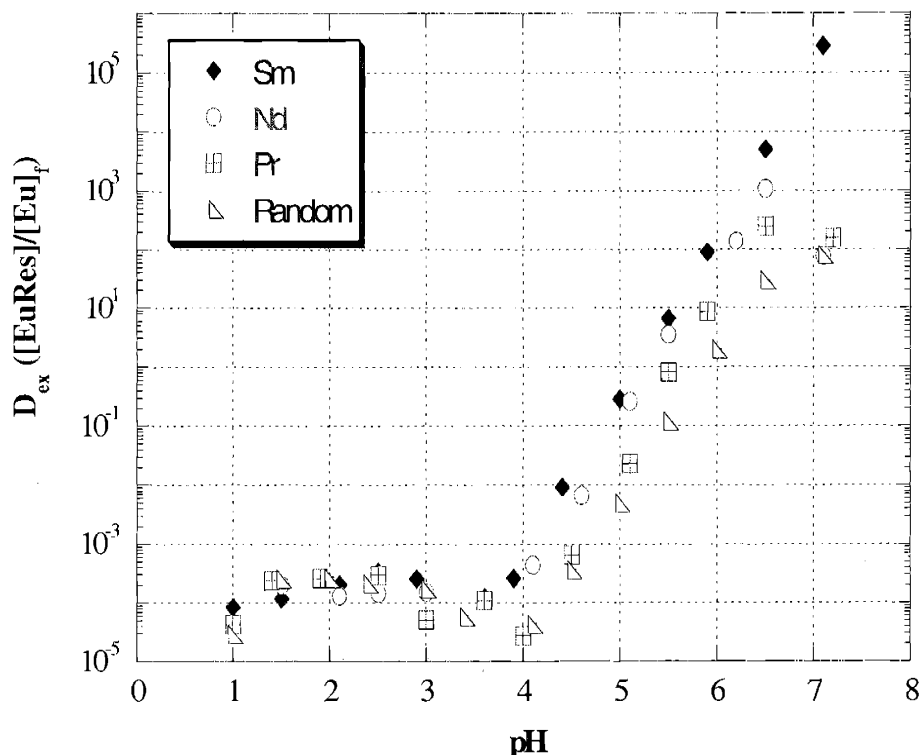
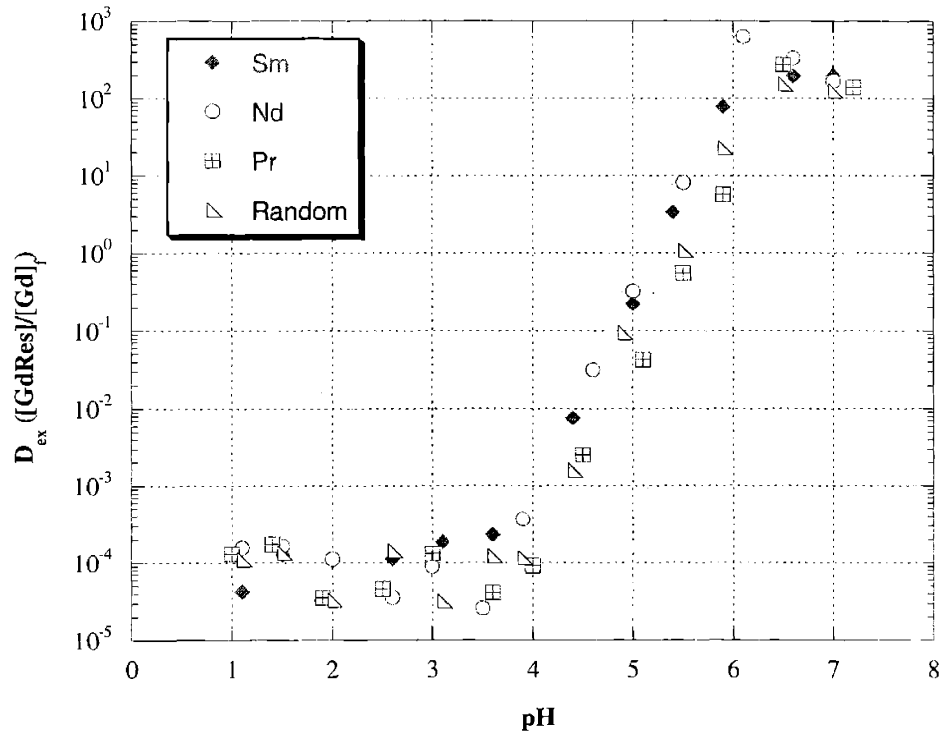


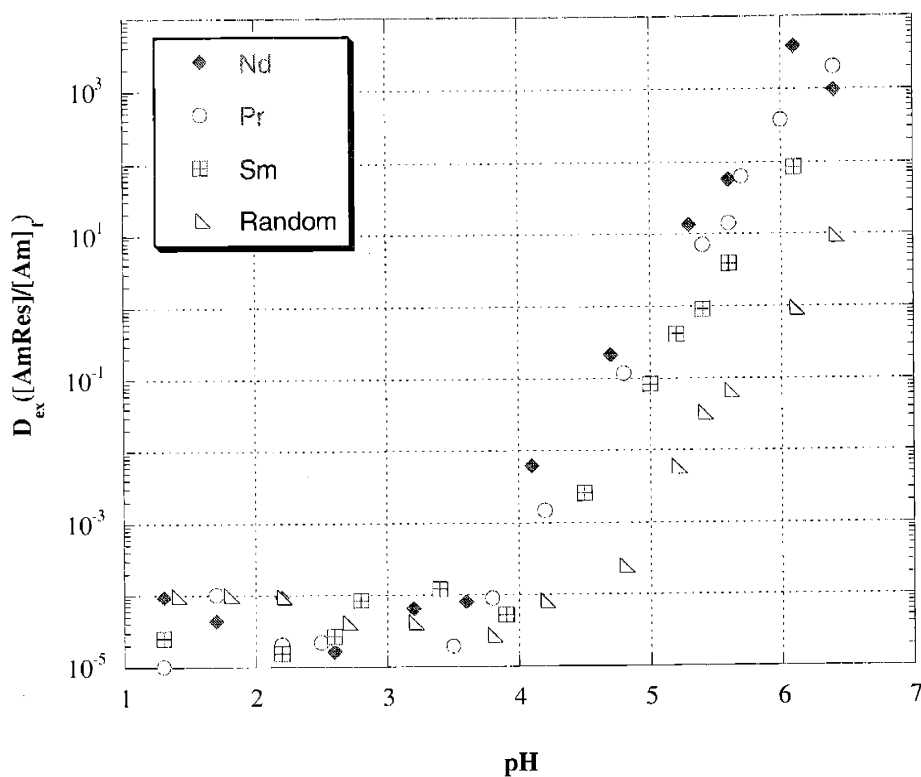
Figure 9.5 shows that, with respect to Eu sorption to the resins, at $4 < \text{pH} < 7$, the Sm-templated resin is showing a slightly higher preference for Eu, followed respectively by the Nd-, Pr-, and non-templated resins. This effect is most clearly observed at pH 7, where there is a clear advantage with the Sm-imprinted resin.

Figure 9.6: D_{ex} values for Gd vs. pH at 200% of loading capacity.



As seen above in **Figure 9.6**, the only interesting results are seen in the $4 < \text{pH} < 6$ range, where there are comparable results between the Nd- and Sm-templated resins, which work better than the non- and Pr-templated resins, which also yielded similar results as a pair. At pH values greater than 6, there is a decrease in D and no imprinting effect is observed.

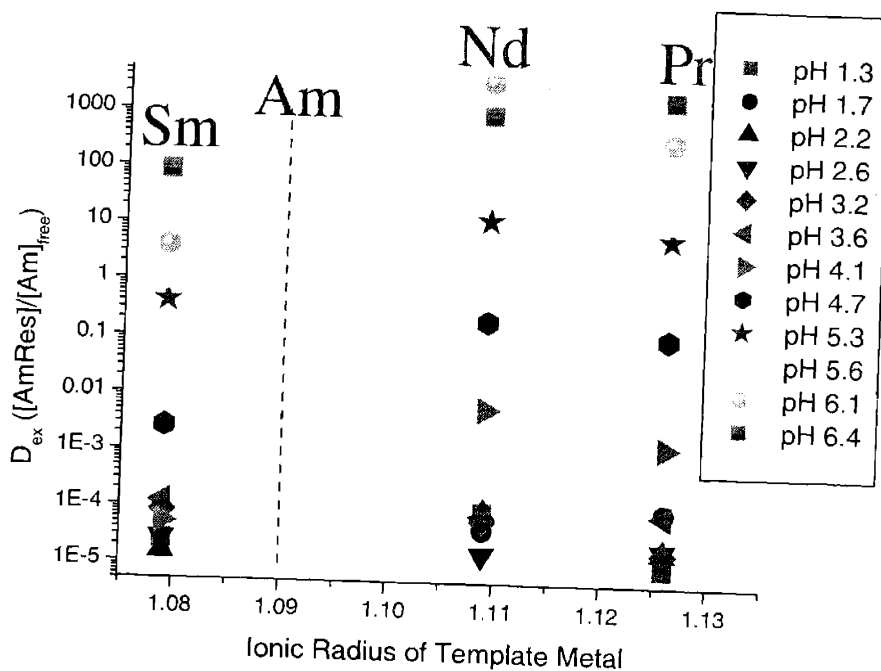
Figure 9.7: D_{ex} values for Am vs. pH at 100 nM.



A general observation gleaned from **Figure 9.5**, **Figure 9.6**, and **Figure 9.7** is that there is no imprinting effect at pH values below 4. The results for Am, shown above in **Figure 9.7**, present a tendency in the range of $4 < \text{pH} < 6.5$ for the Nd-templated resin to have the highest affinity for the target metal, followed by the Pr-, Sm-, and non-templated resins, respectively. As with the other experiments, we see a decrease in D at neutral pH values, in this case beginning at 6.5, where good binding and selectivity is still shown, just not with the Nd-templated resin as observed at lower pH values.

Another interesting way to look at the same data shown above in **Figure 9.7** is to examine the results with respect to the ionic radii of the metals involved in the imprinting process (Pr, Nd, and Sm) and their relationship to Am. This can be seen below in **Figure 9.8**:

Figure 9.8: D_{ex} results for Am, presented with respect to ionic radii at 100 nM.



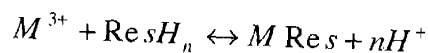
The point of interest in **Figure 9.8** is that it shows, for maximum efficacy, that the template metal must be equal or larger in size than the target metal. As observed in **Figure 9.7**, the Nd-templated resin is providing the highest affinity for Am, the target metal in this case, whereas the Sm-templated resin, which has the smallest available binding cavities, is providing the least selection for Am.

The results show better results for higher pH values, with pH 4 providing reasonable distribution for Am, but with good results through pH 6 with the Nd resin. The trend of better separations at high pH continues with Eu and Gd, with best Eu results at pH 7 with the Sm resin and best results for Gd at pH 6 with the Nd resin.

The subsaturation experiments were also used to calculate values for the selectivity constant K , which is calculated as:

$$K = \frac{[M - Res][H^+]^n}{[M]_{free}[Res]_{free}}$$

This value is obtained from the sorption reaction:



The free resin concentration is determined via the PEC values obtained earlier. Since protons tend to inhibit the formation of the Ln-Resin complex below pH 4 and the system reaches saturation above pH 7, the K values were calculated between pH 4 and 7. For the purposes of calculating K, the value of n was assumed to be 3, since the metals involved are all trivalent. The results for the K values are included below as **Figure 9.9**, **Figure 9.10**, and **Figure 9.11**.

Figure 9.9: K values for Eu vs. pH at 50% of loading capacity.

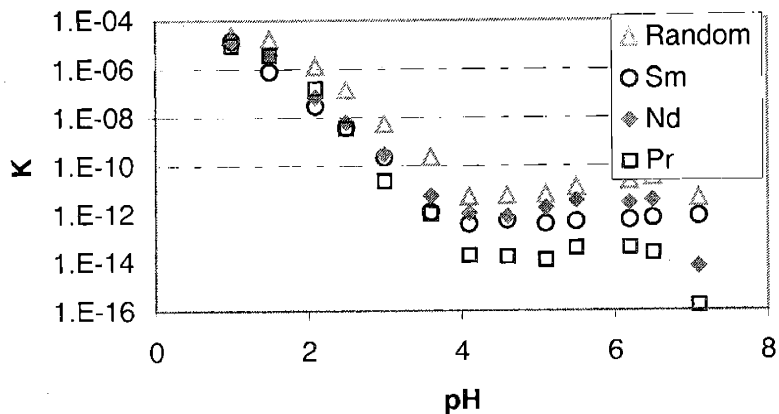


Figure 9.10: K values for Gd vs. pH at 50% of loading capacity.

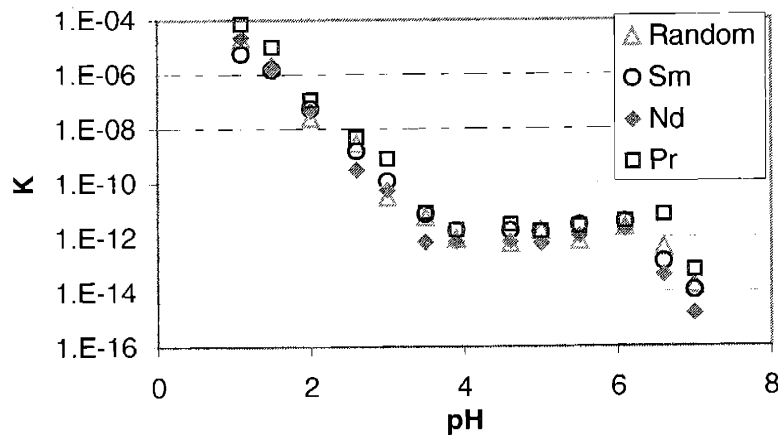
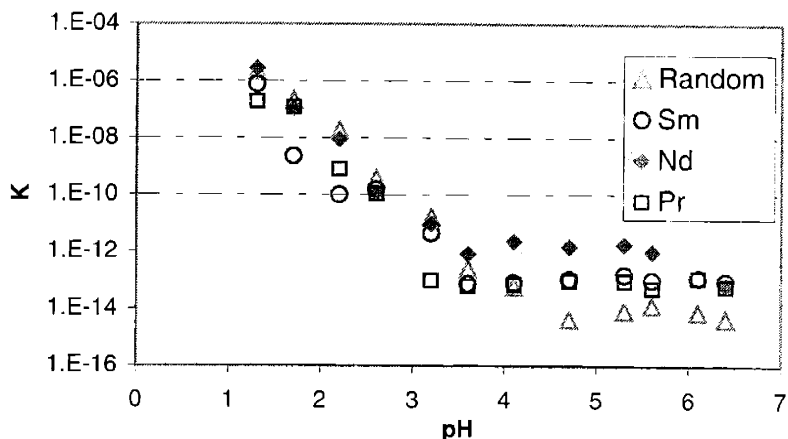


Figure 9.11: K values for Am vs. pH at 100 nM.



For Eu, the best separations are obtained with the random resin, which is a very good result since the templated resins are intended to selectively bind Am. The results for Gd indicate best separations with the Pr resin, which is also a good result, when coupled with the results for Am. The Am results indicate that the best binding is obtained with the Nd resin, which works well given the affinities of the other resins. These results also indicate that the resins bind metals, but more specifically, that they appear useful for Am separations from other trivalent metals.

9.4.5 Comparison with Published Data

When compared with other published results, the results of these syntheses and experiments show that the imprinted resins have lower PEC values than those of phenolic based resins such as CF, RF, CQF, and RQF by factors of 2-3 [5]. Although the D_{ex} values are lower than those for CF, RF, CQF, and RQF, at pH 4, the values are comparable at pH 6 [5]. Other comparisons for K_d values show that the imprinted Nd resin at a pH value of 6 has very comparable values with CMPO, roughly 300 (as calculated in the reference paper) [6]. In comparison with other imprinted polymers, the resins tested for effectiveness with Am can only be compared with a resin meant to complex (i.e. imprinted with) Gd. For this comparison, the values for the Am complexation with the Nd-imprinted resin at pH 6 were compared with the results for the Gd-imprinted resin produced by others; the Am was about 99% complexed by the resin, whereas the Gd was 48% extracted [7]. This may be a bit misleading, as the Gd-imprinted resin is based on a vinylpyridine synthesis, as opposed to my carboxylic acid type, but the two resins do have the same backbone structure.

9.5 Conclusions

So far, the use of lanthanides as templates for ion-imprinted resins for use with Am seems to be working quite well and shows better separation factors than the non-templated resin. The Nd resin shows the most promise and all future work should be concentrated on further evaluating this resin for use in Am separations. Previous issues with slow kinetics have been solved and no Am is needed for the templating process.

The initial testing for reusability via EXAFS analysis shows a good possibility for reuse of the resin, as there is little change in the binding structure after a second loading. Also, the kinetics results show a very fast equilibrium, achieved in 20 minutes or less. The Nd resin shows a higher than theoretical loading capacity for Am, the intended target metal of this process. Column studies also need to be run in the future to determine potential for column separations and elution methods.

Overall, the resins indeed sorb metals and the Nd resin in particular seems very promising for use in Am separations. Since the content of Nd in waste relative to other trivalent metals tends to be small, there is not much concern for the metal used in the templating process significantly interfering with the separation scheme. However, experiments still need to be run to confirm a resin preference for Am when other trivalent metals are in direct competition, as in a realistic waste stream. Based on previous successes along with the successes from the experiments presented in this paper, the same method is currently being applied for templating Np and Pu resins.

9.6 Acknowledgements

Part of this work was performed under the auspices of the U.S. Department of Energy (DOE) by the University of California Lawrence Livermore National Laboratory under Contract No. W-7405-Eng-48. This work was done (partially) at SSRL, which is operated by the Department of Energy, Division of Chemical Sciences.

9.7 References for Section IX

1. H. Nishide, J. Deguchi, E. Tsuchida, *Chem. Lett.*, 1976, 169-174.
2. M. Draye, A. Favre-Reguillon, D. Wruck, J. Foos, A. Guy, K.R. Czerwinski, *Removal of ²⁴³Am with Phenol Based Resins*, *Sep. Sci. Technol.*, 2001, (36), 899-909.
3. G. Saunders, S. Foxon, P. Walton, M. Joyce, S. Port, *A Selective Uranium Extraction Agent Prepared by Polymer Imprinting*, *Chem. Commun.*, 2000, (4), 273-274.
4. K.L. Noyes, M. Draye, A. Favre-Reguillon, J. Foos, A. Guy, K.R. Czerwinski, *Synthesis and Evaluation of Uranium and Thorium Imprinted Resins*, MRS Fall 2001 Meeting Proceedings, Symposium JJ.
5. Draye, M., Favre-Reguillon, A., Wruck, D., Foos, J., Guy, A., and Czerwinski, K. *Sep Sci Tech.*, 2001, 899-909.
6. Barr, M.E., Schulte, L.D., Jarvinen, G.D., Espinoza, J., Ricketts, T.E., Valdez, Y., Abney, K.D., and Bartsch, R.A. *Journal of Radioanalytical and Nuclear Chemistry*, 2001, 457-465.
7. Garcia, R., Vigneau, O., Pinel, C., and Lemaire, M. *Sep Sci Tech.*, 2002, 2839-2857.

X. Capping of Uranium Templated Resin

An ion exchange resin with carboxylic acid functional groups was synthesized based on the templating method to complex UO_2^{2+} from aqueous solutions. The nitrate salt of the target metal ion was dissolved in CCl_2H_2 , while the resin was created around the ions to provide a unique structure based upon each metal, followed by a process to remove potential binding sites which were not involved in the initial imprinting process. This resin was synthesized by a radical polymerization method, producing a reusable organic solid and is based upon the original work as seen in chapter 7. The resin was qualified by obtaining a value for its proton exchange capacity. Proton exchange capacities were determined using an indirect titration and were found to be 14.39 meq/g for the new uranium-based resin. A new resin preparation process was developed in order to prepare this new resin (“capped”) for use in experiments. Once loaded with metal, the ions can easily be removed with 5 M HNO_3 so that the resin can be reused.

10.1 Introduction

Organic based ion selective resins have some similar attributes: ease of synthesis, high metal ion complexation ability, and flexibility for different nuclear waste management applications. For most chelating polymers, the ligand is deemed to be of primary importance for the interaction with the targeted metal ion. The role of the polymer matrix is usually ignored.

The concept of molecular-imprinted polymers was developed more than 20 years ago [1] and shows a potential for applications in analytical chemistry [2-4]. The technique of molecular imprinting can be used for the production of selective ion exchange resins. Both simple organic compounds and polymers have been created using these methods in order to separate lanthanides [5] and actinides [6]. The more traditional simple organic compounds utilized functional groups such as phenols, resorcinol, and catechol. The problems with these previous resins include slow kinetics and difficulty with creating a molecularly imprinted product. These problems lead to the investigation of templated resins with carboxylic functional groups, as seen in chapters 7, 8, 9, and 10.

10.2 Background

A uranium, thorium, and americium selective polymers have yielded promising results and the uranium resin (see chapter 7) was used as the synthetic basis for the work

described in this chapter. This section examines the creation and qualification of a new polymer-based uranium selective resin which has been modified to remove interference from unimprinted binding sites. The separation of uranium from other metals has been used by the nuclear industry, mainly for fuel production and the handling of waste streams. The synthesis of a capped U selective resin can prove the methodology for template synthesis with a high degree of assurance that all binding sites are involved in the imprinting process.

With the success of the uranium-imprinted resin synthesis discussed in chapter 7, a modified synthetic route was developed in order to remove random binding sites. The final, successful process is outlined below and includes modifications to the resin processing procedures. The modifications to the synthesis were based on the methylation reactions presented in two references [7,8]. The proton exchange capacity of the synthesized templated resin was determined.

10.3 Experimental

10.3.1 Reagents

Methacrylic acid, triethylamine, ethylene glycol dimethacrylate, azobisisobutyronitrile (AIBN), tetrahydrofuran (THF), 1,8-diazabicyclo[5.4.0]undec-7-ene (1,5-5) (DBU), and iodomethane were obtained from Aldrich and used without further purification. Dichloromethane and uranium nitrate hexahydrate were obtained from Alfa Aesar and used without further purification.

10.3.2 Resin Synthesis

The metal was added, while stirring, to a mixture of methacrylic acid ($C_4H_6O_2$, 3.80 mmol, 0.33 g) in dichloromethane (CCl_2H_2 , 100 mL) as a nitrate ($UO_2(NO_3)_2 \cdot 6H_2O$), 1.51 mmol, 0.76 g) with triethylamine ($C_6H_{15}N$, 10.77 mmol, 1.5 mL) drop-wise. This reaction mixture was stirred at 40 °C for 2 hours under reflux. Ethylene glycol dimethacrylate ($C_{10}H_{14}O_4$, 12.92 mmol, 2.60 g) was added along with azobisisobutyronitrile (AIBN, $C_8H_{12}N_4$, 1.86 mmol, 0.31 g). The reaction mixture was heated to 60 °C and kept at this temperature overnight while stirring under reflux.

After evaporation, the resulting solid was ground and the template metal was left bound to the polymer. The resin was then washed with ethanol in order to remove any remaining organic residues, filtered, and dried. Once dry, the resin was then washed

combined with tetrahydrofuran (THF, C₄H₈O, 1.23 mol, 100 mL) in a three-neck round-bottom flask with stir bar and an addition funnel. The reaction vessel was then packed with ice and cooled to 0 °C. Once cool, 1,8-diazabicyclo[5.4.0]undec-7-ene (1,5-5) (DBU, C₉H₁₆N₂, 0.407 mol, 61.97 g) was very slowly added while maintaining the temperature. Following this addition, iodomethane (CH₃I, 0.490 mol, 69.57 g) was added and the solution was stirred for 24 hours at room temperature.

To prepare the resin for experiments, it was first placed in a filtration apparatus, washed with ether, washed with 7.5 M HNO₃ to remove the template metal, washed with water until neutral, washed with 0.1 M NaOH, washed with water until neutral, washed with 5 M HNO₃ in order to remove all remaining template metal, and washed with water until neutral. The resin was then transferred to a 60 °C air oven for curing for 2 days.

10.3.3 PEC Determination

Solutions, as prepared below, were titrated with a 736 GP Titrino from Metrohm after equilibration under Ar atmosphere for 1 hour. The titration parameters are 0.1515 mL additions of 0.10 M HCl every 10 minutes to total 15 mL of solution, with the endpoint of the titration used to calculate the PEC of the resins.

For determination of the total proton exchange capacity, samples of 0.05 g resin were equilibrated for 12 h with 25 mL of 0.1 M NaOH containing 5% NaCl solution while shaking. The amount of NaOH consumed in the H⁺ → Na⁺ exchange was determined by titration of the remaining OH⁻ in the supernatant, after preliminary equilibration under Ar atmosphere, with 0.1 M HCl solution.

10.4 Results and Discussion

10.4.1 PEC

From the titration end points, a value of 14.39 meq/g for the capped U resin was obtained. If metal ion charge neutralization is assumed upon sorption, then the molar sorption capacities for the resins need to be normalized to the metal ion charge. For uranyl, a maximum sorption of 7.20 mmol/g resin is expected with charge neutralization. Since the experiments used 0.05 g of resin a theoretic maximum of 0.36 mmoles UO₂²⁺ is expected to sorb. However, the values assume only charge neutralization. Partial hydrolysis of the metal ions will result in lower overall charge, hence sorption values could be seen above the theoretical limit.

10.5 Conclusions

This work proves that the resin synthesis, as developed throughout chapters 7, 8, and 9, can be further modified for both other applications or for more specific separations. This section modifies the synthetic process much more than the previous changes, seen within chapter 7, 8, and 9, which further attests to the robust quality of the final product. The modifications made to the resin in this section (chapter 10) require significantly more processing and caution in the synthesis itself, so the process is no longer as simple as that seen in previous chapters. However, the benefits may end up outweighing the detractions, since it is likely that in future work this capped resin will prove to be more selective than its predecessors. Future work must examine the thermodynamics and kinetics of binding, as well as the efficiency/effectiveness of the resin as applied to competitive separations.

10.6 References for Section X

1. G. Wulff, A. Sarhan, *Angew. Chem. Int. Ed. Eng.*, 1972, **11**, 341 ; R. Arshady, K. Mosbach, *Makromol. Chem.*, 1981, **182**, 687-692
2. a) A. Sarhan, G. Wulff, *Makromol. Chem.*, 1982, **183**, 85-92 ; b) G. Wulff, J. Haarer, *Makromol. Chem.*, 1991, **192**, 1329-1338
3. M. Kempe, K. Mosbach, *J. Chromatogr. A*, 1995, **694**, 3-13
4. a) B. Sellergren, M. Lepistö, K. Mosbach, *J. Am. Chem. Soc.*, 1988, **110**, 5853-5860 ;
b) D. Spivak, M.A. Gilmore, K.J. Shea, *J. Am. Chem. Soc.*, 1997, **119**, 4388-4393
5. K. Uezu, M. Yoshida, M. Goto, S. Furusaki, *Chemtech*, 1999, 12-18
6. Saunders, G., Foxon, S., Walton, P., Joyce, M., and Port, S.: A Selective Uranium Extraction Agent Prepared by Polymer Imprinting. *Chem Commun.*2000, **4**, 273-274.
7. Mal, D. *Synthetic Communications*, 1986, 331-335.
8. Renga, J.M., Wang, P. *Synthetic Communications*, 1984, 77-82.

XI. Conclusions

This chapter gathers the conclusions of all of the previous chapters, along with some overall comments and conclusions, and ideas for future work.

11.1 Phenolic Resin Syntheses

This work has shown that ion imprinting is very difficult to accomplish on phenolic-based resins while maintaining the integrity of the resin. Due to the chemistry of uranium, or actinides in general, the syntheses require significant pH modifications from very basic to at least mildly acidic in order to create an environment suitable for uranium, or actinide, dissolution. Since the ion imprinting technique requires that the target ion be present in solution while the resin is formed, this step is crucial to the successful production of an ion imprinted resin.

In general, the only potential success in this task was the production of a phenol imprinted resin, which is very limiting and may not be applicable with further modifications, such as adding soft donors to the back bone or adding chelators. Given these severe limitations, ion imprinting is not deemed to be a compatible technique with phenolic-type resin syntheses. Other types of resin syntheses could show more promise for this technique and are investigated throughout the remainder of this thesis, as well as by other researchers for use with other, lighter metals.

11.2 Uranium and Thorium Experiments

These studies show that polymer-based resins templated with uranyl and thorium(IV) ions sorb their target metal ions. The ability of the resin to sorb the target metal ion while competing with metal ion of differing oxidation states yielded some unexpected results in that strong competition was coming from unexpected players. This may indicate that a fair amount of binding is occurring at random sites, or binding sites which were not produced via the imprinting process. An addition to the synthesis should be investigated in order to remove these random binding sites, which should further increase the selectivity of the resin.

The breakthrough of solutions containing the target metal in a resin column also must be determined in order to consider column feasibility. The syntheses of this study will also be used as a basis for templating higher actinides, such as neptunium and plutonium. One of the initial goals of this work was to produce a resin with rapid kinetics, and these

experiments have indicated success. The values for the metal binding indicate charge neutralization, which is confirmed with the EXAFS data. The reusability of the resin also remains to be proven, and will be investigated in another experiment.

11.3 Neptunium Experiments

The successful imprinting of a resin with the Np(V) ion proves that it is possible to template both more radioactive metals and run the synthesis on very small scales. Other successes of the synthesis include starting with a wet (i.e. aqueous) target, which is notable since water easily and completely halts the radical synthesis involved in the formation of the imprinted resin. The resin preparation method was also altered in order to account for both the small amount of product and the radioactivity involved. All in all, this is a success which can be further applied to other elements in the future, such as Pu. Future work should include characterization of the resin and an examination of the thermodynamics of binding, as well as the effectiveness of the resin in competitive separation schemes.

11.4 Americium Experiments

When compared with other published results, the results of these syntheses and experiments show that the imprinted resins have lower PEC values than those of phenolic based resins such as CF, RF, CQF, and RQF by factors of 2-3 [1]. Although the D_{ex} values are lower than those for CF, RF, CQF, and RQF, at pH 4, the values are comparable at pH 6 [1]. Other comparisons for K_d values show that the imprinted Nd resin at a pH value of 6 has very comparable values with CMPO, roughly 300 (as calculated in the reference paper) [2]. In comparison with other imprinted polymers, the resins tested for effectiveness with Am can only be compared with a resin meant to complex (i.e. imprinted with) Gd. For this comparison, the values for the Am complexation with the Nd-imprinted resin at pH 6 were compared with the results for the Gd-imprinted resin produced by others; the Am was about 99% complexed by the resin, whereas the Gd was 48% extracted [3]. This may be a bit misleading, as the Gd-imprinted resin is based on a vinylpyridine synthesis, as opposed to my carboxylic acid type, but the two resins do have the same backbone structure.

So far, the use of lanthanides as templates for ion-imprinted resins for use with Am seems to be working quite well and shows better separation factors than the non-

templated resin. The Nd resin shows the most promise and all future work should be concentrated on further evaluating this resin for use in Am separations. Previous issues with slow kinetics have been solved and no Am is needed for the templating process.

The initial testing for reusability via EXAFS analysis shows a good possibility for reuse of the resin, as there is little change in the binding structure after a second loading. Also, the kinetics results show a very fast equilibrium, achieved in 20 minutes or less. The Nd resin shows a higher than theoretical loading capacity for Am, the intended target metal of this process. Column studies also need to be run in the future to determine potential for column separations and elution methods.

Overall, the resins indeed sorb metals and the Nd resin in particular seems very promising for use in Am separations. Since the content of Nd in waste relative to other trivalent metals tends to be small, there is not much concern for the metal used in the templating process significantly interfering with the separation scheme. However, experiments still need to be run to confirm a resin preference for Am when other trivalent metals are in direct competition, as in a realistic waste stream. Based on previous successes along with the successes from the experiments presented in this paper, the same method is currently being applied for templating Np and Pu resins.

11.5 Capping of Uranium Resin

This work proves that the resin synthesis, as developed throughout chapters 7, 8, and 9, can be further modified for both other applications or for more specific separations. This section modifies the synthetic process much more than the previous changes, seen within chapter 7, 8, and 9, which further attests to the robust quality of the final product. The modifications made to the resin in this section (chapter 10) require significantly more processing and caution in the synthesis itself, so the process is no longer as simple as that seen in previous chapters. However, the benefits may end up outweighing the detractions, since it is likely that in future work this “capped” resin will prove to be more selective than its predecessors. Future work must examine the thermodynamics and kinetics of binding, as well as the efficiency/effectiveness of the resin as applied to competitive separations.

11.6 Overall Conclusions from Resin Work

The most important conclusion of this work is that it is possible to apply the ion imprinting method to the synthesis of resins that are applicable for actinide separations processes. This is a notable achievement, since ion imprinted products are well-known to be highly selective for their target metals and that efficient separations processes will likely be needed in the near future for most currently proposed nuclear fuel cycles.

Initially, the ion imprinting technique was applied to phenolic resin syntheses, which have been widely used and synthesized for experiments in actinide/lanthanide separations. Due to the high pH conditions (about 10) inherent to the phenolic-based resin syntheses, the ion imprinting technique was extremely difficult to accomplish in a reliable manner (for details on this section of the work, see chapter 6). For these reasons, a very common application of ion imprinting was tapped: ion imprinted polymers.

Since there had been a previous success with the imprinting of a polymer with the uranyl ion, this work began with a similar synthesis based on that initial work. A resin imprinted with uranyl was successfully produced and tested for effectiveness (see chapter 7 for details on results/tests). This success led to modifications to the synthesis so that a product imprinted with Th(IV) ions was successfully produced. This resin was also tested for effectiveness (results can be seen in detail in chapter 7).

The successes of the imprinting of resins with the uranyl and Th(IV) ions, the work was further adapted for application to Np(V) ions (see chapter 8 for details). Due to the small advantage in selectivity, the synthesis was further modified in order to remove any binding sites which were not involved in the original synthetic imprinting process. This methylation of unimprinted binding sites is referred to as “capping.” The capping technique was only applied to the uranyl ion, which provided the simplest reaction conditions and the least number of preliminary modifications (details on this work can be found in chapter 10).

Although the fruitful application to Np(V) showed that it was possible to template relatively radioactive metals, when the technique was extended to produce a resin for Am(III) separations, four resins were created for use with Am(III), none of which were actually imprinted with Am(III). Given the chemical similarity of Am(III) to the lanthanides, the following four resins were produced: Sm(III)-, Pr(III)-, Nd(III)-, and un-

imprinted. A series of experiments were run in order to test the effectiveness and applicability of each of the resins to Am(III) separations. The most notable conclusion to come out of the work is the following: the most effective resin for application to Am(III) separations was the resin templated with Nd(III). This is notable, since the size of the template ion can be proven to matter. The ion which had a smaller ionic radius than that of Am(III) was not very effective; the most effective turned out to be that which was just slightly larger than Am(III), proving that the cavity produced in the templating process must be at least as large as the desired target (for details on this section, please reference chapter 9).

Based on all of the applications of the ion imprinting technique detailed in this thesis, it can be seen that ion imprinting is a highly adaptable and widely applicable technique that is also useful for potential actinide/lanthanide separation schemes. The work in this thesis can easily be further extended to other actinides, lanthanides, or further still to other sections of the periodic table. The synthetic processes detailed throughout the thesis are easily scalable for either small- or large-scale processes. In cases of high activity or hard to get target materials, suitable resins can be created from chemically similar materials (note: the similarity must be in both size and charge). The creation of a more tailored resin is possible by adding additional synthetic steps onto the back-end of the resin production process, but requires significant and non-trivial modifications to the synthetic conditions. Finally, this work shows that the area of ion imprinting should be investigated further for the renewed development of actinide/lanthanide separation science.

11.7 Recommendations for Future Work

Recommendations for future work are to extend the projects already undertaken in this thesis. The Np(V) resin should be characterized: obtain values for PEC, kinetics, thermodynamics, and potentially even competition-type experimental data. The capped uranyl resin should be characterized: confirmation of PEC value, kinetics, thermodynamics, and competition-type experiments, along with a comparison to the original uranyl-imprinted resin. This work can also be extended to other elements, such as Pu, which are also important to the nuclear industry. Finally, given the known harsh conditions of separations involved radioactive materials, the resins should also be tested for durability under both heat and from irradiation.

11.8 References for Section XI

1. Draye, M., Favre-Reguillon, A., Wruck, D., Foos, J., Guy, A., and Czerwinski, K. *Sep. Sci. Tech.*, 2001, 899-909.
2. Barr, M.E., Schulte, L.D., Jarvinen, G.D., Espinoza, J., Ricketts, T.E., Valdez, Y., Abney, K.D., and Bartsch, R.A. *Journal of Radioanalytical and Nuclear Chemistry*, 2001, 457-465.
3. Garcia, R., Vigneau, O., Pinel, C., and Lemaire, M. *Sep Sci Tech.*, 2002, 2839-2857.

XII. References

12.1 References from section II

1. G. Wulff, A. Sarhan, *Angew. Chem. Int. Ed. Eng.*, 1972, **11**, 341 ; R. Arshady, K. Mosbach, *Makromol. Chem.*, 1981, **182**, 687-692
2. a) A. Sarhan, G. Wulff, *Makromol. Chem.*, 1982, **183**, 85-92 ; b) G. Wulff, J. Haarer, *Makromol. Chem.*, 1991, **192**, 1329-1338
3. M. Kempe, K. Mosbach, *J. Chromatogr. A*, 1995, **694**, 3-13
4. a) B. Sellergren, M. Lepistö, K. Mosbach, *J. Am. Chem. Soc.*, 1988, **110**, 5853-5860 ; b) D. Spivak, M.A. Gilmore, K.J. Shea, *J. Am. Chem. Soc.*, 1997, **119**, 4388-4393
5. K. Uezu, M. Yoshida, M. Goto, S. Furusaki, *Chemtech*, 1999, 12-18
6. Saunders, G., Foxon, S., Walton, P., Joyce, M., and Port, S.: A Selective Uranium Extraction Agent Prepared by Polymer Imprinting. *Chem Commun.*2000, **4**, 273-274.
7. Kazuba, J.P., Runde, W.H.: The Aqueous Geochemistry of Neptunium: Dynamic Control of Soluble Concentrations with Applications to Nuclear Waste Disposal. *Env. Sci. Tech.* 33, 4427-4433 (1999)
8. Nash, K.L. *Solvent Extr. and Ion Exch.*, 1993, 729-768.
9. Draye, M., Favre-Reguillon, A., Wruck, D., Foos, J., Guy, A., and Czerwinski, K. *Sep. Sci. Tech.*, 2001, 899-909.
10. Barr, M.E., Schulte, L.D., Jarvinen, G.D., Espinoza, J., Ricketts, T.E., Valdez, Y., Abney, K.D., and Bartsch, R.A. *Journal of Radioanalytical and Nuclear Chemistry*, 2001, 457-465.
11. Garcia, R., Vigneau, O., Pinel, C., and Lemaire, M. *Sep Sci Tech.*, 2002, 2839-2857.

12.2 References from section III

1. G. Wulff, A. Sarhan, *Angew. Chem. Int. Ed. Eng.*, 1972, **11**, 341 ; R. Arshady, K. Mosbach, *Makromol. Chem.*, 1981, **182**, 687-692
2. a) A. Sarhan, G. Wulff, *Makromol. Chem.*, 1982, **183**, 85-92 ; b) G. Wulff, J. Haarer, *Makromol. Chem.*, 1991, **192**, 1329-1338
3. M. Kempe, K. Mosbach, *J. Chromatogr. A*, 1995, **694**, 3-13
4. a) B. Sellergren, M. Lepistö, K. Mosbach, *J. Am. Chem. Soc.*, 1988, **110**, 5853-5860 ; b) D. Spivak, M.A. Gilmore, K.J. Shea, *J. Am. Chem. Soc.*, 1997, **119**, 4388-4393
5. K. Uezu, M. Yoshida, M. Goto, S. Furusaki, *Chemtech*, 1999, 12-18
6. Saunders, G., Foxon, S., Walton, P., Joyce, M., and Port, S.: A Selective Uranium Extraction Agent Prepared by Polymer Imprinting. *Chem Commun.*2000, **4**, 273-274.
7. Kazuba, J.P., Runde, W.H.: The Aqueous Geochemistry of Neptunium: Dynamic Control of Soluble Concentrations with Applications to Nuclear Waste Disposal. *Env. Sci. Tech.* 33, 4427-4433 (1999)
8. http://www.chem.ubc.ca/courseware/233/5-5_pka.pdf
9. <http://www.chem.ucalgary.ca/courses/351/Carey/Ch19/ch19-1.html>
10. Laidler, J.J. *J. Nucl. Mat. Mgmt.*, 2002, 36-38.
11. Aoki, S. *Progress in Nucl. Energy*, 2002, 343-348.
12. Mukaiyama, T., Takano, H., Ogawa, T., Takizuka, T., and Mizumoto, M. *Progress in Nucl. Energy*, 2002, 403-413.

13. Hoffman, Darleane. *Advances in Plutonium Chemistry, 1967-2000*. American Nuclear Society: 2002.
14. Choppin, G.R. *Chem. Sep. Tech. And Related Meth. Of Nucl. Waste Mang.*, 1999, 1-16.
15. Benedict, M., Pigford, T., and Levi, H.W.: *Nuclear Chemical Engineering*, Second edition. McGraw-Hill: 1981.
16. Manthur, J.N., Murali, M.S, and Nash, K.L. *Solv. Extr. Ion Exch.*, 2001, 357-390.
17. Selvaduray, G., Goldstein, M.K., and Anderson, R.N. *Reprocessing and Recycling*, 1978, 35-40.

12.3 References from section IV

1. Greenwood, N.N., and Earnshaw, A. *Chemistry of the Elements*. Butterworth Heinemann: Woburn, 1997.
2. Seaborg, G.T., and Loveland, W.D. *The Elements Beyond Uranium*. John Wiley & Sons: New York, 1990.
3. Nash, K.L. *Solvent Extr. and Ion Exch.*, 1993, 729-768.
4. Tsukagoshi, K., Murata, M., and Maeda, M. *Techniques and Instrumentation in Analytical Chemistry*, 2001, p. 245-269.
5. Fish, Richard H. "Metal Ion Templated Polymers" from *Molecular and Ionic Recognition with Imprinted Polymers*, Bartsch, R.A. and Maeda, M., ed. Published by the American Chemical Society: Washington, D.C., 1998, p. 238-250.
6. Bartsch, R.A. and Maeda, M. "Molecular and Ionic Recognition with Imprinted Polymers: A Brief Overview" from *Molecular and Ionic Recognition with Imprinted Polymers*, Bartsch, R.A. and Maeda, M., ed. Published by the American Chemical Society: Washington, D.C., 1998, p. 1-8.
7. Zeng, X., Bzhelyansky, A., Bae, S.Y., Jenkins, A.L., and Murray, G.M. "Templated Polymers for the Selective Sequestering and Sensing of Metal Ions" from *Molecular and Ionic Recognition with Imprinted Polymers*, Bartsch, R.A. and Maeda, M., ed. Published by the American Chemical Society: Washington, D.C., 1998, p. 218-237.
8. Nishide, H., Deguchi, J., and Tsuchida, E. *Chemistry Letters*, 1976, 169-174.
9. Mosbach, K., and Ramström, O. *Biotechnology*, 1996, 163-170.
10. Wulff, G. and Sarhan, A. *Angew. Chem., Int. Ed. Engl.*, 1972, 341.
11. Andersson, L., Sellergren, B., and Mosbach, K. *Tetrahedron Lett.*, 1984, 5211.
12. Kuchen, W., and Schram, J. *Angew. Chem. Int. Ed. Engl.*, 1988, 1695-1697.

12.4 References from section V

1. Gill, Robin, *Modern Analytical Geochemistry*, Longman Singapore Publishers, LTD, Singapore, Indonesia 1997 pp. 41-60
2. <http://xray.chm.bris.ac.uk:8000/research/exafs.html>
3. <http://www.chem.orst.edu/ch361-464/ch362/irinstrs.htm>
4. <http://www.uwm.edu/Dept/EHSRM/RAD/HANDOUT.pdf>

12.5 References from section VI

1. Draye, M.; Favre-Reguillon, A.; Wruck, D.; Foos, J.; Guy, A.; Czerwinski, K. **Removal of ²⁴³Am with phenol-based resins.** Separation Science and Technology

- (2001), 36(5 & 6), 899-909; Draye, M.; Czerwinski, K. R.; Favre-Reguillon, A.; Foos, J.; Guy, A.; Lemaire, M. **Selective separation of lanthanides with phenolic resins: extraction behavior and thermal stability.** Separation Science and Technology (2000), 35(8), 1117-1132.
2. Kuchen, W., and Schram, J. *Angew. Chem. Int. Ed. Engl.*, 1988, 1695-1697.

12.6 References from section VII

1. G. Wulff, A. Sarhan, *Angew. Chem. Int. Ed. Engl.*, 1972, **11**, 341 ; R. Arshady, K. Mosbach, *Makromol. Chem.*, 1981, **182**, 687-692
2. a) A. Sarhan, G. Wulff, *Makromol. Chem.*, 1982, **183**, 85-92 ; b) G. Wulff, J. Haarer, *Makromol. Chem.*, 1991, **192**, 1329-1338
3. M. Kempe, K. Mosbach, *J. Chromatogr. A*, 1995, **694**, 3-13
4. a) B. Sellergren, M. Lepistö, K. Mosbach, *J. Am. Chem. Soc.*, 1988, **110**, 5853-5860 ; b) D. Spivak, M.A. Gilmore, K.J. Shea, *J. Am. Chem. Soc.*, 1997, **119**, 4388-4393
5. K. Uezu, M. Yoshida, M. Goto, S. Furusaki, *Chemtech*, 1999, 12-18
6. Saunders, G., Foxon, S., Walton, P., Joyce, M., and Port, S.: A Selective Uranium Extraction Agent Prepared by Polymer Imprinting. *Chem Commun.*2000, **4**, 273-274.

12.7 References from section VIII

1. H. Nishide, J. Deguchi, E. Tsuchida, *Chem. Lett.*, 1976, 169-174.
2. M. Draye, A. Favre-Reguillon, D. Wruck, J. Foos, A. Guy, K.R. Czerwinski, *Removal of ²⁴³Am with Phenol Based Resins*, *Sep. Sci. Technol.*, 2001, (36), 899-909.
3. G. Saunders, S. Foxon, P. Walton, M. Joyce, S. Port, *A Selective Uranium Extraction Agent Prepared by Polymer Imprinting*, *Chem. Commun.*, 2000, (4), 273-274.
4. K.L. Noyes, M. Draye, A. Favre-Reguillon, J. Foos, A. Guy, K.R. Czerwinski, *Synthesis and Evaluation of Uranium and Thorium Imprinted Resins*, MRS Fall 2001 Meeting Proceedings, Symposium JJ.

12.8 References from section IX

1. H. Nishide, J. Deguchi, E. Tsuchida, *Chem. Lett.*, 1976, 169-174.
2. M. Draye, A. Favre-Reguillon, D. Wruck, J. Foos, A. Guy, K.R. Czerwinski, *Removal of ²⁴³Am with Phenol Based Resins*, *Sep. Sci. Technol.*, 2001, (36), 899-909.
3. G. Saunders, S. Foxon, P. Walton, M. Joyce, S. Port, *A Selective Uranium Extraction Agent Prepared by Polymer Imprinting*, *Chem. Commun.*, 2000, (4), 273-274.
4. K.L. Noyes, M. Draye, A. Favre-Reguillon, J. Foos, A. Guy, K.R. Czerwinski, *Synthesis and Evaluation of Uranium and Thorium Imprinted Resins*, MRS Fall 2001 Meeting Proceedings, Symposium JJ.
5. Draye, M., Favre-Reguillon, A., Wruck, D., Foos, J., Guy, A., and Czerwinski, K. *Sep Sci Tech.*, 2001, 899-909.
6. Barr, M.E., Schulte, L.D., Jarvinen, G.D., Espinoza, J., Ricketts, T.E., Valdez, Y., Abney, K.D., and Bartsch, R.A. *Journal of Radioanalytical and Nuclear Chemistry*, 2001, 457-465.

7. Garcia, R., Vigneau, O., Pinel, C., and Lemaire, M. *Sep Sci Tech.*, 2002, 2839-2857.

12.9 References from section X

1. G. Wulff, A. Sarhan, *Angew. Chem. Int. Ed. Eng.*, 1972, **11**, 341 ; R. Arshady, K. Mosbach, *Makromol. Chem.*, 1981, **182**, 687-692
2. a) A. Sarhan, G. Wulff, *Makromol. Chem.*, 1982, **183**, 85-92 ; b) G. Wulff, J. Haarer, *Makromol. Chem.*, 1991, **192**, 1329-1338
3. M. Kempe, K. Mosbach, *J. Chromatogr. A*, 1995, **694**, 3-13
4. a) B. Sellergren, M. Lepistö, K. Mosbach, *J. Am. Chem. Soc.*, 1988, **110**, 5853-5860 ;
b) D. Spivak, M.A. Gilmore, K.J. Shea, *J. Am. Chem. Soc.*, 1997, **119**, 4388-4393
5. K. Uezu, M. Yoshida, M. Goto, S. Furusaki, *Chemtech*, 1999, 12-18
6. Saunders, G., Foxon, S., Walton, P., Joyce, M., and Port, S.: A Selective Uranium Extraction Agent Prepared by Polymer Imprinting. *Chem Commun.*2000, **4**, 273-274.
7. Mal, D. *Synthetic Communications*, 1986, 331-335.
8. Renga, J.M., Wang, P. *Synthetic Communications*, 1984, 77-82.

12.10 References from section XI

1. Draye, M., Favre-Reguillon, A., Wruck, D., Foos, J., Guy, A., and Czerwinski, K. *Sep. Sci. Tech.*, 2001, 899-909.
2. Barr, M.E., Schulte, L.D., Jarvinen, G.D., Espinoza, J., Ricketts, T.E., Valdez, Y., Abney, K.D., and Bartsch, R.A. *Journal of Radioanalytical and Nuclear Chemistry*, 2001, 457-465.
3. Garcia, R., Vigneau, O., Pinel, C., and Lemaire, M. *Sep Sci Tech.*, 2002, 2839-2857.